Investigating the Effect of Dyeing on the Surface of Wool Fibres with Atomic Force Microscopy (AFM)

By

Abduelmaged Abduallah

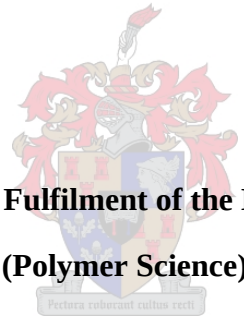

Thesis Presented in Partial Fulfilment of the Degree of Master of Science

(Polymer Science)

at the

University of Stellenbosch

Supervisor: Dr. M. Meincken

Co-supervisor: A. Gericke

Stellenbosch

April 2006

Declaration:

I the undersigned hereby declare that the work contained in this thesis is my own original work and has not previously in its entirety or in part been submitted at any university for a degree.

Signature: ……

Date: …….……..

Abstract

Dyeing has an influence on the characteristic properties of wool fibres. This can result in changes in the final properties of the fibre including fibre elasticity, fibre strength and breaking elongation of the wool fibres, especially in the case of dark colours. Damage that occurs to the fibre surface due to the action of acid, alkali, dyestuff, water, heat, and mechanical stress during the dyeing process can thus have an affect on the fibre breaking elongation and the fibre strength. The aim of this project was to assess the effect of dyeing with different colours (ranging from light to dark) on the surface of wool fibres using atomic force microscopy (AFM).

The results indicated that four different types of surface damage can be discerned: scale raising, scale chipping, fluting and pitting. The findings also indicate that the surface damage to the fibres was greater and more noticeable (especially the scale raising) on fibres dyed with dark colours than to fibres dyed with light colours. The same applied to the fibre strength and elongation, where generally the fibre breaking extension and the breaking load was smaller in the case of darker colours.

The effect of dyeing with different colour shades on the fibre surface was observed with AFM. Several characteristic scale parameters of a statistical significant number of dyed and undyed fibres were measured in order to determine the surface damage caused by dyeing. The correlation between the surface damage, observed by AFM, and the loss in tensile strength and fibre elongation, determined by tensile tests, were investigated. This was done in order to determine the effect of the cuticle damage on the tensile stress/strain behaviour. The results show that AFM is a viable tool to study the effects of different dyes on the fibre surface and for detecting surface modifications with great accuracy.

It was found that dyeing with dark colours caused greater damage to the surface than light colours, and it was possible to distinguish different lightness areas, which could be regarded as light and dark colours.

Opsomming

Die invloed van tekstielkleuring op die karakteristieke eienskappe van wolvesels, kan lei tot veranderinge in vesel gedragseienskappe soos elastisiteit, veselsterkte en breekverlenging – veral in die geval van donker kleure. Beskadiging van die vesel-oppervlak as gevolg van blootstelling aan sure, alkalië, kleurstowwe, water, hitte en meganiese stress gedurende die kleurproses kan dus ‘n direkte effek hê op veral sterkte en breekverlenging. Die doel van die projek was om die effek van kleuring met verskillende kleure kleurstowwe (van lig na donker) op die oppervlak van wolvesels te ondersoek met behulp van ‘n skandeer pylstif mikroskoop (ook bekend as die atoom-kragmikroskoop of in Engels algemeen verwys na as die AFM).

Die resultate het getoon dat vier verskillende tipes oppervlakbeskadiging geïdentifiseer kan word, naamlik verhoging van skubreliëf, skub-afsplintering en die vorming van groewe en gaatjies in die skuboppervlakte. Daar is ook bevind dat die oppervlakbeskadiging van die vesels meer opmerklik was by vesels wat donker gekleur is as by dié in ligter kleure. Dit geld ook vir die eienskappe veselsterkte en –breekverlenging, waar beide laer was in die geval van donker kleure.

In die ondersoek na die effek van kleuring met verskillende skakerings kleure op die vesel-oppervlak van wolvesels met behulp van die AFM is ‘n verskeidenheid kenmerkende parameters op ‘n statisties beduidende aantal gekleurde en ongekleurde vesels gemeet. Die verband tussen die waargeneemde oppervlakbeskadiging en veselbreeksterkte en –verlenging (bepaal deur middel van breektoetse op die Instron) is ondersoek. Die doel hiervan was om die effek van beskadiging aan die kutikulla op die breekverlengingsgedrag van die vesels te bepaal. Die resultate toon duidelik die waarde van die AFM as meetinstrument van die effek van verskillende kleurstowwe op die vesel-oppervlak en vir die akkurate meting van veranderinge in oppervlak-eienskappe.

Daar is bevind dat kleuring met donker kleure meer beskadiging aan die vesel-oppervlak meebring en dat dit moontlik is om onderskeid te tref tussen “ligte” en “donker” areas op grond van mikroskoopwaarnemings.

ACKNOWLEDGMENTS

I would like to express my gratitude and appreciation to my major advisor and supervisor, Dr. M. Meincken, for her sincere supervision, guidance and her help throughout this work. I am also grateful to Ms Adine Gericke, my co-supervisor, for her invaluable advice, guidance and assistance, which led to the completion of this project. It was an honour to know and to work with them.

Furthermore, I am thankful to all the members of Chemistry and Polymer Science Department for their cooperation and time.

I am also grateful to the company Hextex for their cooperation and provision of the wool samples and the dyes, especially to the dyeing manager Mr Eugene Lesch for his time and support.

I also acknowledge the financial support received from the International Centre for Macromolecular Chemistry and Technology in Libya.

I deeply acknowledge the encouragement, support, and patience of my family and friends for their help and support.

A large part of this thesis was presented as a poster at the *44th* *annual conference of the Microscopy Society of Southern Africa* (MSSA 2005).

This conference took place 5-7 December 2005, at the University of KwaZulu-Natal, in Pietermaritzburg.

INVESTIGATING THE EFFECT OF DIFFERENT DYEING COLOURS ON WOOL FIBRES WITH ATOMIC FORCE MICROSCOPY

A. Abduallah, A. Gericke, M. Meincken

Department for Chemistry and Polymer Science, Polymer Science, University of Stellenbosch, Private Bag X1, Matieland 7602, South Africa, email: mmein@sun.ac.za

Introduction

The potential for imaging techniques, particularly atomic force microscopy (AFM), in the field of wool fibre analysis has been reported recently [1,2].
These fibres consist of three morphological components: the cortex layer, which makes up the bulk of the fibre, the cuticle layer, which surrounds the cortex and the cell membrane complex, which bonds the two layers together. The cuticle consists of epicuticle, endocuticle and exocuticle layers [3].
It has been established that dyeing of wool fibres leads to surface damage and decreases the elasticity [4], especially for dark colours [5]. This has been ascribed to a breakdown of cystine linkages to form thiol groups and hydrolysis of peptides to form amino groups [4].

In this study AFM was used to investigate the surface damage of the fibres, link it to their loss in elasticity, and determine the "difference" between light and dark colours.

Materials & Methods

Investigated Samples:
Undyed and dyed merino fibres were supplied by Hextex / Worcester. The samples were dyed with either
- 1:2 metal complex reactive dye (Lanaset) or
- reactive dye (Lanasol)

from Ciba. The samples were ordered from light to dark shades according to their lightness, which was determined by a colorimeter.

Instrumentation:
AFM measurements were performed with a Multimode AFM with a Nanoscope III controller from Veeco under ambient conditions. The AFM was operated in non-contact and contact mode with a scan rate of 0.6 to 0.8 Hz.

Five random wool fibres were picked out of a bundle and four images were acquired on each fibre, resulting in a total of 20 images.
For static measurements, 20 force distance curves were recorded on each sample.

Measured Parameters:
For all fibres the following properties were determined: **scale height** (P1), **cuticle angle** (P2), **scale interval** (P3), **surface roughness** (P4), **normalised contact edge length** (P5), **scale elongation** (P6), **adhesive force** (P7) and the **hardness** (P8).
These surface characteristics were chosen because they are expected to change after dyeing, and it should be possible to observe the effect of different colours or shades.

Results

Comparison with undyed fibres (Fig. 1) shows that after dyeing, significant changes occur in the surface structure of the cuticle scales (Fig. 1c and Fig. 2).

Figure 1: a) Typical surface of an undyed wool fibre, b) 3d image of a) and c) raised scales of a dyed fibre.

Scale raising (Fig. 1c) was the most frequent type of damage. Other observed forms of surface damage are: *chipping* (pieces of the scale are chipped off the edge, Fig. 2a), *pitting* (the formation of holes, Fig. 2b), or *fluting* (etching of the surface without dissolving all proteins or fatty acids, which results in "wrinkles" , Fig. 2c). The fluting could be associated to the natural striations of the surface (Fig. 1b).

Figure 2: Forms of surface damage of dyed fibres a) chipping, b) pitting, c) fluting

Figure 1 and 2 show that the observed parameters, such as scale height or surface roughness, have changed after dyeing and are therefore suitable parameters to observe the effect of dyeing on the fiber surface as well as the influence of colour.

Figure 3 shows the changes in P1 and P2 versus the lightness. Both increase as the colour becomes darker. For both parameters a point can be determined within a lightness range of 30 to 40, at which the gradient changes drastically. Samples with a lightness lower than this point can be expected to show different physical and mechanical properties and could be considered as *dark* colours.

The increase in P1 and P2 can be explained by surface degradation, which breaks the polypeptide structure in the joint areas between two scales during dyeing (Fig 4). This is the weakest area of the fibre.
Lanasol reactive dye (circle) shows less surface damage than Lanaset dye. This could be due to the additional cross-links, which are produced by reactive dyes.
It seems that surface changes depend more on the type of dye than other materials in the dye bath, e.g. acid.

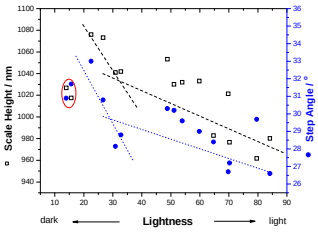

Figure 3: Changes in P1 and P2 as a function of lightness

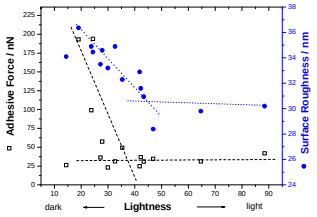

Figure 5: Changes in P3 and P7 as a function of lightness

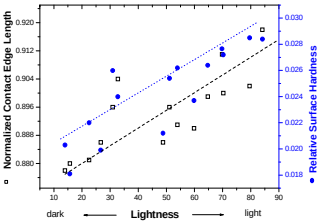

Figure 6: Changes in P5 and P8 as a function of lightness

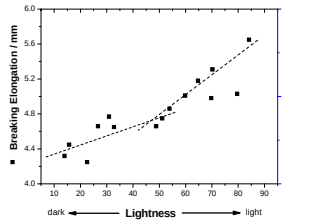

Figure 7: Elongation at break as a function of lightness

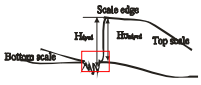

Figure 4: Sketch illustrating the damaged joint area between two scales

Fig. 5 shows that lighter colours influence P3 and P7 less than darker colours, which shows that darker colours cause more surface damage.
The change in P7 is related to the changes of the chemical structure of the fibre surface during dyeing due to the removal of fatty acids, which leads to damage of the epicuticle layer resulting in a more hydrophilic surface with a less homogeneous surface and therefore an increased surface roughness.
A change of P3 and P7 is clearly visible in the colour region of 30 – 45, which can be referred to as the physical separation between *light* (less surface damage, only in the epicuticle layer) and *dark* colours, where the damage reaches deeper into the endocuticle layer, or even into the cortex.

Fig. 6 shows a decrease of P5 and P8 as the colour becomes darker, which confirms the observation that the scale height increases after dyeing, especially for dark colours.
The decrease in P8 indicates that the extensive disulfide bonds in the cuticle layer were damaged, which are responsible for the high rigidity of the outer layer of undyed fibres [2]. As P8 decreases the damage goes deeper into the fibre, which affects the bulk properties, and results in a loss of fibre strength.
Lanasol dyed samples follow the same trend as Lanaset dyed samples, which indicates that the dye type does not influence these parameters.

The observations by AFM were confirmed by tensile measurements. Fig. 7 shows the breaking elongation as a function of lightness where the change in the gradient of the elastic behaviour from light to dark colours is clearly visible.

Conclusions

The results show that AFM is a viable tool to study the effects of different dyes on the surface of wool fibers and detect the surface modifications with great accuracy by measuring various parameters for the cuticle scales.
It was also possible to distinguish different lightness areas, which could be regarded as *dark* and *light* colours.

References

[1] T. L. Phillips, T. J. Horr, M. G. Huson and P. S. Turner, Textile Res. J., 1995, 65, 445-453.
[2] A. N. Parbhu, W. G. Bryson, and R. Lal, Biochemistry, 1999, 38(36), 11755-11761.
[3] J. Sikorki, A. Hepworth and T. Buckley, Applied Polymer Symposium, 1971, 18, 887-893.
[4] M. G. Huson, Textile Res. J., 1992, 62, 9-14
[5] B. Gullbrandson, Textile Res. J., 1958, 28, 965-968.

Acknowledgements

The authors would like to thank the International Centre for Macromolecules Chemistry and Technology in Libya for financial support.

TABLE OF CONTENTS

List of Abbreviations

A	The mean section scale width
a*	Redness-greenness dimension
AFM	Atomic force microscopy
ASTM	American Society for Testing and Materials
B	The mean length of the scale edge
b*	Yellowness-blueness dimension
BS	British standard
C	The length of a scale
CMC	Cell membrane complex
Cp	precision level
CRE	Constant rate of extension
F	Adhesive force
F/d curves	Force versus distance curves
IC-AFM	Intermittent-contact AFM
IF	Intermediate filament
IFAP	Intermediate filament associated proteins
HGT	Glycine–tyrosine-rich proteins
L*	Lightness-darkness dimension
LS	Low-sulphur proteins
k	Spring constant of the AFM cantilever
KAP	Keratin-associated proteins
NC-AFM	Non-contact AFM
P1	Cuticle scale height
P2	Step angle
P3 and Ra	Surface roughness
P4	Scale interval
P5	Normalized contact edge length
P6	Scale elongation
P7	Adhesive force
P8	Relative surface hardness

pH	Potential of hydrogen
SEM	Scanning electron microscope
SFM	Scanning force microscope
SPM	Scanning probe microscope
STM	Scanning tunnelling microscope
TEM	Transmission electron microscope
Tg	Glass transition temperature
UHS	Ultrahigh content of sulphur
US standard	United states standard
X	Displacement of the cantilever
3D	Three dimension

List of Figures

List of Tables

1 Introduction

Wool is one of the oldest textile fibres. Despite its limited availability and high cost it is still one of the most important natural fibres [1], although today it has become more of a luxury fibre. The advantage of wool fibres over artificial fibres is the natural feel and appearance of the fibre. Wool fibres can be successfully dyed into a wide array of colours. The thermo-physiological, sensorial and body-movement comfort of wool fabrics is directly influenced by the fibre structure and its properties. Conditions during processing and dyeing can have a detrimental effect on fibre structure, and consequently, the fibre properties [2].

Chemically wool can be regarded as a composite material consisting of mainly keratinous protein polymers. Keratin in wool is a mixture of chemically linked amino acids with strong hydrogen and covalent bonds [2]. Extensive studies of the morphology and mechanical properties of wool [3, 4, 5] have shown that it is a semi-crystalline polymer, in which crystalline fibrils, aligned along the fibre axis, are embedded in an amorphous matrix that is heavily crosslinked through disulphide bonds.

Microscopic magnification reveals that a wool fibre consists of cuticle and cortical cells linked to each other by the cell membrane complex. The cuticle cells are located on the outermost part of the fibre, forming a layer of scales overlapping one another [6, 7]. Each scale has edges pointing outward and towards the fibre tip. The size and shape of the scales can be used to identify different wool types and to investigate the effect of processing on the wool surface [6, 7].

The surface structure of wool fibres has a great influence on its characteristic properties and any damage to this layer can affect the final properties of the product. Micro-damage, (for example) which is caused by the wool opening process, affects the form of the fracture during tensile tests and leads to a loss in the strength of the wool fibre [8, 9]. The fracture is also influenced by the elastic modulus of the cuticle and the cuticle-cortex boundary, as well as the cortex layer [10].

One of the most important processing stages for fibres is the dyeing process, which gives the wool different colours. Unfortunately this process can lead to a loss in elasticity of the wool fibre, especially for dark colours, which means the fibre becomes brittle and breaks at small elongations under a small load [11, 12]. The loss in elasticity and breaking load and elongation are affected by the amount of damage that occurs on the fibre surface

during the dyeing process due to the action of acid, alkali, dyestuff, water, heat, and mechanical stress [12].

Studies concerning the influence of process parameters on wool properties [13] pointed out that scouring and dyeing cause the most damage to the surface of wool fibres. Four different types of damage to the fibre surface could be discerned: the formation of cracks, scale lifting, fibre breakage and formation of holes [14, 15]. Up to now, little effort has been made to study the changes in fibre topography resulting from either mechanical processing or chemical treatments, and various indirect methods have been used to investigate the fibre damage, such as physical tests of mechanical properties and chemical absorption of the fibre [16].

The main methods used to investigate the cuticle scale structure and possible damage to the scale structure involve direct microscopic observations with optical microscopy, scanning electron microscopy (SEM), transmission electron microscopy (TEM), and atomic force microscopy (AFM) [17-19]. AFM has been used to study wool fibres for the first time in 1995, when Phillips et al. [20] described the use of AFM to examine the surface of wool fibres. In the same year the effect of ultraviolet light on wool fibre surfaces was investigated with AFM [19].

In this study the correlation between the surface changes caused by dyeing, observed by AFM (direct method) and the loss in tensile strength (indirect method) after dyeing was investigated. The scale characteristics of a statistical significant number of dyed and undyed fibres were characterized by AFM. Several researchers [20- 22] have suggested that the measurement of these scale characteristics, such as scale height or scale angle, allow the distinction between different wool fibres, and the determination of surface damage and the effects of treatment on the fibre surface. But it has also been suggested, that measurements of these specific parameters are unreliable [15].

AFM offers several advantages over other techniques, since it is a quantitative, non-destructive technique and provides real three-dimensional information of the surface, while no sample preparation is required. Given the fact that textile materials are insulators, which means that they must be coated with a conducting layer in order to be examined by SEM, AFM shows a clear advantage as a characterization tool for textile fibres [7, 23].

1.1 Problem Statement

Wool fibres are usually dyed with reactive dyes (Lanasol) or metal complex dyes (Lanaset) at a temperature around 100 ºC. The company Hextex in Worcester found that fibres become brittle and tend to break during the manufacturing processes that follow dyeing, especially in the spinning process, which makes it very difficult to produce yarn with desirable strength. This reduces the quality of the final product and decreases its life time. This problem was noticed more often on dark colours and less on light colours [24].

The reasons for this phenomenon are still unknown and until now, the effect of dyes with different colour lightness on the fibres has not been investigated using microscopic techniques such as AFM or SEM. The damaged part of the fibre surface has not been clearly defined and the extent and nature of damage to this surface as a result of dyeing (especially in relation to the lightness value of the dye) has yet to be investigated.

A scientific investigation using AFM was therefore necessary to investigate the effect of dyes with different colour lightness on the fibre surface. Other properties, such as the fibre strength and extensibility were measured on tensile tester to investigate the overall change in the fibre properties.

1.2 Objectives

The objectives of this project were firstly to investigate the feasibility of AFM to characterise wool fibres entirely and to determine any type of surface damage that would occur during dyeing, (particularly for Lanasol reactive dyes and Lanaset metal complex dyes) and then classify the damage according to its severity. The scale characteristics of these fibres were determined by measuring several properties in order to differentiate various degrees of surface damage.

The second objective was to investigate the effect of the cuticle damage on the strength of the fibres and the breaking extension (stress / strain behaviour). In order to do this the data obtained from AFM of the surface features were regarded statistically, and then compared to results obtained from tensile tests on individual fibres, which describe the breaking strength and breaking extension of the bulk fibres.

The third objective was to identify the influence of depth of shade on the fibre damage and to study the effect of different dye concentrations on the surface changes and on the loss in the tensile strength. Various sources in the literature [9] and from industry [24] indicated a tendency for dark colours to cause greater damage than light colours. An

additional aim of this study was to determine the degree of the lightness value from which on the colour can be referred to as dark colour, this value can be used to distinguish between “light” and “dark” dyed colours according to its propensity to be damaged during dyeing. It was determined if one could discerns dark colour from light colours by measuring physical properties as a function of lightness.

The study was limited by the dependency on sample availability from the factory that supplied the dyed slivers for testing. In some areas a shortage of colours was experienced. This was overcome by dyeing raw fibres of the same lot with the desired colours in the laboratory. Blank dyed sample was also prepared, where the dyeing process was carried out in absence of the colorant materials. Another limitation was the nondisclosure of the chemical structure of the commercial dyes such as Lanaset dyes from Ciba Spezialitäten Chemie. This made a discussion of the results based on the chemical dye structure difficult or impossible.

1.3 Thesis Outline

In the theoretical background (chapter 2) the structure of wool fibres and their properties are discussed with a special focus on the fibre surface. A background of the dyeing process for wool fibres is also given in this chapter. The AFM and its operation and control modes as well as the tensile strength test method are described in chapter 3. The experimental chapter (chapter 4) describes the empirical part of the study, where the sample selection and the experimental design are described. The experimental work was performed in two stages. The first stage was the surface characterisation of the fibres by AFM. The second stage was tensile test measurements. In chapter 5 the data obtained from both techniques is statistically analysed in order to obtain acceptable information. All results obtained for dyed and undyed wool fibres are presented and discussed. Finally a conclusion is drawn from the obtained results and suggestions for future research are given in chapter 6.

1.4 References

1. S. J. Kadolph, A. L. Langford, N. Hollen and J. Saddler, *Textiles.* 1st ed., New York, Macmillan Publishing Company, 2002. p. 50.
2. A. R. Horrocks and S. C. Anand, *Handbook of Technical Textiles.* 1st ed., England Cambridge, Woodhead Publishing Ltd. and CRC Press LLC, 2000. p. 25.
3. F. J. Wortmann, B. J. Rigby, and D. G. Philips, *Glass Transition Temperature of Wool as a Function of Regain*. Textile Res. J., 1984. 54: p. 6-8.
4. J. R. Cook and B. E. Fleischfresser, *Ultimate Tensile Properties of Normal and Modified Wool.* Textile Res. J., 1990. 60(1): p. 42-49.

5. M. Feughelman, *A Model for the Mechanical Properties of the α-Keratin Cortex.* Textile Res. J., 1994. 64(4): p. 236-239.
6. J. Sikorki, A. Hepworth and T. Buckley, *Scanning Electron Microscope Techniques in Wool Research and Processing.* John Wiley & Sons, Inc., Appl. Polym. Symp., 1971. 18: p. 887-893.
7. P. Jovanèiæ, P. Erra, J., R. Molina, D. Jociæ and M. R. Julia, *Study of Surface Modification of Wool Fibres by Means of SEM, AFM and Light Microscopy*. Eur. Microsc. Anal., 1998. 51: p. 15.
8. A. A. Gharehaghaji, N. A. G. Johnson and X. Wang, *Wool Fibre Microdamage Caused by Opening Process, Part III: In Situ Studies on the Tensile Failure of Damage Induced Fibres.* Journal Text. Inst, 1999. (part 1 and 2), (90): p.1-34.
9. W. Yu, R. Postle and H. Yan, *Characterization of the Weak Link of Wool Fibres*. J. Appl. Polym. Sci., 2003. 90(5): p. 1206-1212.
10. M. W. Andrews, *The Fracture Mechanism of Wool Fibres under Tension.* Textile Res. J., 1964. 34(10): p. 831-835.
11. M. G. Huson, *The Mechanism by Which Oxidation Agents Minimize Strength Losses in Wool Dyeing*. Textile Res. J., 1992. 62(1): p. 9-14.
12. B. Gullbrandson, *Fibre Damage in the Stock-Dyeing of Wool*. Textile Res. J., 1958. 28(11): p. 965-968
13. C. Popescu, J. Chelaru, C. Magrini, S. Pall and V. Corneanu, *Influence of Technological Processes on Tear Strength of Finished Wools*. Textile Res. J., 1985. 55, p. 72-74.
14. M. E. Campbell and H. Baumann, *Surface Topography of Blank Dyed Merino Wool.* Textile Res. J., 1981. 51(1): p. 52-54.
15. T. Baba, N. Nagasawa, H. Ito, O. Yaida and T. Miyamoto, *Recovery of Surface Properties of Damaged Wool Fibres*. Textile Res. J., 2001. 71(10): p. 885-890.
16. E. J. Wood, P. Stanley-Boden and G. A. Carnaby, *Fibre Breakage during Carding, Part II: Evaluation*. Textile Res. J., 1984. 54: p. 419-424.
17. D. H. Tester, *Fine Structure of Cashmere and Superfine Merino Wool Fibres*. Textile Res. J., 1987. 57: p. 213-219.
18. F.-J Wortmann, and W. Arns, *Quantitative Fibre Mixture Analysis by Scanning Electron Microscopy, Part I; Blends of Mohair and Cashmere with Sheep's Wool,* Textile Res. J., 1986, 56: p. 442-446.
19. J. W. S. Hearle B. Lomas and W. D. Cooke, *Atlas of Fibre Fracture and Damage to Textiles.* 2nd ed., University of Manchester Institute of Science and Technology, 1998, P 20-21.
20. T. L. Phillips, T. J. Horr, M. G. Huson, P. S. Turner and R. A. Shanks, *Imaging Wool Fiber Surface with a Scanning Force Microscope.* Textile Res. J., 1995. 65(8): p. 445-453.
21. F.-J. Wortmann, and K.-H. Paba, *Cuticle Scale Heights of Wool and Specialty Fibres and Their Changes Due to Textile Processing.* Textile Res. J., 1999. 69: p. 139-144.
22. J. R. Smith, *A Quantitative Method for Analysing AFM Images of the Outer Surface of Human Hair.* J. Microsc., 1998. 191: p. 223-228.
23. P. A. Tucker, *Scale Height of Chemically Treated Wool and Hair Fibres*. Textile Res. J., 1998. 68(3): p. 229-230.
24. E. Lesch, Dyeing Manager, Hextex Company in Worcester, *Personal Conversation*. 2005. E-mail: elesch@romatex.co.za, Tel: (27) 23-3470814, Fax: (27) 23-3476117.

2 Theoretical Background

2.1 Structure of Wool Fibres

Wool is one of the first fibres that was spun into yarn and woven into cloth and used to be one of most widely used textile fibres. Today it has become more of a luxury fibre. Due to its unique natural properties, wool fibres have been popular in commodity and specialised textile products for the last 2000 years [1, 2]. The importance of wool fibres lies in its combination of properties, which are unequalled by any other fibre, such as elasticity, water absorption, felting and dyeing qualities [3]. Today many other natural or artificial textile fibres are used, but as yet science has not been able to produce fibres containing all the natural properties of wool [1]. Scientific and technological necessity has led to the accumulation of a great deal of knowledge about the structure of wool. In the past 70 years, extensive investigations have been carried out on the structure of wool fibres, using optical microscopy, infra-red spectroscopy, X-ray diffraction, electron microscopy and atomic force microscopy [4-12]. The general structure of animal fibres was established in the 1950s and was reviewed by Sikorski, Bendit and Feughelman [13-16].

2.1.1 Chemical Composition

Wool fibres are biological composite materials consisting of regions of morphological components that differ from each other both physically and chemically [17]. The obvious heterogeneity of the wool fibre led to attempts to separate different cell components and to look for chemical differences. Thus as early as 1952 evidence was obtained that showed that the cuticle (Fig. 2.5) of wool contained more sulphur than the cortex (Fig. 2.6), a finding that has since been confirmed repeatedly [18]. In water-free wool, 97 % of the weight consists of wool proteins, the remainder is made up of 2 % structural lipids and 1 % mineral salts, nucleic acids, and carbohydrates (wax). The bulk of the material forming keratins consists of a number of amino acids, which are linked through amino and carboxyl groups to form a polypeptide chain of the following form:

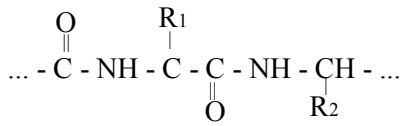

Figure 2. 1: Polypeptide polymer chain

where R_1 and R_2 are the side chains of the amino acids with twenty different varying proportions [19, 20]. Chemical analysis has shown that the protein of a wool fibre consists

of 50.5% carbon, 6.8 % hydrogen, 22.0 % oxygen, 16.5 % nitrogen, 3–4% sulphur and 0.5% ash, where the ash contains other elements, such as potassium, sodium, calcium, silicon, sulphate, and chloride [19, 21]. The proteins with low sulphur content represent 50 - 60 % and the high sulphur proteins 20 - 30 % of the wool fibre [18]. The high sulphur content is due to the high content of cystine [22], a double amino acid containing two sulphur atoms in a disulfide bond:

HOOCCH(NH2)CH2 - S - S - CH2CH(NH2)COOH

Figure 2. 2: A disulfide bond in the amino acid structure

The structural lipids, in contrast, are components of the cell membrane complex, which bind together the cuticle and cortex cells [8, 23].

Wool can act either as an acid or an alkali, which means that both alkalis and acids will react with it, therefore the wool fibre is considered as amphoteric [19, 24]. The amino acids are classified in five groups: acidic amino acids, basic amino acids, amino acids with hydroxyl groups, sulphur-containing amino acids, and amino acids with no reactive groups in the side chain. The free amino groups at the ends of the peptide chains result in the cationic character, and the anionic groups are present as dissociated side chains of aspartic and glutamic acids and as carboxyl end groups [25]. The amino groups of lysine, histidine, the amino end groups, and the thiol groups of cystine are possible sites for the covalent attachment of reactive dyes [19]. The side chains, which account for about 50 % of the protein material in the wool fibre, interact with each other to form several different kinds of non-covalent and covalent bonds or interactions, which stabilize the peptide by forming links between the chains and rings within a chain [16, 19].

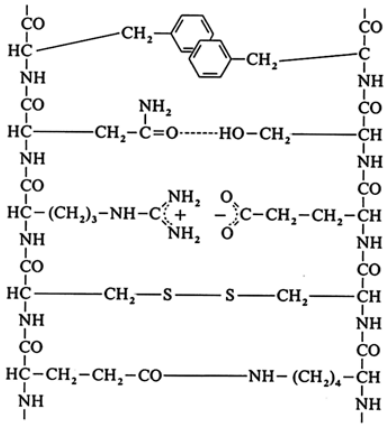

Figure 2. 3: Possible covalent and non covalent bonds between two keratin chains [19].

The three-dimensional structure of wool proteins is stabilized by a wide variety of electrostatic interactions between amino acid constituents. Figure 2.3 shows hydrophobic

interactions, hydrogen bonds, a salt bridge or electrostatic bonds, a disulfide bridge, and an isodipeptide bridge [22]. According to Weigmann and Dansizer [26, 27] the fibre cannot be stabilized in an extended state by the formation of covalent crosslinks unless the crystallization of beta-crystallites is permitted. On the other hand, the extended state of the fibres cannot be stabilized by the formation of beta-crystallites unless this configuration is supported by the formation of stable covalent crosslinks.

The matrix proteins are collectively classed as intermediate filament associated proteins (IFAP). As many as a hundred different proteins are found in the matrix, of which three general classes have been distinguished: the sulphur-rich proteins, proteins with an ultrahigh content of sulphur (UHS), and the glycine–tyrosine-rich (HGT) proteins. A detailed account of the occurrence and characterization of IFAP in trichocyte keratins has been given by Gillespie [29] and Powell and Rogers [30]. The filament proteins, initially referred to as low-sulphur proteins (LS), are members of this family and have several features that make them structurally and functionally unique [28]. The keratins in wool originate from microfibrils, which together with some other protein filaments are classified as intermediate filaments [13, 31].

2.1.2 Wool Fibre Morphology

Morphologically, wool fibres consist of two components, outside layers of protecting cells, called cuticles, which enfold the cortex that consists of elongated cells lying parallel to the fibre axis [18, 32]. The cuticle and the cortical cells are linked to one another by the cell membrane complex (CMC) [33, 34].

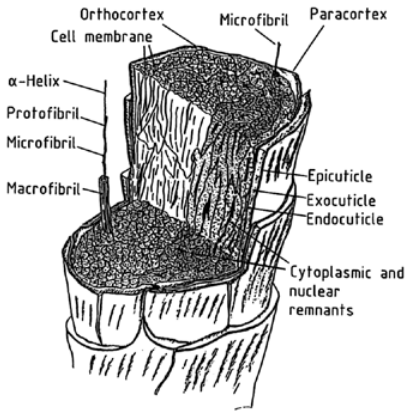

Figure 2. 4: Longitudinal and cross section of a fine merino wool fibre [19]

In coarse fibres, there is also a central medulla. Figure 2.4 shows the general composition of wool fibres, and shows more clearly the major structural features found in the cortical cells of a wool fibre.

2.1.2.1 The cuticle cells

The cuticle cells, which are about 1 μm thick and plate-shaped, form the outer part of the fibre surrounding the cortical cells in layers of flat scales peripherally overlapping one another [34, 35]. Each type of animal fibre has a characteristic scale pattern, by which they can be described. This entails the scale interval, step height, cuticle interface angle and surface roughness [36-39]. These characteristics provide good identification features, although they vary along the length of one fibre [40, 41].

In wool, the cuticle layer is only one scale in thickness over most of its area, except where one scale ends and another commences. All the scales point in the same direction: outwards along the fibre towards the tip. As most animal fibres, the surface of the wool fibre has a serrated appearance when examined under the microscope, though the scale patterns differ depending on the parent animal. This difference is very small and makes fibre identification a very skilled and tedious task [19, 24].

Each cuticle cell is formed by three layers of different cystine and isodipeptide contents: the epicuticle, exocuticle (A- and B- layers in Figure 2.5), and endocuticle [4, 34]. The cell membrane complex lies between overlapping cuticle cells [42]. The existence of a thin chemically resistant layer, the epicuticle, close to the surface of all undamaged mammalian keratin fibres, has been known since 1916 [4], but the identification of such a specific structure within the cuticle has remained elusive. Recently, through transmission electron microscopy investigation of stained transverse sections of wool from various animal species, the epicuticle has been tentatively identified [32], and it was showed that the epicuticle membrane is 5-7 nm thick [43] and consists of about three quarters proteins and one quarter lipids [44, 45], including covalently bound 18-methyleicosanoic acid [46], as schematically summarized in Figure 2.5

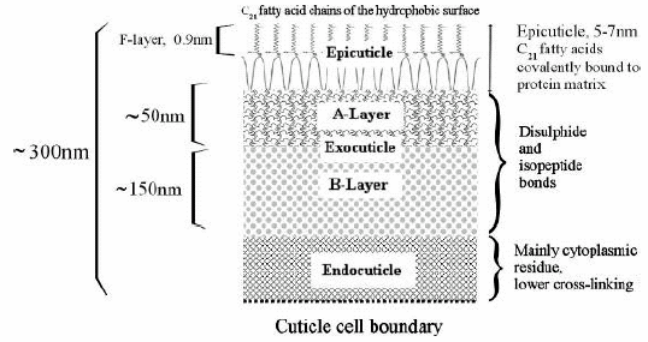

Figure 2. 5: Diagram of the layered structure of the cuticle cell [34]

The protein component contains around 12% cystine and the lipid component is a mixture

of fatty acids, predominantly 18-methyleicosanoic acid (18-MEA), covalently bound to proteins by means of cystine residues [44, 47]. Fatty acid chains are oriented away from the fibre to produce a "polyethylene-like" layer at the fibre surface [35]. This is why wool is known to have a hydrophobic water-repellent surface even after removal of the wool grease. However, the epicuticle has microscopic pores through which water vapour can permeate into the internal structure of the fibre [20].

Beneath the epicuticle lies the exocuticular layer. This compact amorphous keratin constitutes about half of the cuticle. The endocuticular layer consists of modified cellular residues and is resistant to alkali extraction but not to proteolytic enzymes such as trypsin and papain [18].

2.1.2.2 The cortex

The cortex forms the principal body of the wool fibre [48] and comprises more than 90 percent of the total weight of fine wool fibres. It consists of small spindle-shaped cells that are in turn consisting of fibrils, which are oriented along the length of the cell [49]. This layer is enclosed by the cuticle layer [20]. The inner part of the wool fibre is divided into two different parts: the paracortex and the orthocortex (Figure 2. 6).

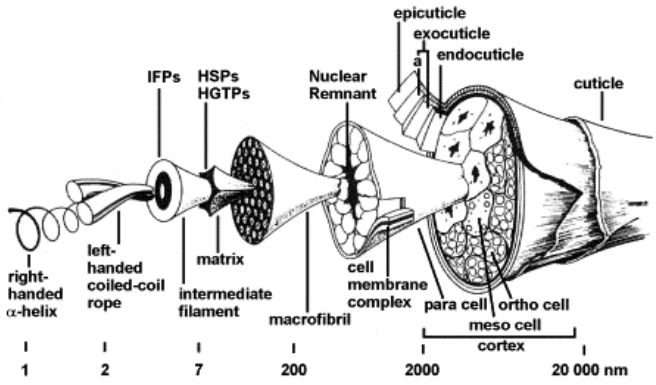

Figure 2. 7: The major structural features found in the cortical cells of wool fibre [50].

The growth of wool fibres is asymmetric, as the hardening of the paracortex begins earlier than the hardening of the orthocortex. This asymmetry results in a crimp that is typical for wool. The composition of the orthocortex is looser than that of the paracortex, which causes the greater ability of the orthocortex to absorb water. If wool gets wet, the crimp increases, and the coiled springs of molecular chains contribute to the fibre's resilience. In addition to the ortho and para, there are meso-cells, which differ in their cystine content and staining behaviour with silver salts [24, 40, 51].

The chemical compositions of the orthocortex and the paracortex in the mature fibre are

substantially different. Transmission electron microscope studies of thin sections of fine Merino wool have shown that the mode of assembly of the IF into macrofibrils is quite different in the two types of cortical cells. In the paracortex the macrofibrils are large, irregularly shaped, and the predominant mode of IF packing is quasi-hexagonal [52] (Figure 2.7a), whereas in the orthocortex the macrofibrils are smaller and approximately cylindrical in cross-section (Figure 2.7b), and the fibrils are packed in circular sheets around a central core. Coarser wool fibres have less clearly aligned arrangements of ortho- and para-cells [53, 54]

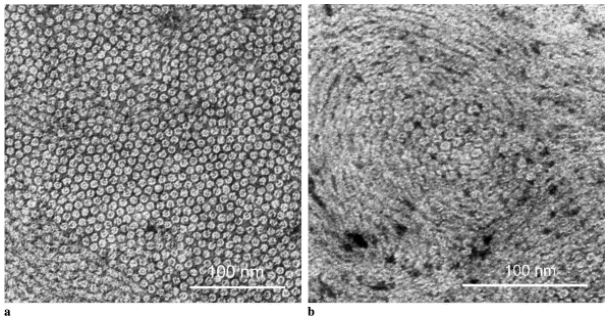

Figure 2. 8: Cross-sections of fine Merino wool illustrating: the quasi-hexagonal packing of the IF observed in (a) the macrofibrils of the paracortex; (b) macrofibrils in the orthocortex [54].

The cortex contains fibril-structured keratin proteins, which have a large molecular size, and amorphous keratin polymers, which have a smaller molecular size. Microfibrils are organized to form macrofibril structures, which are held together by amorphous proteins.

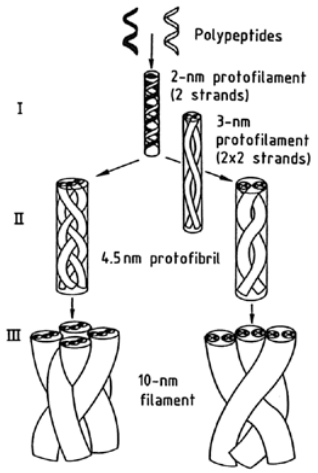

Figure 2. 9: Schematic representation of the three distinct levels of fibrillar organization in keratin filament assembly and architecture [19].

A cortex cell of wool contains around 5 – 8 macrofibrils. Between them are cytoplasmic and nuclear remnants of keratinocytes. A macrofibril is a bundle of 500 – 800 keratin intermediate filaments (microfibrils). Keratin-associated proteins (KAP) are intercalated, enveloping individual microfibrils and their aggregates [9, 54]. An individual microfibril

consists of protofibrils, which again consist of protofilaments (Fig. 2.8).

2.1.2.3 The medulla

The medulla is a hollow canal in the centre of the fibre [55] with a skeleton of amorphous proteins and fine filaments [19]. In coarser wool fibres, the medulla may occupy up to 90% of the cross-sectional area, whereas in fine wool fibres, the medulla is small and may be discontinuous along the length of the fibre [48]. The cuticular and medullary tissues contain specific protein constituents, which might play an important part in the behaviour of the wool fibre during the processing and application.

2.1.3 Molecular Form and Packing in Wool

Two different crystal structures of keratin can be observed with x-ray diffraction, which represent two different chain conformations. In ordinary un-stretched wool fibres, α-keratin prevails, which shows the diffraction pattern of α-helices. But if wool is stretched, there is a gradual and reversible transformation to a form known as β-keratin [56-58].

In α-keratin, the peptide chains are twisted like a right-handed helix, Figure 2.9.

Figure 2. 10: α -helix structure of α-keratin suggested by Pauling [19].

The α-helix is stabilized by intramolecular hydrogen bonds and intra-helical salt linkages [59-61]. It contains 18 amino acid units in five turns, in other words 3.6 amino acid units per turn. In the β-keratin structure, the peptide chains are largely stretched to form what is called a pleated sheet structure, each sheet has hydrogen bonds between the peptide groups of opposing chains (Fig. 2.10). The sheet is folded along the –CHR groups of the polymer chains [60-62].

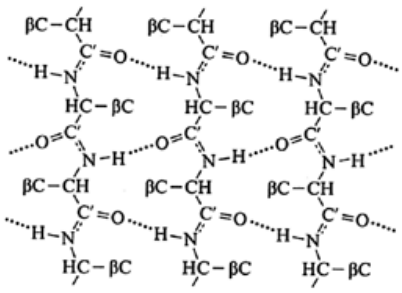

Figure 2. 11: Pleated sheet structure of β-keratin [19].

2.1.4 Two-Phase Model

In order to simplify the complex morphological and molecular structure of wool and interpret properties such as the elasto-mechanical behaviour of wool fibres, Feughelman [63, 64] suggested a two-phase model. He proposed that the wool fibre consists of a water-absorbing matrix, in which non water-absorbing cylinders are embedded. Table 2.1 shows the morphological structures of the wool fibre split into the most important components.

Table 2. 1: Two-component (phase) structures of the wool morphology [19].

Composite system	Type	Component 1	Component 2
Wool fibre	ring/core structure	cuticle	cortex
Cortex	filament in matrix	cortex cell	cell membrane complex
Cortex cell	filament in matrix	macrofibrils	intermacrofibrillar matrix
Macrofibril	filament in matrix	microfibrils	intermicrofibrillar matrix

The elastic-mechanical behaviour of wool fibres is satisfactorily represented by the simple two-phase model. The difference in the degree of order between the components, which form the wool fibre, is the reason for differences in elastic properties. About 30 % of the wool fibre is crystalline if only the α-helical crystal is taken into account. The other components make up the non-crystalline phase, which includes the cuticle, the cell membrane complex, the intermacrofibrillar and the intermicrofibrillar matrix [57, 65]. When the fibre is stretched in the linear-viscoelastic region, the behaviour of the crystalline phase is linearly elastic in contrast to the non-crystalline matrix, which is linearly viscoelastic.

2.2 Wool Characteristics

The complex internal structure of wool fibres is already well known, and current studies in this area are aimed at determining the impact of each structural component on the fibre properties. Wool fibres without medulla have a density of 1.31 g/cm^3 at 25 °C and 65 % relative humidity. The average fibre diameter varies between 16 and 40 µm and the average fibre length between 2.5 and 25 cm, depending on type and origin. Every wool fibre has a natural elasticity and wave or crimp that allows it to be stretched about one third of its lengths and then spring back into place [66]. However wool fibres have certain properties, which distinguish them from all other raw textile materials and can not be equalled by any other manufactured fibre: the ability to be shaped by heat and moisture, good moisture absorption, excellent heat retention, water repellence and flame-retardancy [67]. These properties are common to all wool fibres, whether coarse or fine. The following four basic properties will be discussed

1) surface characteristics
2) water absorption
3) mechanical properties and
4) chemical properties.

2.2.1 Surface Characteristics

The cuticle of wool fibres is obviously of great practical importance since it forms the interface between the fibre and the environment, including chemical processing media and the wearer of the product. A better understanding of the surface properties of wool fibres might promote new product development of wool. The microscopic appearance of wool is sufficiently characteristic to distinguish it from all other fibres, and the scales on the surface of the fibre can easily be discerned. Each wool fibre has small scales on the surface, which, together with other structural features determine the surface properties [68]. The exact nature, structure and arrangement of the scales differ considerably for different varieties of wool. In fine merino wools, for instance, the individual scales are in the form of cylindrical cusps, one somewhat overlapping the other. In other varieties of wool, on the other hand, two or more scales occur in the circumference of the fibre. Because of the cuticle scales on the fibre surface, entanglement and felting may occur during processing, which is seen as a defect, as it causes shrinkage. On the other hand softer yarns can be produced from wool because of the gripping effect of the surface

scales [16].

The outermost layer of proteolipid material on the surface of the cuticle cells (or scales) is chemically bound to the wool surface [69] and it plays an important role in controlling the diffusion rate of dyes into the wool fibre. The understanding of the chemical structure of this layer can help in the development of new techniques to manipulate the surface of wool fibres.

There are many benefits to be gained from manipulating the wool fibre surface, such as the development of a new generation of improved low-add-on, shrink-resistant processes and an increase in the rate of the dyeing process [70]. This will be especially important in future as restrictions on chemical processes are tightened due to environmental concerns [71, 72].

The number of scales per mm for Merino fibres with a diameter of 25 μm is 72, and the scale height might reach up to 1.3 μm [73]. Some researchers [41, 74] have suggested that the measurement of the scale height, scale edge angle and other scale characteristics allows the distinction between different wool fibre types, as well as investigation of the surface damage and the effect of the treatment process on the fibre surface. It has, however, also been suggested, that measurements of these specific parameters can be unreliable [75].

The fibre surface can be damaged by processing as explained by Andrew et al. [76], who found that fatty acids are removed by the dyeing process, leading to a decrease in the resistance of the surface to acetic acid, water and other treatment chemicals. Studies have shown that fibre processing results in damage to the fibre surface, such as the formation of cracks and holes, scale lifting, and fibre breakage [75]. The amount of scale lifting has been related to an increase in dye susceptibility [77]. The cuticular material is largely amorphous and highly crosslinked, mainly with disulphide bonds, which are very susceptible to degradation at high dyeing temperatures [41].

The strength of the wool fibre was found to be affected by the degradation of the wool surface during the dyeing process, which leads to a breakdown of cystine linkages and hydrolysis of peptide chains to form shorter chains with thiol groups. This leads to surface damage or micro-damage of the wool fibre [78]. The cuticle layer has a great effect on the fracture, according to Andrew's research [79]. He pointed out that pieces of cuticle frequently projected from the broken fibres, indicating that the fracture is influenced by the cuticle or the cuticle-cortex boundary. Transverse micro-cracks develop to grow into

larger cracks during tensile testing. The micro-cracks initiate at critical points, such as natural micro-voids, within the fibre and the weak region at the root of overlapping scales where the stress is concentrated. Another characteristic feature is the craze, a special form of transverse crack, which eventually grows rapidly and becomes a rupture site [80].

2.2.2 Water Absorption

Wool can absorb moisture up to 30% of its weight without feeling damp or clammy. This makes wool feasible for all climates since it aids the body's cooling mechanisms as it allows moisture from the skin to evaporate [81]. Although wool is hygroscopic, its surface is hydrophobic and therefore difficult to wet [82]. The scales on the outside of the fibre cause liquid to roll off the surface of the wool fabric [83].

The amount of absorbed water depends on the relative humidity, temperature, and the history of the wool [84]. An increase in the amount of absorbed moisture from 0 % to 33 % leads to a longitudinal swelling of 2 % and a radial swelling of 16 %. The degree of fibre swelling is the lowest at the isoionic point (pH 4.9), at which there is no excess of ionic groups. Above and below this point, the number of stabilizing salt bridges decreases and the wool carries excess negative or positive charges, which cause electrostatic repulsion of the peptide chains, thereby increasing the swelling.

Many physical and mechanical properties of wool depend on its moisture content, which has two important effects. Increased moisture decreases the strength and lowers the glass temperature of wool [21, 85]. Thus, for example, dry, undamaged wool has a tensile strength of 150 – 200 N/mm^2 in its initial state, whereas a wet fibre has a tensile strength of only 70 – 80 % of this value. While the tensile strength of wool decreases with increasing moisture content, the fracture strain increases. The relative humidity of the atmosphere must therefore be controlled to ensure optimum processing and to obtain correct results during fibre testing such as tensile tests [86, 87].

The temperature dependency of the physical properties of wool water systems has been investigated by many authors using a variety of methods [88, 89]. Knowledge of the glass transition temperature T_g of wool [89] as a function of the water content is of central importance for understanding its viscoelastic properties, especially under the varying conditions of moisture content and temperature that can exist during the manufacturing of wool.

2.2.3 Mechanical Properties (Stress / Strain Behaviour)

Wool is characterized by a high extensibility and relatively low breaking strength. It has very unusual elastic properties, particularly when the fibre is wet [87]. Wool has a natural elasticity, greater than that of any other fibre, which makes it comfortable to wear because it fits the shape of the body. The ability of wool to recover its original length after stretching is very high compared to other fibres. Under certain controlled test conditions wool will recover 89%, and cotton fibres only 45% [16]. A dry wool fibre can be extended by about 30 %. When wet it will stretch by between 60 and 70 % [57, 66].

As mentioned before, an extensive study of the mechanical properties of wool was carried out by Feughelman et al. [14, 90, 91]. Other elaborate investigations were performed by other researcher groups, such as designing a tensile test stage can be used under SEM to observe the surface changes of the fibre in the different stages of elongation until fracture [92]. They recognized that a crack developed in the cuticular cell until the cortical cell was exposed and that the cuticle then slid over the cortex after the breakdown of the intercellular cement between the cortex cells [92]. In addition to that Gharehaghaji et al. [93] reported the effects of wool fibre microdamage, caused by the wool opening processes, on the tensile fracture, using scanning electron microscopy.

A typical stress – strain curve, as displayed in Figure 2.11, can be divided into three regions, which are affected to different extents by increasing humidity.

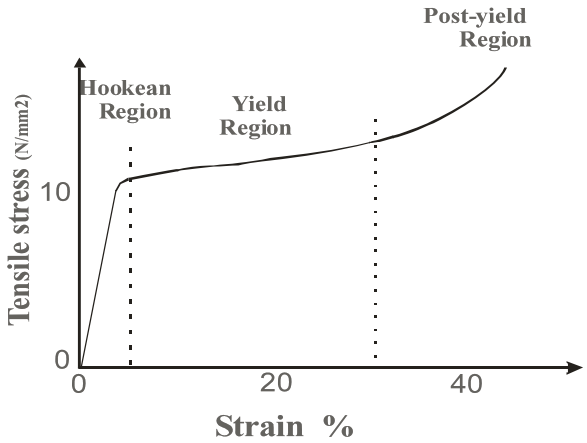

Figure 2. 12: Mechanical behaviour of a wool fibre extended at a constant rate.

After decrimping, the tension in the fibre increases rapidly and almost linearly up to a strain of 1 – 2 %. This initial region is referred to as the "Hookean region". The second section of the curve is known as the yield region, which ends at an elongation between 25 and 30 %. The third region of the stress – strain curve is known as the post-yield region, and is terminated by the rupture of the fibre. In this section of the curve, the increase in tension that accompanies an increase in elongation is larger than that of the second section [59, 94]. The Young modulus determined from this curve ranges from 3.52 to 5.40 GPa [19].

This deformation can principally be explained by the arrangement of the covalent disulfide bonds and the transformation of the α-helices into an unfolded form (α→ β transformation) [62]. In the Hookean region the bonds stretch and the bond angles deform [57]. Above 2% strain the fibre yields and the α-helix begins to unfold [95]. The unfolding however, is not completed and the fibre breaks at an extension of 50-70% [21]. Weigmann and Dansizer [26, 27] studied the role of the disulfide interchange in the fibre deformation, particularly at the turnover point from the yield to post yield region. The unique role of the disulfide linkage interchanges mechanism, which is catalyzed by sulfhydryl groups, can be described as follows:

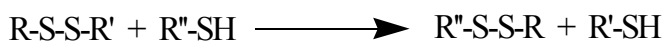

Figure 2. 13: Disulfide linkages interchange mechanism.

The strength of wool fibres is influenced by the proportions of the different classes of cortical cells present, and the protein composition [59]. The content of matrix proteins may influence some mechanical properties of fibres during compression [96]. The fibre cuticles contain few filaments and are rich in proteins that are similar to the ultra-high-sulphur proteins of the cortex [97]. It is not considered that the cuticle contributes significantly to the longitudinal mechanical properties of wool fibres, but any damage in this layer could lead to a stress concentration and a subsequent loss in the fibre strength. The cell membrane complex forms a continuous network that acts as an adhesive between the individual cuticle and cortical cells. Longitudinal extension may lead to preferential fracture along the cell boundaries, but the exact contribution of the cell membrane complex to the longitudinal strength of fibres is not known [59, 98].

2.2.4 Chemical Properties

The most important chemical characteristics of wool related to this work are the dye ability, the effect of heat, and the action of acids and alkalis especially during the dyeing process. Wool absorbs many dyes deeply, uniformly, and directly without the use of chemicals and the range of colours is limitless [55, 99]. This property allows wool to assume beautiful and rich colours when dyed. The scales on the surface of the wool fibre tend to diffuse light resulting in less reflection and a softer colour. Because the proteins in the core of the fibre are reactive, they can absorb and combine with a wide variety of dyes. This means that the wool holds its colour well as the dye becomes part of the fibre [66].

2.3 Dyeing of Wool Fibres

Textile finishing consists of a variety of processes that improve the appearance, texture or performance of a textile material. The dyeing process is usually the first finishing step, which involves chemical, mechanical and thermal treatment [99]. Textiles derive their colour from colorants. The two types of colorants are dyes and pigments. Pigments are insoluble, micrometer-sized colour particles that are usually held on the surface of a fibre by a binding agent, which works like glue [67, 100]. Dyes on the other hand are substances that add colour to textiles, and they can be dissolved in water or some other carrier in order to penetrate into the fibre [67]. They are incorporated into the fibre by a chemical reaction, absorption or dispersion.

The dye exhaustion, fixation and levelness depends on several factors, such as the fibre properties, the molecular structure of the dye and the medium of the dye-bath [101]. In recent years, many attempts have been made to improve various aspects of dyeing, and new technologies have been developed to reduce the fibre damage, decrease the energy consumption and increase the productivity.

Dyeing of wool can take place at any of the following three processing stages;

1) immediately after scouring and before spinning (stock dyeing), [67, 100]

2) after spinning but before fabric construction (yarn dyeing) [67] and

3) after fabric formation e.g. knitting or weaving (piece-dyeing).

Garment dyeing is also possible if the fabric had been previously shrink-resist treated [102].

2.3.1 Chemical Constitution and Colour of Dyes

If white light is spread out by a prism, it can be observed that it is composed of different colours. Each colour corresponds to a different wavelength. The colour of a compound depends on the wavelength of light that is absorbed. If a compound does not absorb any visible light it will appear colourless. If a compound absorbs light the human eyes will perceive the complementary colour, because the light that reaches the eye is missing the absorbed wavelengths [103]. Table 2.2 shows the wave lengths the absorbed light and the resultant colours.

Table 2. 2: Relationship between absorbed wavelengths and the colour [55].

Wavelength of light, nm	**Colour (absorbed light)**	**Complementary colour**
400-440	violet	green-yellow
440-480	blue	yellow
480-490	green-blue	orange
490-510	blue-green	red
510-530	green	purple
530-570	yellow-green	violet
570-580	yellow	blue
580-610	orange	green-blue
610-700	red	blue-green

The ability of a dye molecule to absorb light depends on the presence of chromophores, which are largely responsible for its colour. A chromophore is usually an extended conjugated system, particularly with different resonance contributing forms. If there is a conjugated system, with only C=C bonds, a long chain of conjugated bonds is required to result in a coloured system as illustrated in the following table [104].

Table 2. 3: Relationship between the coloured system and the conjugated bonds

H-(CH=CH)n-H	
n =	**Absorbed wavelength (nm)**
1	180
2	217
3	268
4	310
5	335

The ultimate conjugated system is graphite (Figure 2.13), which contains large sheets of fused rings and is black because it absorbs all wavelengths of visible light.

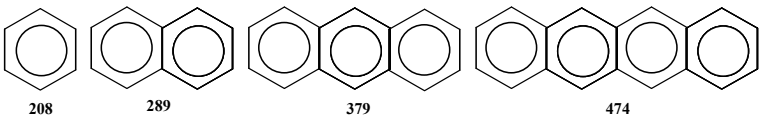

Figure 2. 14: Possible aromatic groups found in the graphite structure and their absorbed wavelength

Chromophores contain unsaturated groups, such as C=O and -N=N-, which are often part of extended delocalized electron systems involving aromatic rings [105]. Smaller molecules can be coloured if they have polar functional groups. One example of this is the Chrysoidine dye shown in Figure 2.14, where two NH_2 groups interact with the chromophore to produce orange colour.

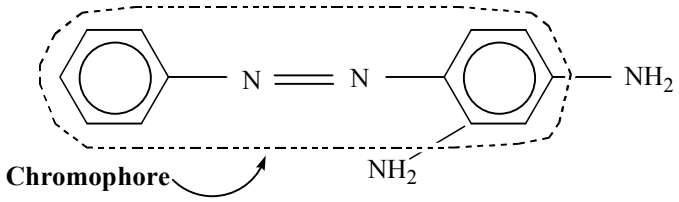

Figure 2. 15: A basic dye molecule, called Chrysoidine [82]

The relation between colour and constitution is explained based on the behaviour of electrons in molecular orbitals in literature [82]. Other functional groups may be added to the dye structure in order to:

1) modify or enhance the colour of the dye,
2) make the dye more soluble in water and
3) attach the dye molecules to the fibres of the dyed object, in reactive dyes.

2.3.2 Colour Identification

Colour can be identified by three factors: colour name, saturation and lightness. The colour name is the distinction between classes of colour; e.g. red, yellow-blue, blue etc. This is referred to as hue. The colour saturation indicates the strength of the colour, or the amount of pure colour present. It is the distinction between, for example, a pale green and a dark green. The pale green would have a low degree of green saturation, while the dark green would have a high degree. The colour lightness indicates the amount of light that is reflected. The lighter the colour is, the more light is reflected. In other words, a darker colour reflects less light. It is the distinction between, for example, white and black. White is the lightest colour, and black is the darkest. The term "value" is sometimes used instead of lightness [55, 106].

The lightness of the colour can be measured with a spectrophotometer or a colorimeter. These instruments respond to the spectral distribution of light in the same manner as the

human eyes do and they provide rapid and precise measurements and make it possible to quantify colour differences. Differences between similar colours can be determined by considering the three values L*, a* and b* as coordinates in a three-dimensional colour space as it is illustrated in Figure 2.15 [55]. In this colour space, L* refers to the lightness-darkness dimension, a* refers to the redness-greenness dimension and b* refers to the yellowness-blueness dimension.

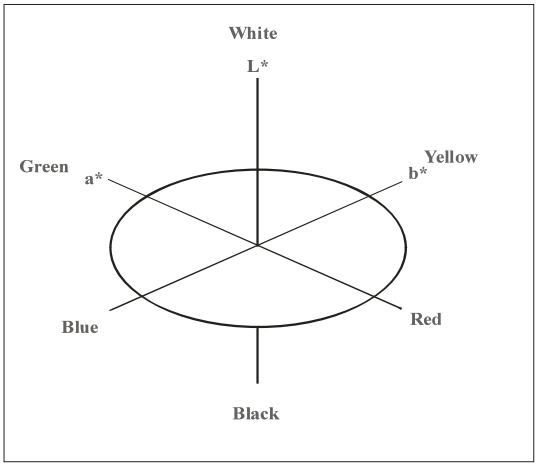

Figure 2. 16: Three dimensional colour space [107].

L* can assume values between 0 (black) and 100 (white), which will be used in this study to arrange the dyed wool samples according to their lightness [55, 108].

2.3.3 Theory of Dyeing

The theory of dyeing includes a number of inter-related factors such as surface and colloid chemistry and biochemistry [109]. Because of this no unified theory of dyeing has been developed so far, which accounts for all the observed phenomena. In addition to this, the thermodynamic and the kinetic aspects of processes occurring within the dye bath are also important. These involve the interaction between the dye molecules and the external and internal wool fibre surface, the transfer of the dye molecules from the external to the internal fibre surface, the transfer of the dye molecules from these surfaces by diffusion processes to the inner part of the fibre and finally the subsequent behaviour of the dye, once equilibrium has been achieved [110, 111].

Generally the dyeing process of textile materials is divided into four fundamental stages:

1) Diffusion in solution: In this stage dye molecules are transported through the solution to the solid-liquid interface.

2) Adsorption on the fibre surface: Dye molecules are attracted to the fibre surface and adsorbed (phase boundary).
3) Diffusion into the fibre: Diffusion of the dye molecules from the surface into the fibre. The dye molecules migrate from place to place on the fibre due to the high concentration of the deposited dye on the surface [107].
4) Fixation of the dye at specific sites in the wool fibre [112, 113].

It is assumed that the dye molecules in solution are adsorbed on the substrate surface and diffuse into the substrate as individual entities, particularly at a low dye concentration and high dyeing temperature. A partial explanation for this phenomenon could be as following, the entry of the dye molecules into the fibre from the interfacial layer happens rapidly and can exceed the speed at which the dye molecules are replaced from the bulk of the solution. This stresses the importance of turbulence of the dye liquor during dyeing [109].

According to the classical Flory-Rehner polymer swelling theory, which is applied to keratin fibres, the swelling is directly related to the density of the disulfide crosslink [114]. The morphological structure of the fibre determines the pathway that dyes can take during dyeing and is of decisive importance for the rate and extent of the dye uptake [19, 115]. The cuticles and epicuticles play an important role in controlling the diffusion rate of dyes and other molecules into the fibre. It has been shown by Leeder [114] that dyes enter the fibre at the junctions between the cuticular cells and diffuse through the wool via the relatively lightly crosslinked, non-keratinous regions. This is called intercellular diffusion (Figure 2.16). In later stages of the dyeing cycle, the dyes migrate into the sulphur-rich keratinous regions [116].

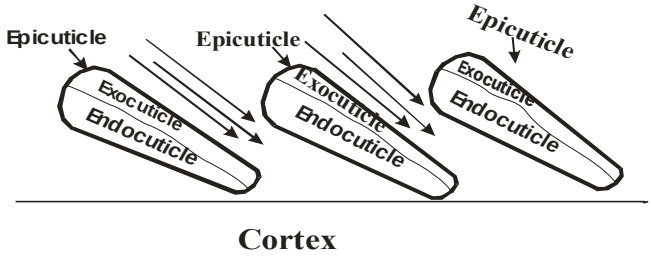

Figure 2. 17: Intercellular diffusion of the dye molecules into the wool fibre

The transcellular diffusion is illustrated in Figure 2.17. It becomes possible after preceding processes, such as chlorination, which modifies the cuticle layer chemically [117, 118].

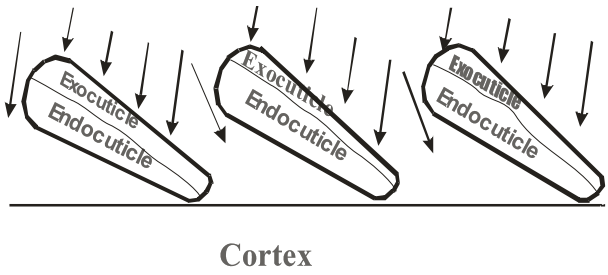

Figure 2. 18: Trans-cellular diffusion of the dye molecules into the wool fibre

2.3.4 Bonding Forces between Dye Molecules and Fibres

Dyes and the fibres to which they are applied usually have an inherent attraction for each other. There are four kinds of forces, by which dye molecules are bound to fibres: ionic forces, hydrogen bonds, van der Waals forces, and covalent bonds [107].

1) Ionic bonds: Positively charged amino groups in wool attract the anions of acid dyes, whilst negatively charged carboxyl groups attract basic dyes. However, these forces are weak and need to be supplemented by other forces [119].
2) Hydrogen bonds: During dyeing, hydrogen bonds are set up between the azo-, amino-, alkyl-amino, and other groups in the dyestuff, and the amido -CO-NH- groups on the wool fibre [19].
3) Van der Waals' forces: These are non-polar attractions between molecules, acting when they are sufficiently close to each other. The strength of the interaction is proportional to the area of possible contact. Large flat dye molecules will therefore interact stronger [119].
4) Covalent bonds: Strong permanent bonds resulting from chemical reactions between a reactive dye molecule containing a chemically reactive centre, and amino-, hydroxyl- and thioal- groups of a wool fibre [19].

These forces seldom act individually and usually at least two of them operate simultaneously.

2.3.5 Dye Classes

There are several different types of dyes that are suitable for the use on wool fibres. These are metal-complex, chrome, acid and reactive dyes [120]. Most manufacturers of dyestuffs have responded to the concerns over chromium by promoting alternative metal-free dyes. New reactive dyes (e.g. Lanasol CE from Ciba) and optimised ranges of metal-free acid dyes, such as Sandolan MF and Lanasets have been developed to achieve a balance of ecological friendliness and performance comparable to that of chrome dyes

[121]. In this project two different dye types were used; namely reactive dyes (Lanasol) and a mixture of 1: 2 metal complex dyes (Lanaset).

2.3.5.1 Reactive dyes

This dye class was introduced to the market in 1956. Reactive dyes react chemically with the fibre and if correctly applied, cannot be removed by washing or boiling [122]. They result in bright shades and provide a good wash fastness. Reactive dyes might assume greater importance for wool dyeing, due to a growing perception that chrome and premetallised dyes are environmentally undesirable [71]. Reactive dyes present an alternative method to chrome dyes, whilst eliminating the problem of heavy metal contamination and scouring liquors [123].

There are two types of reactive dyes: cold and hot dyeing types. Cold dyeing is used mainly for batik work. The wool fibres evaluated in this study were dyed with hot reactive dyes. These dyes have a reactive site, which can form a covalent bond to the fibre, and the dye molecule becomes attached to the fibre and cannot be removed without another chemical reaction [124, 125]. The general structure of a fibre-reactive dye is shown in Figure 2.18:

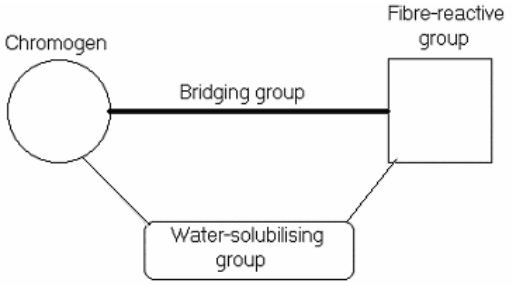

Figure 2. 19: Model of the general structure of a fibre-reactive dye molecule

The four different components of the dye molecule are:

1) the chromogen (chromophore), which normally has a small, simple structure with limited or no attraction at all to the fibre, such as the monoazo [107],
2) the bridging group, which links the chromophore and the fibre-reactive group (frequently an amino group),
3) water soluble groups (ionic groups, often sulphonate salts), which improve the solubility, since reactive dyes must be in solution to be able to diffuse into the wool fibre and

4) the fibre-reactive group, which is the only part of the molecule able to react with the fibre. It has no or little influence on the colour [107], but to achieve level dyeing on wool with a good dye distribution, the reactivity of the reactive group of the dye must be controlled or even reduced using an auxiliary agent.

Table 2.4 shows the commercial names of some reactive dyes and their reactive group.

Table 2. 4: Reactive groups in various dye molecules [19]

Reactive anchor groups	**Dye ranges**
N-Methyltaurine ethylsulfone	Hostalan E, Procilan E
β-Sulfatoethylsulfone-	Remalan
Acrylamide- chloroacetyl-	Procilan
α-Bromoacrylamide-	Lanasol

Lanasol reactive dyes are specifically intended for the application to wool and comprise more than nine dyes. The reactive group of the Lanasol dyes is α-Bromoacrylamino Figure (2.19) [19].

Figure 2. 20: α-Bromoacrylamino in the Lanasol dyes

Lanasol dyes are claimed to combine clarity and brightness of shade with a high wet fastness. They are applied to wool under acidic conditions (pH 4-5.5) and after dyeing, the acid in the dye-bath is neutralized with ammonia, after which the unfixed dye is removed by washing [122].

Wool contains many reactive groups such as primary ($-NH_2$) and secondary (-NH-) amino groups, thiol groups (-SH), and hydroxyl groups (-OH), which are considered the most important reactive groups in the wool fibre. Reactions of the dye with the fibre occur in a weakly acidic medium and include either nucleophilic substitution of leaving groups, such as Cl, Br, sulphonate and ammonium groups or addition reactions to polarized aliphatic double bonds. Both of these reactions might occur simultaneously [19, 124]. The two reaction types for the amino reactive group can be seen in Figure 2.20.

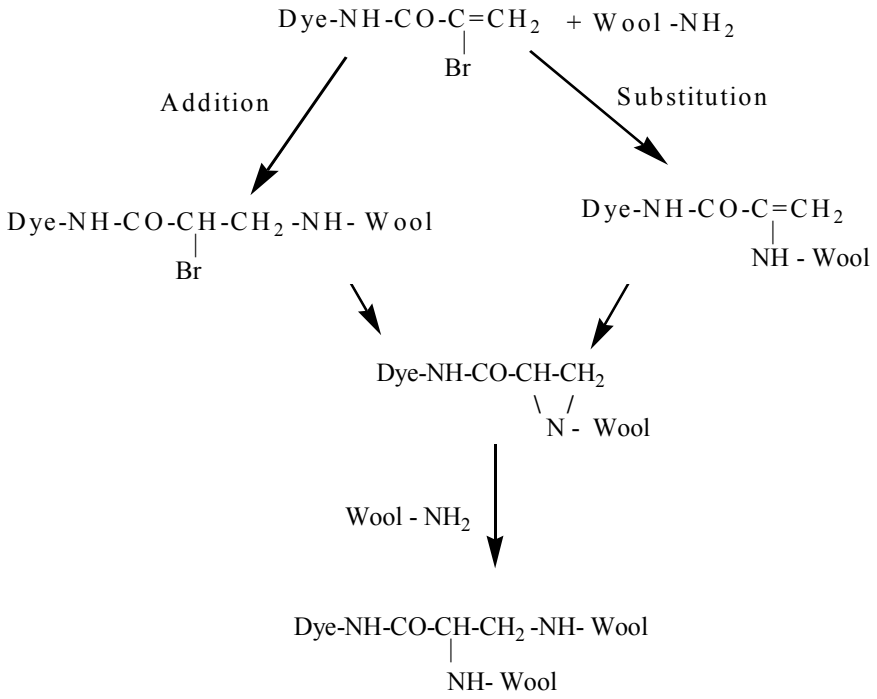

Figure 2. 21: Addition and substitution reaction of the amino groups of the wool fibre and the dye

It is clear that both the substitution and the addition lead to the formation of an aziridine ring (Fig. 2.20), which will react with other amino groups of the fibre to form new crosslinks. The covalent bonds of the crosslinks can be superimposed on secondary and ionic bonds as well [126].

Similar reactions can be observed for thiol and hydroxide groups. The example of a thiol group reaction is illustrated in Figure 2.21.

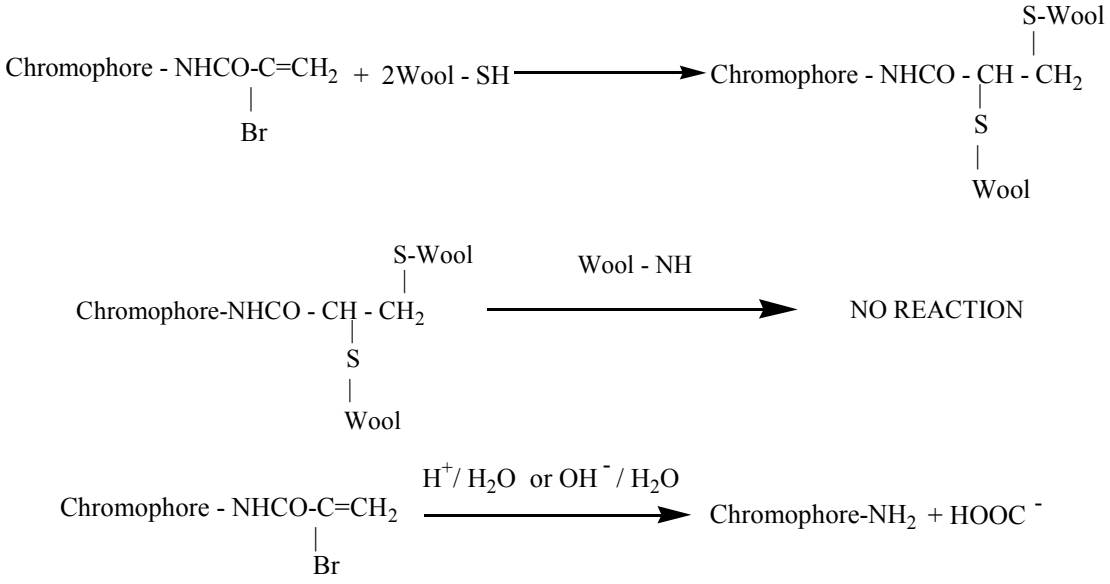

Figure 2. 22: Addition and substitution reaction of the thiol groups of the wool fibre and the dye

2.3.5.2 1:2 Metal complex dyes

Metal-complex dyes are chemically very similar to chrome dyes. The risk of fibre damage is reduced because the complex is formed during the dye production. This group of dyes is, along with reactive dyes, gradually replacing other types of acid dyes, because of their superior fastness properties [99]. 1: 2 Metal complex dyes are premetallized acid dyes, in which one metal ion (Cr or Co) is complexed with two molecules of monoazo dyes (chromophores). The chromophores contain groups (-OH, -NH_2, -COOH) capable of coordinating with the metal ions [21, 127].

The metal atom is located between the two chromophores, which are usually arranged perpendicular to each other. The high affinity for the fibre is based on the large size of the dye molecules, their compact, often almost spherical shape and their negative charge. The dye molecule can form strong links with the fibre and tends to migrate little [19, 99]. On the other hand these molecules can aggregate in dye solution, which slows down the diffusion rate into the wool fibre [99].

There are three distinct types of 1:2 metal complex dyes: unsulphonated, monosulphonated and disulphonated. The disulphonated types are the most soluble and have a greater pH dependence. This means that they have a low neutral affinity and require more acid to achieve exhaustion, but they also have the advantage of the highest fastness to domestic washing, since any desorbed dye has only limited affinity for adjacent fibres at the pH conditions experienced in domestic detergents. Disulphonated dyes are, however, more fibre selective than the mono or unsulphonated dyes [128].

Only limited information is available of modern commercial dye ranges, such as Lanaset (Ciba) and Lanasan CF (Clariant). Generally Lanaset dye consists of optimised mixtures of all three different types of 1:2 metal complex dyes (unsulphonated, monosulphonated and disulphonated), which are formulated to give good combinability, good coverage of fibre irregularities and good overall fastness properties. 1:2 metal complex dyes are often applied in combination with acid dyes to brighten the shades obtainable with metal complex recipes [21].

2.3.6 Degradation of the Wool Fibre Surface

The necessity to obtain satisfactory penetration and better distribution of the dye throughout the fibre results in harsh dyeing conditions. Generally the wool surface can be damaged by any type of wet treatment, such as washing and dyeing processes. Damage of

the wool during dyeing is due to the action of acid, alkali, oxidizing agents (chromates), water, heat, and mechanical stress. All of these factors might lead to permanent damage of keratin, because of an irreversible shortening of the main peptide chains and rupture of disulfide bridges, which form the crosslinking bonds between the polymer chains [8]. The addition of alkali causes the deposited dyes to react with the fibre.

The damage of the surface is shown by a loss of elasticity, loss in abrasion resistance or by felting [129, 130]. The ability of certain reactive dyes to crosslink the wool fibre has been confirmed by solubility experiments [126, 131], and there is evidence to suggest that thiol groups are reactive towards reactive dyes, which can influence the mechanical and physical properties of the fibre [132].

The tenacity of wool is often reduced in stock-dyeing processes. As a result of this, many fibres are damaged or even broken. Besides the surface damage a reduction in fibre strength can be observed, which could be due to setting of bends or curvatures in the fibres caused by the hot water treatment. Chemical stress relaxation via the thiol-disulphide interchange reaction results in strained wool fibres being set in a new configuration, especially when the dyeing temperature is above 70 °C [78, 133]. Such set fibre bends are non-uniformly strained by tensions and can not resist the same loads as fibres set in a straight state [133]. Additionally, other internal changes in the wool fibre can occur during the dyeing process, which lead to changes in mechanical properties. One example is the extraction of soluble proteins from the cell membrane complex, which changes the crosslinking density and the degree of crystallinity especially in the case of reactive dyes [78, 133].

All these factors affect the wool surface directly and cause some sort of surface degradation in the wool fibre. In general it is agreed that there is not one single factor that causes serious fibre damage, but rather a combination of a number of factors. The damage also depends on the history and the conditions to which the fibre has been exposed on the sheep, in storage and before the dyeing process [134].

2.3.6.1 Effect of the pH value

For some dye types (acid dyes, metal complex and some of reactive dyes) a high dyeing rate is required in order to obtain good colour distribution in a short time. For this the dyeing bath should have a pH of between 4 and 5.5, or lower. The amount of free fatty acids remaining on the wool surface decreases significantly with treatment in dye baths at pH values above 2 [76]. Acidic and alkali media can cause severe damage to the protein

fibres, during dyeing. The main chain of the keratin polymer undergoes hydrolytic attacks in the peptide linkages and the amide side chains, especially in a strong acidic solution and if subjected to prolonged treatment in hot water [129]. In the acidic range, ionic bonds are formed between the dye and the fibre, with the dye still being capable of migration. At a pH of 5 covalent binding to the fibre predominates [19].

When wool fibres are subjected to an alkaline solution and heat, the fibres start to swell and uncurl and the scales open up. In alkaline solutions the principle attack is on the cystine linkages, as shown in Figure 2.22:

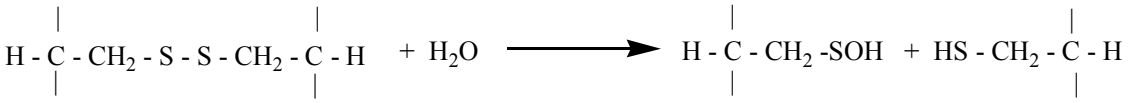

Figure 2. 23: Breakage of the cystine linkages in the peptide chain [99].

Hydrolytic degradation increases with increasing distance from the isoelectric point [135]. The presence of sodium sulphate increases hydrolysis, which is closely connected to a deterioration of mechanical properties**.**

2.3.6.2 Effect of the temperature

For any dyeing process, and all types of dye, heat must be applied to the dye bath. The energy is used to transfer dye molecules from the solution to the fibre and swell the fibre in order to render it more perceptive. The temperature should be at the boil (95 -105 °C) and the dyeing time between 1 and 2 hours or longer depending on the type of dye and the darkness of the colour. Generally the darker the desired colour the longer the dyeing time. The optimal processing conditions should ideally not inflict any damage to the main peptide chains [136].

Exposure to boiling water for a longer time results in cleavage of the cystine crosslinks. New bridges are formed, such as lysinoalanine, which can contribute to crease fixation. Therefore, woollen fabrics should be set before dyeing. Permanent setting in wool fibres requires the rupture of disulfide bonds in addition to the hydrogen bonds in the fibre. Most authors believe that thiol – disulfide exchange reactions at temperatures above 60 °C are required to impart permanent set [137]. Others consider the transition temperature for the onset of thiol – disulfide exchange reactions as the temperature required for chemical cysteine degradation and H_2S formation [19].

Cohesive setting in wool fibres is thought to involve rearrangement of the hydrogen bonds in the fibre, and is imparted whenever wool is distorted at temperatures above the glass-transition temperature of the fibre and cooled while distorted. This set configuration of the fibre is stable as long as the fibres remain below their T_g [138].

2.3.6.3 Effect of the water

Although dry fibrous proteins are very stable, wool can be damaged by extended treatment in boiling water [99]. The fibres become weaker and water decreases the stability further. This is due to strong interactions between the water and the hydrophilic groups in the keratin proteins, whereby hydration shells are formed that weaken the interactions between adjacent polar groups. In addition to these interactions, interactions between water and polar side chains may also occur [139]. Hydrolysis of the peptide, however, leads to the formation of amino groups under the severe dyeing conditions, which causes a huge loss in elasticity of the wool fibre [78, 133].

A particular property of wool is the structural change that readily occurs in boiling water. Thiol and cystine disulphide bonds can undergo interchange reactions that essentially set wool fibres in their conformation in compacted loose fibres and yarns. Colourless chemicals capable of reacting with thiol groups have been suggested as a means of restricting permanent set developing during dyeing [19].

When the wool fibre is placed in the dye solution the fibre tends to twist and revolve rapidly until it comes to rest. When the same fibre is then placed in a dry atmosphere it will return to its original dry form. This can be explained by the fact that the cortex tends to contract more than the cuticle under wet conditions, which causes a curl of the fibre that will stop when dried [140]. This behaviour increases when the chemical stress relaxation via the thiol-disulphide interchange reaction, resulting in strained wool fibres, is set in a new configuration, especially when the dyeing temperature is above 70°C, which produces bends in the fibres [141].

2.3.7 Minimizing the Dyeing Damage

Great care should be taken during the dyeing processing to ensure that the inherent properties of the fibres are maintained. During loose fibre dyeing, the degree of damage must be minimised in order to reduce the amount of waste in carding and to prevent an excessive number of end breaks during spinning. To do this the dyeing time at the boil must be kept at a minimum, or the dyeing should happen at temperatures below the boil.

Acid dyes and metal complex dyes can be successfully applied at temperatures of 80–90°C in conjunction with a low temperature dyeing auxiliary. The auxiliary promotes dyestuff exhaustion, diffusion, and produces fast results with well penetrated dyes [129] .

Research has been performed [142] to dye wool from non-aqueous media, i.e. from supercritical carbon dioxide with hydrophobic dyes. Improved fastness properties are achieved by application of these reactive disperse dyes.

The decisive role of cysteine thiol groups as initiators of the reaction that leads to permanent set is well known and all industrially proven methods of minimizing dyeing damage due to permanent set are therefore based on the same principle, namely the blockage or oxidation of the cysteine thiol groups during dyeing. Compounds that are capable of blocking the thiol-disulphide interchange can in fact be very effective protective agents [130].

Reactive dyes have been shown to reduce permanent set because they are mostly attached to thiol groups. The major advantages of restricting permanent setting in loose wool is the superior spinning property compared to chrome dyed wool, for example [143].

2.4 References

1. J. Harris, *5000 Years of Textiles.* 1st ed., London, British Museum Press, 1993. p. 16, 18, 54-55, 66-68.
2. K.Wilson, *A History of Textiles*. 1st ed., New York, Westview Press, 1979. p. 23-27.
3. M. Feughelman, *Natural Protein Fibres,* J. Appl. Polym. Sci., 2002. 83(3): p. 489-507.
4. L. Wolfram, *Topography of Some Cuticle Cells.* Textile Res. J., 1971. 41(12): p. 252-254.
5. J. Sikorki, A. Hepworth and T. Buckley, *Scanning Electron Microscope Techniques in Wool Research and Processing.* John Wiley & Sons, Inc., Appl. Polym. Symp., 1971. 18: p. 887-893.
6. A. L. Woodhead, F. J. Harrigan and J. S. Church, *Assessment of Wool Chlorination by Infrared Spectroscopy: II. The Chemometric Approach.* Vibr. Spectrosc., 1997. 15(2): p. 179-189.
7. L. Rivettq, N. Jones and E. Donald, *The Role of 18-Methyleicosanoic Acid in the Structure and Formation of Mammalian Hair Fibres.* Micron, 1997. 28(6): p. 469 485.
8. J. Fonollosa, L.Campos, M. Martí, A. Maza, J. L. Parra and L. Coderch, *X-Ray Diffraction Analysis of Internal Wool Lipids.* Chem. and Phys. Lipids, 2004. 130(2): p. 159-166.
9. R. D. Bruce Fraser and David A. D. Parry, *Macrofibril assembly in trichocyte (hard α-keratins).* J. Structural Biol., 2003. 142(2): p. 319-325.
10. L. D'orazio, E. Martuscelli, G. Orsello, F. Riva, G. Scala and A. Taglialatela, *Nature, Origin and Technology of Natural Fibres of Textile Artefacts Recovered in the Ancient Cities around Vesuvius.* J. Archaeol. Sci., 2000. 27(9): p. 745-754.

11. I. Mark, L. Saika and S. Siddiqui, *Are Natural Protein Networks Similar to Synthetic Elastomeric Networks? Structural Implications of the Characteristic Pentapeptide Repeat from the Elastic Protein Network of Wool.* Polym. Gels Netw., 1996. 4(3): p. 167-188.
12. J.M. Maxwell and M.G. Huson, *Scanning Probe Microscopy Examination of The Surface Properties of Keratin Fibres*. Micron, 2005. 36(2): p. 127-136.
13. J. W. S. Hearle, *A Critical Review of the Structural Mechanics of Wool and Hair Fibres.* Int. J. Biol. Macromol., 2000. 27(2): p. 123-138.
14. M. Feughelman, D. Lyman, E. Menefee and B. Willis, *The Orientation of the α-Helices in α-keratin Fibres.* Int. J. Biol. Macromol., 2003. 33(1-3): p. 149-152.
15. A. Hepworth, J. Sikorski, D. J. Tucker and C. S. Whewell, *The Surface Topography of Chemically Treated Wool Fibres.* J. Textile Inst. 1969. 60: p. 513-546.
16. B. J. Toomey, *Handling, Grading and Disposal of Wool*. 1st ed., Rome, Food and Agriculture Organization of the United Nations 1983. p. 21-33, 60-63.
17. D. M. Lewis, G. Yan, R. M. Julia, L. Coderch and P. Erra, *Chromium Distribution in Wool by Electron Microscopy and X-Ray Energy Dispersion Analysis.* Textile Res. J., 2000. 70(4): p. 315-320.
18. T. Haylett, *The Amino Acid Sequence of a Homogeneous Wool Protein*. University of South Africa,1969. p. 1-22.
19. W. Gerhartz and Y. S. Xamamoto, *Ullmann's Encyclopedia of Industrial Chemistry*. 5TH ed., Germany, Wiley-VCH Verlag GmbH & Co. KGaA, 1985. (A.9): P. 73-123 and (A.28): P. 395-42.
20. B. C. Goswami, R.D.Anandjiwala, D. M. Hall, *Textile Sizing*. 1st ed., New York, Basel. Marcel Dekker, Inc, 2004. p. 51-55.
21. G.H.Crawshaw, and W.S.Simpson, *Wool: Science and Technology*. 1st ed., Cambridge England. 2002. p. 84-86, 249-250.
22. L. Haylett, S. Swart and M. Thomas, *Studies on the High Sulphur Proteins of Reduced Merino Wool.* Biochem. J., 1973. 133: p. 641-654.
23. R. H. Peters, *Textile Chemistry*: *The Chemistry of Fibres*. London and New York, Elsevire Publishing Company, 1963. 1: p. 264-275.
24. G. E. Hopkins, *Wool as an Apparel Fibre*. 1st ed., New York, 1953 p.12-29.
25. R. L. Hill, J. R. Kimmel and E.L. Smith, *The Structure of Proteins.* Annu. Rev. Biochem., 1959. 28: p. 97-144.
26. H. D. Weigmann and C. J. Dansizer, *Effects of Cross-links on the Mechanical Properties of Keratin Fibres.* , John Wiley & Sons, Inc., Appl. Polym. Symp., 1971. 18: p. 795-807
27. H. D. Weigmann and C. J. Dansizer, *The Stabilization of Irreversible Deformed Keratin Fibres Part II: Mechanism of Stabilization.* Textile Res. J., 1971. 41: p. 576-585.
28. D. A. D. Parry and P. M. Steinert, *Intermediate Filaments: Molecular Architecture, Assembly, Dynamics and Polymorphism.* Q. Rev. Biophys, 1999. 32: p. 99-187.
29. J. M, Gillespie, *The Proteins of Hair and Other Hard α-keratins*. Cell. Mol. Biol., Plenum, New York. 1990. p.95-128.
30. G. E., Powell and B.C. Rogers, *The Role of Keratin Proteins and Their Genes in the Growth, Structure and Properties of Hair*. Formation and Structure of Human Hair. Birkhäuser Verlag, Basel. 1997. p. 59-148.
31. M. L. Josepl, *Introductory Textile Science*. 4th ed., London and Toronto, CBS College Publishing, 1981. p. 51-55.
32. J. R. Smith and J. A. Swift, *Microscopical Investigations on the Epicuticle of Mammalian Keratin Fibres.* J. Microsc., 2001. 204(3): p. 203-211.
33. E. Wojciechowska, A. Wlochowicz and A. Weselucha-Birczyn´ska, *Application of*

Fourier-transform Infrared and Raman Spectroscopy to the Study of the Influence of Orthosilicic Acid on the Structure of Wool Fibre. J. Mol. Struct., 2000. 555: p. 397-406.
34. P. Jovanèiæ, P. Erra, J., R. Molina, D. Jociæ and M. R. Julia, *Study of Surface Modification of Wool Fibres by Means of SEM, AFM and Light Microscopy*. Eur. Microsc. Anal., 1998. 51: p. 15.
35. Ludger Pille, Jeffrey S. Church and Robert G. Gilbert, *Adsorption of Amino-Functional Polymer Particles onto Keratin Fibres*. J. Colloid Interface Sci., 1998. 198(2): p. 368-377.
36. D. Robson, *Animal Fibre Analysis Using Imaging Techniques Part I: Scale Pattern Data.* Textile Res. J., 1997. 67(10): p. 747-752.
37. D. Robson, P. J. Weedall, and R. J. Harwood, *Cuticular Scale Measurements Using Image Analysis Techniques.* Textile Res. J., 1989. 59: p. 713-717.
38. F.-J. Wortmann, and W. Arns, *Quantitative Fibre Mixture Analysis by Scanning Electron Microscopy, Part I: Blend of Mohair and Cashmere with Sheep's Wool.* Textile Res. J., 1986, 56: p. 442-446.
39. K. D. Langley and T. A. Kennedy, JR., *The Identification of Specialty Fibres.* Textile Res. J., 1981. 51: p. 703-709.
40. M. L. Ryder, *Wool Biology.* Textile magazine, 2001. 30(1): p. 16-21.
41. T. L. Phillips, T. J. Horr, M. G. Huson, P. S. Turner and R. A. Shanks, *Imaging Wool Fibre Surface with a Scanning Force Microscope.* Textile Res. J., 1995. 65(8): p. 445-453.
42. W. E. Morton and J.W.S. Hearle, *Physical Properties of Textile Fibres*. 2nd ed., London. 1975, p.51-60.
43. C. F. Allen, S. A. Dobrowski, , P. T. Speakman, , and P. S. Truter, *Membrane from Wool Cuticle Cells.* Biochem. Soc. Trans., 1985. 13: p. 170-172.
44. A. P. Negri and H. J. Cornell, *A Model for the Surface of Keratin Fibres.* Textile Res. J., 1993. 63(2): p. 109-115.
45. C. M.Carr, I. H. Leaver, and A. E. Hughes, *X-Ray Photoelectron Spectroscopic Studies of Wool Fibres.* Textile Res. J., 1986. 56: p. 457-461.
46. G. Mazingue, P. Ponchel, and J. P. Lubrez, *The Composition and Properties of the Wool Cuticle.* , John Wiley & Sons, Inc., Appl. Polym. Symp., 1971. 18: p. 209-216.
47. H. Zahn, H. Messinger, and H. Hocker, *Covalently Linked Fatty Acids at the Surface of Wool: Part of the "Cuticle Cell Envelope".* Textile Res. J., 1994. 64(9): p. 554-555.
48. A. R. Urquharr and F. O. Howitt, *The Structure of the Textile Fibre*. 1st ed. London, C. Tinling and Co. Ltd., 1953.p. 69-90.
49. M. Feughelman, D.J.L. and B.K.W., *The Parallel Helices of the Intermediate Filaments of α-keratin.* Int. J. Biol. Macromol., 2002. p. 95-96.
50. J. E. Plowman, *Proteomic Database of Wool Components.* J. Chromatogr. B, 2003. 787(1): p. 63-76.
51. Jonathan P. Caldwell , D.N.M., Joy L. Woods , Warren G. Bryson, *The Three Dimensional Arrangement of Intermediate Laments in Romney Wool Cortical Cells.* J. Struct. Biol., 2005. 151(3): p. 298-305.
52. M. Feughelman and V. James, *Hexagonal Packing of Intermediate Filaments (Microfibrils) In α-Keratin Fibres.* Textile Res. J., 1998. 68(2): p. 110-114.
53. H. Wang, D.A.D.P., Leslie N. Jones, *In Vitro Assembly and Structure of Trichocyte Keratin Intermediate Filaments: A Novel Role for Stabilization by Disulfide Bonding.* J. Cell Biol., 2000. 151(7): p. 1459-1468.
54. R. D. Bruce Frasera, G.E.R.a.D.A.D.P., *Nucleation and Growth of Macrofibrils in Trichocyte (Hard-) Keratins.* J. Struct. Biol., 2003. 143(1): p. 85-93.

55. S. J. Kadolph, *Quality Assurance for Textiles and Apparel*. 1st ed., New York. 1998. p. 302-319.
56. F. A. Bovey and F. H. Winslow, *Macromolecules an Introduction to Polymer Science*. 1st ed., Academic Press Inc., 1979. p. 474,488.
57. D. R. Rao and V. B. Gupta, *Properties Structure Correlation in Wool Fibres.* Textile Res. J., 1991. 61(10): p. 609-617.
58. J. Sikorski, *Fibre Structure.* 1st ed., Manchester and London, Butterworth and co. Ltd., 1963. p. 391-401.
59. M. Feughelman, and G. Danilatos, *The Microfibril Matrix Relationships in the Mechanical Properties of Keratin Fibres.* Textile Res. J., 1980. 50(9): p. 568-574.
60. J. Cao, *Is the α-ß transition of keratin a transition of α-helices to ß-pleated sheets. Part I. In situ XRD studies.* J. Mol. Struct., 2000. 553(1-3): p. 101-107.
61. J. Cao, *Is the α-ß transition of keratin a transition of α-helices to ß-pleated sheets. II. Synchrotron investigation for stretched single specimens.* J. Mol. Struct., 2002. 607(1): p. 69-75.
62. J. W. S. Hearle, B. M. Chapman, and G. S. Senior, *The Interpretation of the Mechanical Properties of Wool.* John Wiley & Sons, Inc., Appl. Polym. Symp., 1971. (18): p. 775-794.
63. M. Feughelman, *A Two Phase Structure for Keratin Fibres.* Textile Res. J., 1959. 29: p. 223-228.
64. M. Feughelman, *The Relationship between Structure and the Mechanical Properties of Keratin Fibres.* John Wiley & Sons, Inc., Appl. Polym. Symp., 1971(18): p. 756-774.
65. M. I. Liff. and S.S.Siddiqui, *NMR Evidence of Formation of Cyclocystine Loops in Peptide Models of the High Sulphur Proteins from Wool.* Int. J. Biol. Macromol., 1996. 19: p. 139-143.
66. M. Franck, and L. Vanderhafl, *Textiles for Homes and People*. 1st ed., Lexington, Massachusetts. Ginn and Company a Xerox Education Company. 1973. p. 2, 29-35, 101.
67. S. J. Kadolph, A. L. Langford, N. Hollen and J. Saddler, *Textiles,* 1st ed. New York, Macmillan Publishing Company. 2002. p. 315.
68. E. Wojciechowska, A. Wlochowicz, and A. Weselucha-BirczynLska, *Application of Fourier-Transform Infrared and Raman Spectroscopy to Study Degradation of the Wool Fibre Keratin.* J. Mol. Struct., 1999. 511-512: p. 307-318.
69. J. H. Rahman, and M. S. Brook, *Surface Energy of Wool.* Textile Res. J., 1986. 56: p. 164-171.
70. L. Coderch, and C. Soriano, *Role of Treatment Medium in Degradative Wool Shrink-proofing Processes.* Textile Res. J., 1993. 63(6): p. 369-370.
71. X.-P. Lei, D. M. Lewis, X.-M. Shen and Y.-N. Wang, *Crosslinking Nucleophilic Dyes on Wool.* Dyes Pigments, 1996. 30(4): p. 271-281.
72. W. Y. Kwok, J. Xin, and K. M. Sin, *Predicting the Degree of Toxicity of Effluent from Reactive Dye Mixtures.* Textile Res. J., 2003. 73: p. 625-630.
73. J. Curiskis and X. Wang, *Australian Mohair Processing Performance and Fabric Properties.* Rural Industries Research and Development Corporation, 1999.
74. F.-J. Wortmann, and K.-H. Paba, *Cuticle Scale Heights of Wool and Specialty Fibres and Their Changes Due to Textile Processing.* Textile Res. J., 1999. 69: p. 139-144.
75. T. Baba, N. Nagasawa, H. Ito, O. Yaida, and T. Miyamoto, *Recovery of Surface Properties of Damaged Wool Fibres.* Textile Res. J., 2001. 71(10): p. 885-890.
76. A. P. Negri, H. J. Cornell and D. E. Rivett, *Effect of Processing on the Bond and Free Fatty Acid Levels in Wool.* Textile Res. J., 1992. 62: p. 381-387.

77. E. J. Wood, P. Stanley-Boden and G. A. Carnaby, *Fibre Breakage during Carding, Part II: Evaluation.* Textile Res. J., 1984. 54: p. 419-424.
78. N. Brack, R. N. Lamb, D. Pham, T. Philips and P. Turner, *Effect of Physical Processing on the Wool Fibre Surface.* Textile Res. J., 2001. 71: p. 911-915.
79. M. W. Andrews, *The Fracture Mechanism of Wool Fibres under Tension,* Textile Res. J., 1964. 34(10): p. 831-835.
80. J. W. S. Hearle B. Lomas W. D. Cooke, *Atlas of Fibre Fracture and Damage to Textiles*. 2nd ed. Manchester. 1998. p. 20-21, 178.
81. N. Kohara; M. Kanel and T. Nakajima, *Effect of Reduction and Succinylation on Water Absorbance of Wool Fibres.* Textile Res. J., 2001. 71(12): p. 1095-1099.
82. E. R. Trotman, *Dyeing and Chemical Technology of Textile Fibres*. High Wycombe : Griffin,1984. p. 254-271.
83. R. Jovanović, J. Jakŝevac and M. Rogulić, *The Porosity of Wool Fibres of Different Origin and Fineness.* John Wiley & Sons, Inc., Appl. Polym. Symp., 1971. 18: p. 915-923.
84. F.-J. Wortmann, P. Augustin, and C. Popescu, *Temperature Dependence of The Water-Sorption Isotherms of Wool,* J. Appl. Polym. Sci., 2001. 79(6): p. 1054 - 1061.
85. J. R. Cook and B. E. Fleischfresser, *Ultimate Tensile Properties of Normal and Modified Wool.* Textile Res. J., 1990. 60(1): p. 42-49.
86. A. P. Pierlot, *Water in Wool.* Textile Res. J., 1996. 69(2): p. 97-103.
87. K. Othmer, *Encyclopaedia of Chemical Technology*. 2nd ed. John Wiley & Sons, Inc., 1970. Vol. 22. p.396-397.
88. J. M. Kure, A. P. Pierlot, and I. M. Russell, *The Glass Transition of Wool: an Improved Determination Using DSC.* Textile Res. J., 1997. 67(1): p. 18-22.
89. F.-J. Wortmann, B. J. Rigby, and D. G. Phillips, *Glass Transition Temperature of Wool as a Function of Regain*. Textile. Res. J., 1984. 54: p. 6 - 8.
90. M. Feughelman and A. R. Haly, *The Mechanical Properties of the Ortho-and Para-like Components of Lincoln Wool Fibres.* Textile Res. J., 1960. 30(11): p. 897-900.
91. M. Feughelman, *A Model for the Mechanical Properties of the α-Keratin Cortex.* Textile Res. J., 1994. 64(4): p. 236-239.
92. W. Yu, R. Postle, and H. Yan, *Characterization of the Weak Link of Wool Fibres*, J. Appl. Polym. Sci., 2003. 90(5): p. 1206-1212.
93. A. A. Gharehaghaji, N. A. G. Johnson, and X. Wang, *Wool Fibre Microdamage Caused by Opening Process, Part III: In Situ Studies on the Tensile Failure of Damage Induced Fibres.* Journal Text. Inst, 1999. Part 1 and 2.(90): p.1-34.
94. F.-J. Wortmann and H. Zahn, *The Stress/Strain Curve of α-Keratin Fibres and the Structure of the Intermediate Filament.* Textile Res. J., 1994. 64(12): p. 737-743.
95. I. C. Watt, *Modification of Physical Properties of Wool Fibre.* John Wiley & Sons, Inc., Appl. Polym. Symp., 1971(18): p. 905-914.
96. E. G. Bendit and J. M. Gillespie, *The Probable Role and Location of High-Glycine-Tyrosine Proteins in the Structure of Keratins.* Biopolym., 1978. 17(27): p. 43-45.
97. R. C. Marshall and K. F. Ley, *Examination of Proteins from Wool Cuticle by Two-dimensional Gel Electrophoresis.* Textile Res. J., 1986. 56: p. 772- 774.
98. P. J. Reis, *Variations in the Strength of Wool Fibres: A Review.* Aust. J. Agric. Res., 1992. 43(13): p. 37-51.
99. A. D. Broadbent, *Basic Principles of Textile Coloration,* 1st ed., Thane Prees Ltd, Kent. 2001. p. 6, 32, 120-121, 264, 267.
100. K. L. Hatch, *Textile Science*. 1st ed., New York, West publishing company. 1993. p. 431-433, 435.
101. R. Paul, C. Solans and P. Erra, *Study of a Natural Dye solubilisation in o/w*

Microemulsions and its Dyeing Behaviour. Colloids and Surf., A: Physicochemical and Engineering Aspects, 2005. 253(1-3): p. 175-181.
102. M. Hardy and N. Walker, *Textile Hand Book*. 5th ed. The American Home Economics Association, 1974. p. 58-62.
103. B. F. Smith and I. Block, *Textiles in Perspective*. USA. Prentice-Hall Inco., 1982. p. 329-330.
104. P. Gregory, *High-technology Applications of Organic Colorants*. New York and London, Plenum press, 1991. p. 38, 220, 239.
105. H. K. Rouerre, J. K. Wilshire, I. Yamase and H. Zollinger, *Dye-Fibre Bond Stabilities of Some Reactive Dyes with Wool.* Textile Res. J., 1971. 41(6): p. 518-525.
106. A. C. Cohen, *Beyond Basic Textiles*. 1st ed., New York Fairchild Publications. 1982. p. 175-190.
107. W. S. Perkins, *Textile Coloration and Finishing*. 1st ed., North Carolina. 1996. p. 87, 140.
108. R. A. Chatvat, *Colouring of Plastics Fundamentals*. 2nd ed., Canada. John Wiley and Aons, Inc., 2004. p. 16-20.
109. M. D. Gibbs, *The Effect of Various Fibre Properties of Cotton on Its Dyeing Behaviour*. University of Port Elizabeth, 1987, p. 25-46.
110. E. G. McFarland, W. Carr and S. Michielsen, *Determining Diffusion and Convective Mass Transfer Coefficients in Dyeing a Thin Flat Film*. Textile Res. J., 2002. 72(9): p. 756-763.
111. S. Scharf, E. Cleve, E. Bach, E. Schollmeyer and P. Naderwitz, *Three-Dimensional Flow Calculation in a Textile Dyeing Process.* Textile Res. J., 2002. 72(9): p. 783-788.
112. L. Codrch, O.Lopez, A. De La Maza, A. M. Manich, J. L. Parra and J. Cegarra. *Internal Lipid Wool Structure Modification Due to a Nonionic Auxiliary Used in Dyeing at Low Temperatures.* Textile Res. J., 1997. 67(2): p. 131-136.
113. R. W. Moncrieff, *Man-Made Fibres*. 6th ed., London, Butterworth and Co. Ltd., 1975. p. 810-811.
114. J. D. Leeder, *Comments on "Pathways for Aqueous Diffusion in Keratin Fibres".* Textile Res. J., 1999. 69(3): p. 229.
115. M. Kärrholm, and J. Lindberg, *The Effect of Solvents on Wool Dyeing.* Textile Res. J., 1956. 26: p. 528-530.
116. F. J. Wortmann, G. Wortmann and H. Zahn, *Bath Ways for Dye Diffusion in Wool Fibre.* Textile Res. J., 1997. 67(10): p. 720-724.
117. H. K. Kittan, and G. Rouette, *Wool Fabric Finishing*. 1st ed., UK, Warm Red Graphics Company Halifax, 1991. p. 10-15, 286-287.
118. W. Snyder, G. Berkstresser, B. Smith, K. Beck, R. Mcgregor and W. Jasper, *Correlating Optical and Kinetic Deviations from Ideality in Fibre Reactive Dye Mixtures.* Textile Res. J., 1997. 67(8): p. 571-579.
119. S. M. Broderick, *Wool Carbonising with Special Reference to the Use of Oxidising Agent*. University of Port Elizabeth: Port Elizabeth. 1989. p. 85.
120. V. G. Lukanova, *Dyeing A Wool/Polyamide Blend with Lanaset Dyes.* Vlàkna a textile, 2004. 11(2): p. 50-53.
121. J. Hall, *The Standard Handbook of Textiles*. 8th ed., London, Butterworth & Co (Publishers) Ltd, 1975. p. 253-259.
122. W. F. Beech, *Fibre Reactive Dyes*. 1st ed., London, J. W. Arrowsmith Ltd., 1970. p. 243-279.
123. W. J. Epolito, Y. H. Lee., L. A. Bottomley and S. G. Pavlostathis, *Characterization of the Textile Anthraquinone Dye Reactive Blue 4.* Dyes Pigments, 2005. 67(1): p.

35-46.
124. J. S. Church, A. S. Davie, P. J. Scammells and D. J. Tucker, *Lanasol Dyes and Wool Fibres. Part I: Model Studies on the Mechanism of Dye Fixation in a Mixed Solvent System.* Dyes Pigments, 1998. 39(4): p. 291-312.
125. J. S. Church, A. S. Davie, P. J. Scammells and D. J. Tucker, *Lanasol dyes and wool fibres. Part II: model studies on the mechanism of dye fixation in an aqueous system.* Dyes Pigments, 1998. 39(4): p. 313-333.
126. P. Ball, U. Meyer, and H. Zollinger*, Crosslinking Effects in Reactive Dyeing of Protein Fibres.* Textile Res. J., 1986. 56(7): p. 447-456.
127. V. Golob, S. C. Benkovic, D. Golob, and D. Fakin, *Influence of Anionic Dye Sorption Properties on the Colour of Wool Top.* Textile Res. J., 2004. 74(7): p. 587-592.
128. E. R. Trotaman, *Dyeing and Chemical Technology of Textile Fibres.* High Wycombe : Griffin, 1984. p. 254-271.
129. R. S. Asquith, *Chemistry of Natural Fibre*. 1st ed., New York. 1977. p. 327-330.
130. Q. Liao, P. R. Brady and M. T. Pailthorpe, *Preserving Wool Fabric Properties during Dyeing Using Some Maleic Acid Derivatives.* Textile Res. J., 2004. 74(7): p. 617-622.
131. B. M. Smith, P. L. Spedding, M. S. Otterburn and D. M. Lewis, *Reactions of ß-Sulphatoethyl Sulphone Crosslinking Agent with Wool. Part V: Effects during Reactive Dyeing.* Dyes Pigments, 1995. 28(2): p. 101-122.
132. J. Garcia, R. Postle and M. T. Pailthorpe, *Changes in the Chemical Composition of Wool During Dyeing and Finishing and Their Effects on Fabric Properties.* Textile Res. J., 1995. 65(8): p. 477-485.
133. B. Gullbrandson, *Fibre Damage in the Stock-Dyeing of Wool.* Textile Res. J., 1958. 28(11): p. 965-968.
134. H. P. Lundgren, *Highlights of Papers on Physical and Protein Chemistry.* Textile Res. J., 1956. 26: p. 372-376.
135. J. Labarthe, *Elements of Textiles*. 1st ed., New York, Macmillan publishing co., Inc. 1975. p. 63.
136. T. Leksophee, S. Supansomboo and N. Sombatsompop, *Effect Of Crosslinking Agents, Dyeing Temperature and pH on Mechanical Performance and Whiteness of Silk Fabric.* J. Appl. Polym. Sci., 2004. 91(2): p. 1000-1007.
137. D. Robson , M. J. Williams, and J. M. Woodhouse, *Colouring Matters.* J. Text. Inst., 1969. 60: p. 140 - 151.
138. P. Dreyfuss and R. Quirk, *Encyclopaedia of Polymer Science and Engineering*. 2nd ed., John Wiley and Sons. Inc., 1987. (8): p.566-600.
139. G. Ebert and J. Wendorff, *Physical Structure and Behaviour of Keratin Fibres Immersed in Liquids.* John Wiley & Sons, Inc., Appl. Polym. Symp., 1971(18): p. 873-877.
140. B.E. Harsuch, *Introduction to Textile Chemistry*. 1st ed., New York, John Wiley and Sons, Inc., 1950. p. 252-255.
141. M. G. Huson, *The Mechanism by Which Oxidizing Agents Minimize Strength Losses in Wool Dyeing*. Textile Res. J., 1992. 62(1): p. 9-14.
142. A. Schmidt, E. Bach and E. Schollmeyer, *The Dyeing of Natural Fibres with Reactive Disperse Dyes in Supercritical Carbon Dioxide.* Dyes Pigments, 2003. 56(1): p. 27-35.
143. K. Parton, *Alternatives to the After-chrome Dyeing of Wool: Fibres to Finished Fabrics Proceeding*. Fibre Science/Dyeing and Finishing Groups Joint Conference. 8-9 December, 1998. p. 93-103.

3 Characterisation Techniques

The ability to measure surface characteristics of fibres and subsequently categorize them remains an important scientific goal, particularly in the field of textile science [1, 2]. The most common techniques to investigate the structure, structure-modification and damage to the wool fibre surface are microscopic observations with optical, transmission electron, scanning electron or atomic force microscopes [3]. The potential range of techniques available these days is so wide that it seems as if capital expenditure is the only restriction when selecting an examination method.

A considerable amount of work has been performed on the surface structure and morphology of wool fibres [4-6]. Some earlier studies were carried out by optical microscopy, but no valuable results could be obtained on the surface damage due to a limited magnification. The problem was not only the great difficulty of establishing reasonable viewing conditions and interpreting what was seen, but that one could easily be misled [3, 7]. In the 1950`s frictional wear was showed clearly by using a conventional electron microscope to observe a fibre directly in the rarely employed reflection mode [7]. Transmission electron microscopy offered little help because it was not possible to obtain a model of complicated fibre breaks with different depth or multiple splitting. Even the simplest fibre structures would be difficult to study in three-dimensions.

With the SEM it became possible for the first time to obtain detailed images of broken fibres and to examine the form of damage and failure in textiles [3, 8]. This high resolution technique has led to an extended knowledge of fine morphological details of wool fibres. The obtained information, however, does not cover the entire range of wool types [9]. Most fibres are electrical insulators and therefore have to be coated with metal in order to be examined with SEM. This conductive layer (normally gold) could mask or distort features of the damaged area or fractures and therefore limit the information which can be obtained by SEM.

This led to the search for a more powerful technique, which could be used without any modification to the wool surface. The solution was found in the atomic force microscope. This instrument allows the investigation of the surface microstructure of fibres in a normal environment (air, atmospheric pressure) and it has shown a clear advantage as a characterization tool for textile fibres [10].

The impact of AFM in the field of textile technology, however, has so far been relatively modest. AFM has been used to study wool fibres for the first time in 1995, when Phillips et al. [6] described the use of AFM to examine the surface of wool fibres. In the same year the effect of ultraviolet light on wool fibre surfaces was investigated with AFM [7]. Since that time AFM has been used to investigate the surface of wool fibres in different environments, for example by Maxwell and Huson [11], who used the AFM to examine the morphology of the surface of wool fibres and human hair in water. Titcombe et al. [5] studied the cortical structure, and Gibson et al. [12] used force-distance measurements to examine the effect of aqueous exposure on the mechanical properties of the fibre surface.

AFM has the further advantage of providing actual three-dimensional information of the surface. The instrument can be used to obtain images of a sample with a nanometer resolution, as well as information of the physical properties of a material, which can be obtained by operating the instrument in force mode [11].

3.1 Atomic Force Microscopy

Since the 1980's various scanning probe microscopes (SPM) have been developed. These microscopes use a very small, sharp tip to sense a range of surface properties such as electrical, chemical, thermal, and mechanical properties at an atomic scale. One such microscope is the atomic force microscope (AFM) or scanning force microscope (SFM), which is considered one of the most important tools for imaging surfaces of polymer fibres and generating a wide range of information about surface features and properties. AFM was invented in 1986 by Binnig et al. [13]. It detects the atomic forces interacting between the sample surface and the AFM probe as the probe is scanned across the surface. These force values can be represented as a topographic profile of the scanned sample area. In addition, the tip is a force sensor and can be used to study mechanical and physical properties of small objects, e.g. determine the surface roughness or the adhesive force [14, 15] and detect changes in local elasticity across the sample surface [16]. Unlike the scanning tunnelling microscope (STM), AFM employs an optical technique to detect the motions of the cantilever, to which the probe is fixed. AFM can be operated in various modes, which differ in the way they sense the interaction forces to create an image.

3.1.1 Components of an AFM

A schematic illustration of a typical AFM is shown in Figure 3.1, which displays the essential components [17]:

1) a tip attached to the free end of a cantilever
2) piezoelectric translators (scanners)
3) a segmented photodiode detector
4) a laser beam focused on the back of the cantilever, and
5) a computer interface.

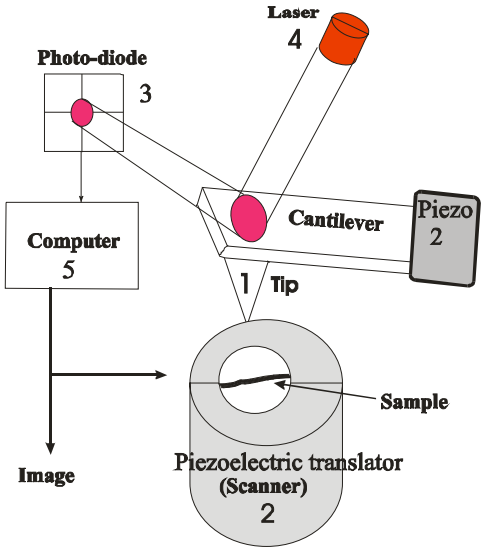

Figure 3. 1: Schematic illustration showing the components of an AFM.

The movement of the AFM probe with piezoelectronic scanners is controlled by a computer. The control software communicates with the AFM hardware and determines the tip motion, the scan-size and the location of the probe on the sample. The probe is several microns long with a curvature-radius at the tip between 10 - 50 nm. The cantilever length ranges typically from 100 – 200 μm, and the spring constant ranges from 0.2 N/m (contact) to 50 N/m (non-contact).

Topographic images with a resolution in the nanometre range, as well as changes in the surface energy due to damage can easily be obtained with the AFM, therefore it is possible to examine the changes in surface topology and measure any changes in the adhesive force between the probe and the sample surface of the fibre, before and after dyeing [14].

3.1.2 AFM Operating Modes

A very sharp probe is raster-scanned across a sample surface. It is attached to the free end of a soft cantilever, which bends easily in response to the forces acting between the probe and the sample. To detect the deformation of the cantilever a laser beam is reflected from the cantilever into a segmented, position-sensitive photodiode. As the probe moves across the sample, the cantilever is bent according to the surface features and the photodiode registers a position change of the laser reflection. Two piezos generate the scanning movement of the cantilever in x- and y-direction. The signal from the photodiode controls a z-piezo, which moves the cantilever up or down to compensate for any shift in the laser deflection. This mode of operation is known as constant force mode, and provides a topographical image of the scanned area. If the feedback electronics are switched off, the microscope is said to be operating in constant height mode. This is particularly useful for imaging very flat samples at high resolution [14, 17].

Depending on the net forces acting between the probe and the sample, the AFM imaging modes can be classified into three types: contact, non-contact and intermittent contact (tapping) mode.

3.1.2.1 Contact mode (repulsive mode)

Contact mode is the simplest operation method of the AFM. In this mode the probe scans across the sample in close contact with the surface. The force between the tip and the sample is repulsive with a value of around 10^{-9} N.

As the probe and the sample are gradually brought closer, they first weakly attract each other. This attraction increases until the atoms are so close together that their electrons begin to repel each other electrostatically. This electrostatic repulsion progressively weakens the attractive force as the interatomic separation continues to decrease. The force reaches zero at a distance of a couple of angstroms, which is about the length of a chemical bond. When the total force becomes positive (repulsive), the tip and the sample are said to be in contact. In the case of the AFM this means, the cantilever is bent upward, if the distance decreases further. This cantilever deflection can be detected and is used to generate the topography image [18].

The deflection of the cantilever is sensed and compared to a set deflection value in a DC feedback amplifier. If the measured deflection is different from the set value the feedback loop applies a voltage to the z-piezo to raise or lower the tip relative to the sample in order

to restore the set deflection value. The voltage applied to the z-piezo is a measure of the height of features on the sample surface and can be displayed as a function of the lateral position of the sample. In this way a topography image is generated [14, 19].

3.1.2.2 Non-contact mode (attractive mode)

The non-contact mode is used when tip contact might influence or alter the sample surface. In this mode the probe oscillates about 50 - 150 Angstrom above the sample surface. Attractive van der Waals forces are detected, and topographic images are constructed by scanning the tip across the surface. The oscillation amplitude or the resonance frequency of the cantilever changes in response to the force acting between the probe and the sample. Because the distance between the probe and the sample is large in the non-contact regime, the resolution is not as good, as in the contact mode. Cantilevers used for the non-contact mode must be stiffer than those used for contact mode in order to obtain an oscillation with a high enough resonance frequency [14, 19, 20].

3.1.2.3 Intermittent-contact mode (tapping mode)

Intermittent-contact or tapping mode is a mixture of both the above modes, with the difference that the tip taps on the sample surface at each cycle of the oscillation. As for NC-mode, the cantilever's oscillation amplitude changes in response to the tip-sample spacing. An image representing the surface topography is obtained by monitoring these changes. Some samples are best handled using IC-AFM instead of contact or non-contact AFM. IC-AFM is less likely to damage the sample than contact AFM because it eliminates lateral forces such as friction between the tip and the sample. In general, it has been found that IC-AFM is more effective than NC-AFM, because of its better resolution [14, 19].

3.1.3 Force Distance Relationship

As mentioned before, the AFM operates by measuring the forces between the probe and sample. The AFM can be operated in the static 'force-versus-distance' **(*F*–*d*)** mode, whereby the approaching/retracting tip senses interactions at the interface. Forces commonly detected by AFM are van der Waals, electrostatic and capillary forces. These forces are either attractive or repulsive, depending on the nature of the sample, the distance between the probe and sample, the probe geometry, and possible contaminations on the sample surface [20].

The AFM probe is first lowered into contact with the sample, then slightly indented into

the surface, and finally lifted off of the sample surface. The cantilever deflection is measured as a function of the distance between the sample and the probe, resulting in a deflection versus distance curve. Knowing the spring constant, the cantilever deflection can be converted into a force to produce a force-distance curve (Figure 3.2) [18].

The deflection can be converted into a force value by applying Hooke's law for small displacements (38):

$$F = - kx \qquad \text{(Eq. 3.1)}$$

where k is the spring constant and x is the displacement of the cantilever [14]. These curves can be used to study surface properties, such as stiffness or the surface polarity of the sample [20].

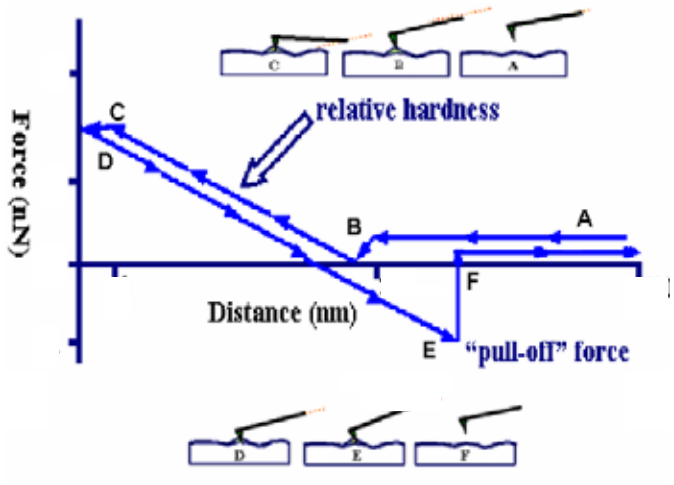

Figure 3. 2: Forces between the probe and sample as the probe approaches the sample surface.

Figure 3.2 shows the interaction force between the tip and the sample surface, which is detected via the deflection of the cantilever. Generally two distance regions are shown on the figure; the contact region and the non-contact region. In section (AB) no interaction forces between the tip and surface are detected and the cantilever is free. At point (B) a long-range attractive force bends the cantilever downwards and it jumps into contact with the surface. As soon as the tip contacts the surface, the cantilever deflection increases with decreasing distance (section BC). If the cantilever is sufficiently stiff, the probe might indent into the surface at this point.

After the maximum set load is reached, the process is reversed. As the cantilever is withdrawn, adhesion between the cantilever and the surface can cause the cantilever to stick to the sample some distance past the initial contact point on the approach curve

(section DE). Eventually the tip springs free (EF) depending on the strength of the adhesive force. This is known as the pull-off point. The pull-off force is a measure for the adhesive force acting between the probe and the surface [15, 19, 20].

3.1.4 Resolution and Artefacts

As with nearly all techniques, the AFM has a number of limitations to go with its many advantages, one of which is imaging artefacts. Great care must be taken to avoid artefacts, when imaging with the AFM [21]. There are three primary sources of artefacts in AFM images [22]:

1) probe geometry,
2) scanner linearity and
3) vibrations (electric and thermal vibration)

Because the AFM depends on the interaction between the probe and the surface, most existing artefacts, are due to the size, shape, and cleanliness of the probe. Features in the image, which remain the same in each frame, are considered part of the sample surface. Often structures on the surface seem larger and broader than they really are. The height of the structure however, is correct. The broadening in the image is caused by the shape of the probe, as displayed in Figure 3.3.

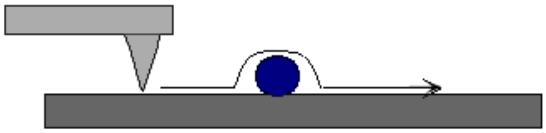

Figure 3. 3: The AFM probe scans over a sphere. The resulting image is broadened because of the shape of the tip [22].

If the probe needs to scan a feature that is below the surface, its size will appear too small.

Figure 3. 4: The AFM probe scans over a hole in a surface. Because of the width of the probe, it does not reach the bottom of the hole [22].

It is obvious that both contact and non-contact AFM cannot trace caves, overhangs and slopes that are steeper than the side angle of the tip [23]. Artefacts from the probe geometry can be avoided by using the optimal probe for each application. If the probe tip

is much smaller than the structure of interest the probe-generated artefacts are minimal and the dimensional measurements derived from the images are accurate.

Artefacts can also be introduced into images because of the geometry of the scanner, and the positioning of the sample relative to the scanner. Also environmental vibrations in the laboratory (acoustic and mechanic) can cause the probe in the microscope to vibrate. Typically, these artefacts appear as low frequency oscillations in the image. In addition to this, artefacts could be due to electronic noise of the control system or faulty electronics. These are normally high frequency oscillations in an image, such as in Figure 3.5

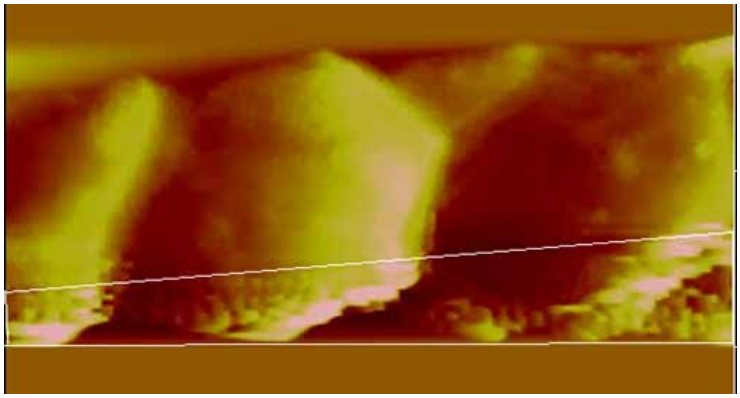

Figure 3. 5: Image of a test sample with electronic noise at the bottom of the scan.

3.2 Mechanical Tensile Testing

According to the literature [24, 25] the most common and universal way to assess the degradation of textile materials is by measuring the tensile strength and the extension at break. Changes in tensile strength and elongation behaviour are an indication of degradation [25].

Tensile strength is defined as the maximum resistance of a material to deformation in a tensile test carried to rupture, or in other words the breaking load or force per unit cross-sectional area of the unstrained specimen [24, 26]. Hatch [27] defines the tensile strength as the ability of a fibre to resist a longitudinal pulling force without rupturing. The breaking strength is the force required to break a textile when it is pulled and it can be used to investigate the effect of different treatment conditions on textile materials [28].

The tensile strength is determined by applying a load to the sample in its axial direction, which develops a tension. This will cause the sample to deform or strain and eventually break as the load is increased. The amount of deformation is called breaking extension and breaking load is usually used as an expression for tensile strength. It is measured in

Newton or Newton per unit area, and is commonly used as an expression for the textile material strength [24].

Two main types of tensile tests are used to observe the effect of pulling forces on textile materials: a constant rate of extension and a constant rate of load. The first type is more common [24]. Each instrument has the same basic components, which include loading-clamping- and recording-mechanisms [29].

The tensile strength of the fibres observed in this study was tested on an Instron tensile strength tester (Model 4444), with a constant rate of extension (Figure 3.6). This machine can be used to investigate different mechanical properties, such as tensile, tearing, flex, compression, and shear properties, with a load cell that can be adjusted according to the strength of the sample to improve accuracy.

Figure 3. 6: Instron Tester Model 4444

For this project the steady strain rate mode was used. The sample was mounted in the pneumatic jaws and the program allowed to run until the sample broke. For data recording the Instron software of Series IX Automated Materials Testing was used.

The tensile properties that can be recorded include: displacement at maximum load (load at break), load, stress, strain, maximum percentage strain (displacement at break), the modulus and a load/elongation curve or a stress/strain curve. The parameters of interest in this study were the displacement at break and the load at break.

3.3 References

1. D. H. Tester, *Fine Structure of Cashmere and Superfine Merino Wool Fibres*. Textile Res. J., 1987. 57: p. 213-219.
2. F.-J Wortmann, and W. Arns, *Quantitative Fibre Mixture Analysis by Scanning Electron Microscopy, Part I; Blends of Mohair and Cashmere with Sheep's Wool.* Textile Res. J., 1986. 56: p. 442-446.
3. S. K. Mukhopadhyay, *Advances in Fibre Science*. 1st ed. Manchester, The Textile Institute, 1992. p. 47-54.
4. L. J. Wolfram, *Topography of Some Cuticle Cells.* Textile Res. J., 1971. 41(12): p. 252-254.
5. L. A. Titcombe, M. G. Huson and P. S. Turner, *Imaging the Internal Cellular Structure of Merino Wool Fibres Using Atomic Force Microscopy.* Micron, 1997. 28(1): p. 69-71.
6. T. L. Phillips, T. J. Horr, M. G. Huson and P. S. Turner, *Imaging Wool Fiber Surfaces with a Scanning Force Microscope.* Textile Res. J., 1995. 65: p. 445-453.
7. J. W. S. Hearle, B. Lomas and W. D. Cooke, *Atlas of Fibre Fracture and Damage to Textiles.* 2nd ed., University of Manchester Institute of Science and Technology, 1998. P 20-21.
8. J. Sikorki, A. Hepworth and T. Buckley, *Scanning Electron Microscope Techniques in Wool Research and Processing.* John Wiley & Sons, Inc., Appl. Polym. Symp., 1971. 18: p. 887-893
9. J. Sikorski, *Fibre Structure.* 1st ed., Manchester and London, Butterworth and co. Ltd., 1963. p. 391-401.
10. P. A. Tucker, *Scale Heights of Chemically Treated Wool and Hair Fibres.* Textile Res. J., 1998. 68: p. 229-230.
11. J. M. Maxwell and M. G. Huson, *Scanning Probe Microscopy Examination of the Surface Properties of Keratin Fibres.* Micron, 2005. 36(2): p. 127-136.
12. C. T. Gibson, G. S. Watson, L. D. Mapledoram, H. Kondo and S. Myhra, *Characterisation of Organic Thin Films by Atomic Force Microscopy-Application of Force vs. Distance Analysis and Other Modes.* Appl. Surf. Sci., 1999. 144-145: p. 618-622.
13. G. Binnig and C. F. Quate, *Atomic Force Microscope.* Phys. Rev. Lett., 1986. 56(9): p. 930-933.
14. S. N. Magonov, *Comprehensive Polymer Science the Synthesis Characterization Reaction & Application of Polymers. "Atomic Force Microscopy in Analysis of Polymers"*. 1989. p. 7433-7455.
15. A. L. Weisenhorn, P. Maivald, H.–J. Butt, and P. K. Hansma, *Measuring Adhesion, Attraction, and Repulsion between Surfaces in Liquids with an Atomic-Force Microscope.* Phys. Rev. B, 1992. 45(19): p. 11226-11232.
16. S. N. Magonov and M. -H. Whangbo, *Surface Analysis with STM and AFM: Experimental and Theoretical Aspects of Image Analysis.* 1st ed., VCH Verlagsgesellschaft mbH, Weinheim, 1996. (1): p. 21-63.
17. N. Jalili and K. Laxminarayana, *A review of Atomic Force Microscopy Imaging Systems: Application to Molecular Metrology and Biological Sciences.* Mechatronics, 2004. 14(8): p. 907-945.
18. S. O. Vansteenkiste, M. C. Davies, C. J. Roberts, S. J. B. Tendler and P. M. Williams, *Scanning Probe Microscopy of Biomedical Interfaces.* Prog. Surf. Sci., 1998. 57(2): p. 95-136.
19. P. Worsfold, A. Townshend and C. Poole, Encyclopaedia of Analytical Science, Microscopy *Techniques/Atomic Force and Scanning Tunnelling Microscopy*. 2nd ed., Elsevier Academic press, 2005. 6: p143-150.

20. H.-Y. Nie, M.J.Walzak, B. Berno and N.S. McIntyre, *Atomic Force Microscopy Study of Polypropylene Surfaces Treated by UV and Ozone Exposure: Modification of Morphology and Adhesion Force.* Appl. Surf. Sci., 1999. 144-145: p. 627-732.
21. S. S. Sheiko, *Imaging of Polymers Using Scanning Force Microscopy: from Superstructures to Individual Molecules.* Advances in polymer science, 2000. (151): P. 61-174.
22. P.West and N. Starostina, *A Guide to AFM Image Artefacts*. Pacific Nanotechnology Advancing Nanotechnology; 2002. p. 3-4.
23. G. Kaupp, A. Herrmann and M. Haak, *Artefacts in Scanning Near-field Optical Microscopy (SNOM) Due to Deficient Tips.* J. Phys. Org. Chem., 1999. 12: p. 797-807.
24. J. E. Booth, *Principle of Textile Testing*. 3rd ed., London, The Millbrook, press Ltd. Southampton, 1968. p. 371-373, 353-357.
25. M. G. Huson, *The Mechanism by Which Oxidizing Agents Minimize Strength Losses in Wool Dyeing*. Textile Res. J., 1992. 62(1): p. 9-14.
26. M. Robert, *Textile Product Serviceability*. 1st ed., New York, 1991. p.156.
27. K. L. Hatch, *Textile Science*. 1st ed., New York, 1993. p. 16, 431-433, 435.
28. G., Tortora, *Understanding Textile*. 2nd ed., New York, Macmillan Publishing Co. Inc., 1982. p. 408-409.
29. A. C. Cohen, *Beyond Basic Textiles*. 1st ed., New York, Fairchild Publications, 1982. p 44-69.

4 Experimental Work

4.1 Sample Selection

Undyed and dyed merino wool fibre slivers, from which fibres were selected randomly for investigation, were supplied by Hextex in Worcester, a textile factory specialising in the production of wool fabrics. Three sample sets of slivers, each set including dyed and undyed slivers, were investigated. The dyed slivers covered a range of colours, from light to dark, and were dyed with two dyes from Ciba - either a 1:2 metal complex reactive dye (commercial name: Lanaset) or a reactive dye (commercial name: Lanasol). Lanasol and Lanaset are commonly used in the industrial dyeing of wool as major dyes in the production output process of wool. The pre-treatment, to which the fibres were submitted included cleaning, bleaching and scouring and was the same for all the samples. Due to a dependency on the production at the factory for sample colours, a shortage of some colours was experienced. To make up a full range of colours (according to lightness values) to investigate, some of the undyed wool fibres from the lot were laboratory dyed in an exhaust dyeing machine. For laboratory dyeing, the dye profile and conditions, dyes and auxiliaries were the same as in the factory conditions. Different concentrations of blue Lanaset dye from Ciba were used to achieve the desired lightness range. Lanaset was chosen over Lanasol for laboratory dyeing because it is more suitable to achieve light colours, which were needed for this study.

To simplify the description of the fibres the samples were arranged from light to dark shades. The degree of lightness of undyed and dyed fibres was determined with a colorimeter produced by BYK-Gardener. It determines the colour degree in three dimensions. For this project only the value for lightness (L*) was used to arrange the samples. L*, a*, b* measurements were taken with the apparatus set to its normal aperture (daylight).

4.2 Sample Description

Samples were divided into three sets for evaluation of the results.

The **first sample set** included four slivers from two different lots of wool. These samples were studied in a pilot study in order to obtain an indication of the surface characteristics which should be investigated and the number of samples needed for the tensile tests.

- The first lot had a nominal diameter of 18.5 μm. Undyed as well as dyed fibres were observed. The dyed samples were dyed black with Lanasol reactive dye. The dyeing time was 356 minutes with a maximum temperature of 100ºC.

- The second lot had a nominal diameter of 20 µm. Undyed and dyed fibres were studied. The dyed samples were dyed navy with Lanasol reactive dye. The dyeing time was 273 minutes with a maximum temperature of 100ºC.

The **second sample set** included undyed and dyed slivers, all from the same lot. They were dyed in a range of colours (eight in the factory + seven in the laboratory) with a metal complex dye (Lanaset) as well as a reactive dye (Lanasol). The maximum temperature (100 ºC), and the concentration of the acetic acid (2 %) were the same for both dyes, but the dyeing times, according to the dyehouse report, was 178 minutes for the Lanaset and 356 minutes for the Lanasol dye. The Lanasol dyed fibres were rinsed with a solution of 3% ammonia. The advantage of this set of samples was that all the samples came from the same original lot, which means less variation in the wool structure. Pre-treated but undyed fibres as well as the blank dyed samples were available for testing. This made the specimens much more comparable since the variables were better defined. The diameters of the fibres were determined with the AFM and average values were calculated. The dyed wool samples used in this sample set were divided into two groups, namely commercially dyed samples from the factory and the laboratory dyed samples, of which the dyeing method is described in appendix A. The sample properties are described in table 4.1.

Table 4. 1: Description of the fibres in the second sample set sorted according to their lightness value.

Sample Colour	Lightness Value	Dye Type	Dye Concentration %	Average Diameter (µm)
Un-dyed	84.18	Undyed	0.000	19.20±1.41
Yellow	69.86	Lanaset	0.340	19.47±1.56
Green	32.78	Lanaset	1.150	19.22±1.35
Grey I	30.90	Lanaset	1.015	19.47±1.45
Blue	26.65	Lanaset	1.295	19.40±1.65
Grey II	22.52	Lanaset	1.015	19.31±1.32
Black I	15.66	Lanasol	6.500	19.02±1.23
Black II	13.94	Lanasol	6.500	18.91±1.65
Blank	79.61	No dye	0.000	19.20±1.51
Blue 1	70.24	Lanaset	0.080	19.30±1.47
Blue 2	64.73	Lanaset	0.100	19.22±1.39
Blue 3	59.83	Lanaset	0.300	19.39±1.41
Blue 4	53.91	Lanaset	0.500	19.11±1.64
Blue 5	51.62	Lanaset	0.800	19.69±1.48
Blue 6	48.31	Lanaset	1.000	19.40±1.31

The **third sample set** consisted of fourteen slivers of different colours, dyed with metal complex dyes (Lanaset), at a maximum temperature of 100 ºC, a standard time of 178 minutes and an acetic acid concentration of 2 % at the beginning. Samples were rinsed with a solution of water containing 0.4 % acetic acid. The slivers were not all from the same lot and variables are therefore not fully controlled. Consequently it was expected that some properties would not be entirely comparable. The average fibre diameter in the samples ranged from 17.5 ± 1.12 μm to 18.88 ± 1.53 μm. The sample properties are described in table 4.2.

Table 4. 2: Description of the fibres in the third sample set sorted according to their lightness value.

Sample Colour	Lightness Values	Dye Type	Dye Concentration %	Average Diameter (μm)
Un-dyed	88.45	Undyed	0.000	18.21±1.32
Lt-blue green	64.69	Lanaset	0.128	18.10±1.60
Ginger	46.86	Lanaset	0.620	18.13±1.94
Dkl-taupe	43.35	Lanaset	0.881	17.57±1.65
Olive	42.18	Lanaset	1.112	18.51±1.48
De-petrol	41.84	Lanaset	1.170	18.88 ± 1.53
Tobacco	35.31	Lanaset	1.215	17.96±1.65
Khaki	32.61	Lanaset	1.015	18.45±1.62
Brown I	29.93	Lanaset	1.460	17.96±1.54
Brown II	27.83	Lanaset	1.770	18.23±1.32
Grey	27.20	Lanaset	1.960	18.76±1.41
Blue-grey	24.39	Lanaset	2.200	18.58±1.60
Dr-grey	23.78	Lanaset	2.160	18.66±1.50
Olive-green	19.10	Lanaset	2.310	17.50 ±1.12
Brown III	14.50	Lanaset	2.720	18.07 ±1.82

4.3 AFM Imaging

AFM was acquired on a multimode AFM with a Nanoscale III controller. AFM images of the wool fibres were acquired in non-contact and contact mode, using a low resonance frequency silicon cantilever with a resonance frequency of about 60 kHz, and a spring constant of K = 50 N/m or a silicon contact cantilever with a spring constant of K = 0.2 N/m . Wool fibres were attached to the sample holder with adhesive tape that fixed the two ends of the fibre to the substrate. Images were acquired with the J-scanner, with a maximum scan range of 130 X 130 μm^2. All experiments were carried out at ambient conditions (room temperature, atmospheric pressure and 75% humidity). The scan rate was set in the range of 0.6 to 0.8 Hz.

The fast scan direction (x-axis) was set parallel to the fibre axis, thus minimizing the possibility of the tip moving the fibre. Topography and phase images were captured simultaneously for tapping mode. Noise was removed with the Veeco imaging software.

Five random wool fibres were picked out of a bundle and imaged in tapping mode. Four images were acquired on each fibre, resulting in a total of 20 images. All parameters (such as scale height etc.) were measured several times in each image, resulting in an average value and a standard deviation. These average values were used in order to ensure that the results represent the surface characteristics of the entire wool fibre statistically correct. This allowed easier comparison of the surface characteristics of different fibres. Some of the measured surface parameters are illustrated in Figures 4.1- 4.8. Measurements were only performed on scales that were not severely damaged.

4.3.1 Cuticle Height (P1) and Step Angle (P2)

The scale height is a measure of how far the cuticle scale edge protrudes above the main shaft or body of the fibre. The step angle represents the steepness of the scale edge as displayed in Figure 4.1. The graph shows the cross-section profile along the line in the image below with the parameters P1 and P2.

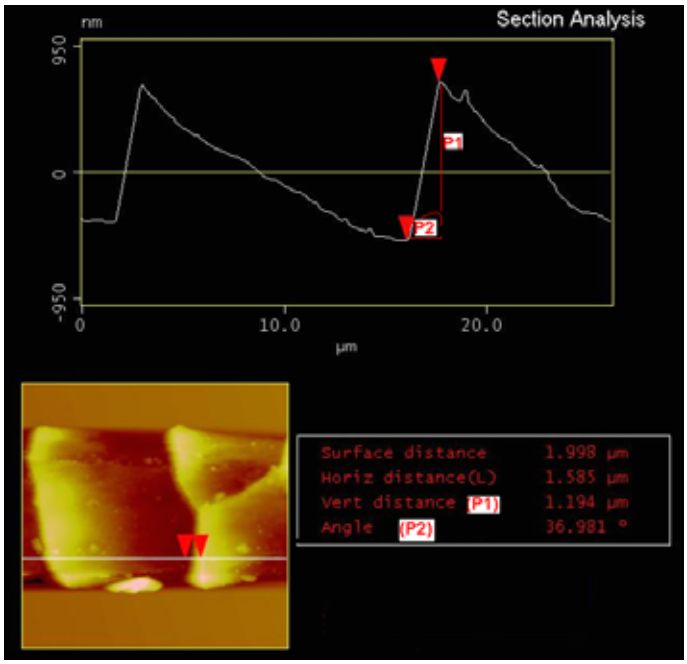

Figure 4. 1: Measurement of the height and the angle of the scale edge

For each sample (colour) twenty images were captured and from them a total of a hundred measurements of the height and the angle were taken at different places along the length of the scale edges.

4.3.2 Surface Roughness of the Scale Top (P3)

The roughness of the scale represents the corrugation of the surface on the scale top of the wool fibre. The surface roughness was measured on three different places on each scale on different scales in an area of 5 x 5 μm^2 as illustrated in Figure 4.2.

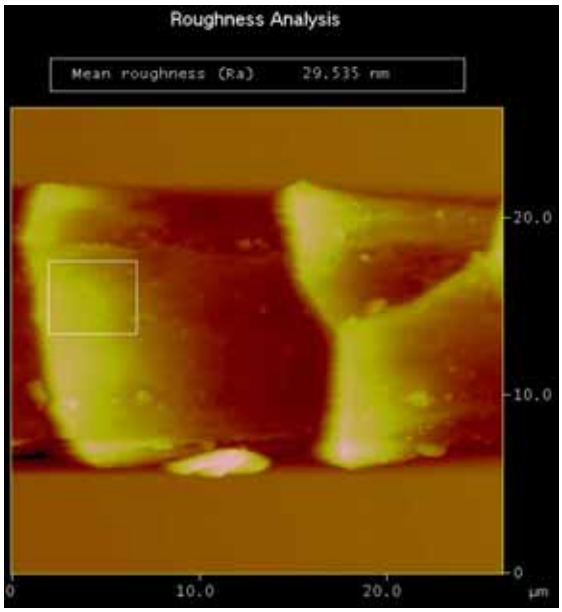

Figure 4. 2 : Measurement of the surface roughness of the scale top

The mean roughness (Ra) or P3 is the arithmetic average of the surface height deviation from the mean plane within the box marked, as illustrated in Figure 4.2. P3 is calculated according to the equation 4.1.

$$\textbf{Ra (P3)} = \textbf{1/n} \left(\sum_{i=1}^{n} |Zi|\right) \qquad \textbf{(Eq. 4.1)} \quad [1]$$

For the twenty images, which were taken for each sample (colour) the surface roughness was consequently determined in sixty measurements.

4.3.3 Scale Interval (P4)

The scale interval is the lateral distance between two scale edges. AFM images were used to measure the scale interval, for each sample forty measurements were taken. An example is displayed in Figure 4.3. The graph shows the cross section profile along the line in the image below, and the parameter P4.

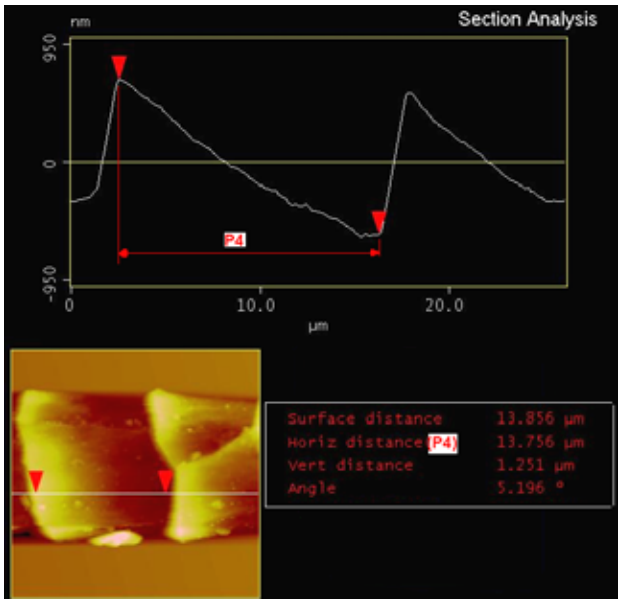

Figure 4. 3: Measurement of the scale interval

4.3.4 Normalized Contact Edge Length (P5)

The normalized contact edge length equals the mean length of the scale edge and / or fibre scale edge junctions (B), divided by the mean section width (A).

P5 is calculated according to the equation number 4.2.

$$P5 = B/A \qquad \text{(Eq. 4.2)}$$

Figure 4.4 shows the mean section width (A) and the mean length of the scale edge (B)

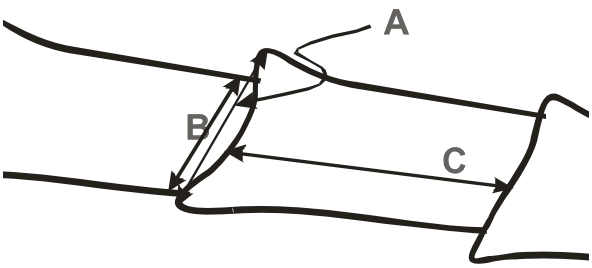

Figure 4. 4: The mean section width (A), the mean length of the scale edge (B) and the length of the scale (C)

For each sample twenty five measurements was taken. An example of the two parameters (A) and (B) is shown in Figure 4.5.

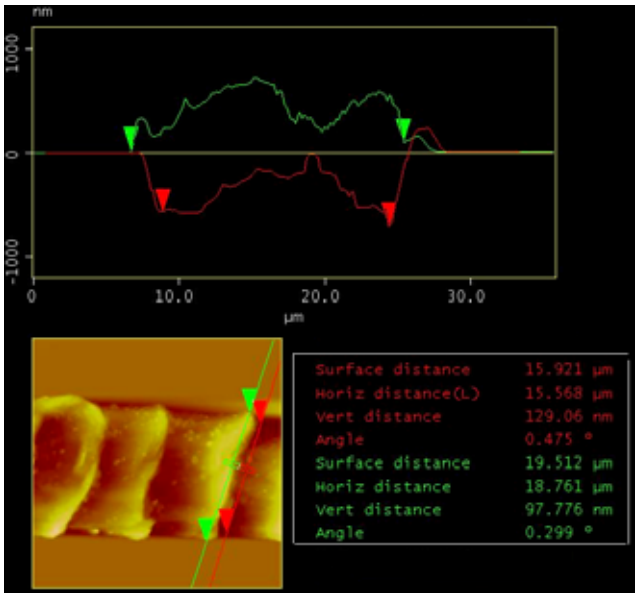

Figure 4. 5: Example of a normalized contact edge length measurement

4.3.5 Scale Elongation (P6)

This parameter measures the ratio between the length of the scale (C) parallel to the fibre and the width of the scale (A) perpendicular to the fibre. Examples of measuring the scale length and the scale width are illustrated in Figure 4.6.

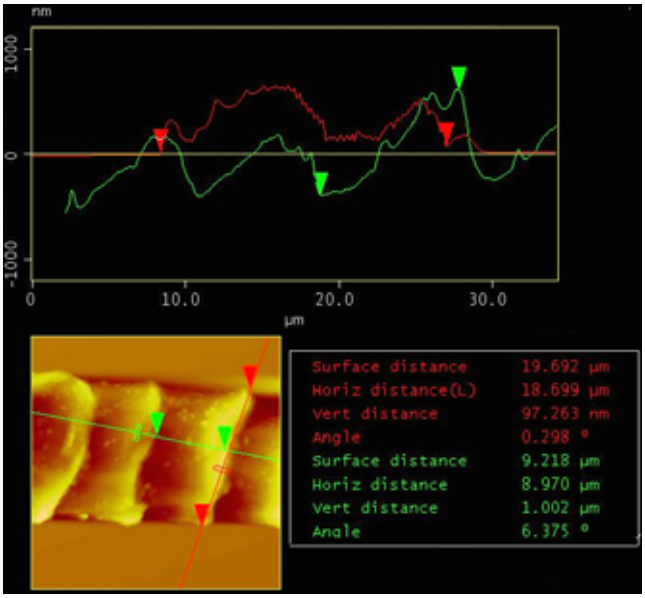

Figure 4. 6: Measurement of the scale elongation

P6 is calculated according to equation 4.3.

$$P6 = C / A \qquad \text{(Eq. 4.3)}$$

Where A is the mean section width and C is the length of the scale and both are illustrated in Figure 4.4. For each sample twenty five measurements was taken.

4.4 Force- Distance (F/D) Curves

Force-Distance curves were acquired in order to measure the surface energy (adhesive forces) of the wool fibres and in order to obtain an indication for the hardness of the fibre surfaces. These curves were recorded in contact mode, using a contact cantilever with a spring constant of K 0.2 N/m. For each sample twenty five F/D curves were captured. The same tip was used to measure all adhesive forces in order to avoid inconsistencies due to a variation in tip radii or spring constants.

4.4.1 Adhesive Forces (P7)

The adhesive force (F) is calculated using Hooke's law. The pull-off cantilever deflection X (the sudden vertical displacement in Figure 4.7) is multiplied by the spring constant (K = 0.2 N/m) of the cantilever:

$$F = -KX \qquad \text{(Eq. 4.4)}$$

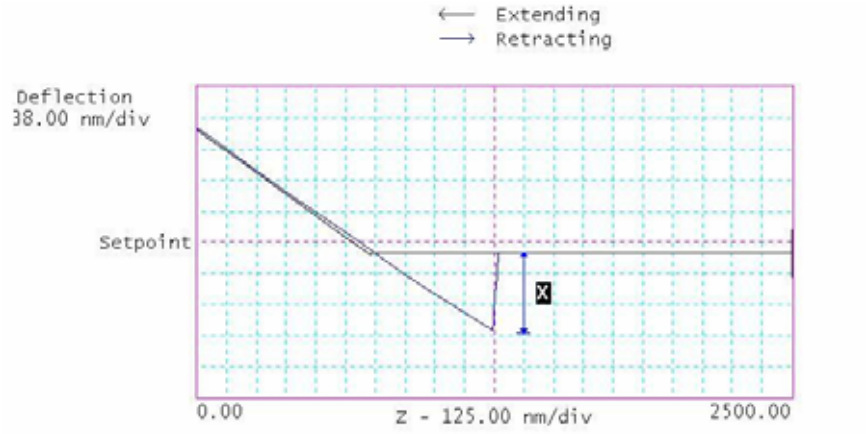

Figure 4. 7: General approach and retract force distance curves and measuring of P7

4.4.2 Relative surface hardness (P8)

The hardness of the sample surface is directly proportional to the gradient of the contact region of the F/D curve (Figure 4.8). The higher the slope, the harder is the sample surface. The slope is calculated according to equation 4.5.

$$S = (Y_2 - Y_1) / (X_2 - X_1) \qquad \text{(Eq. 4.5)}$$

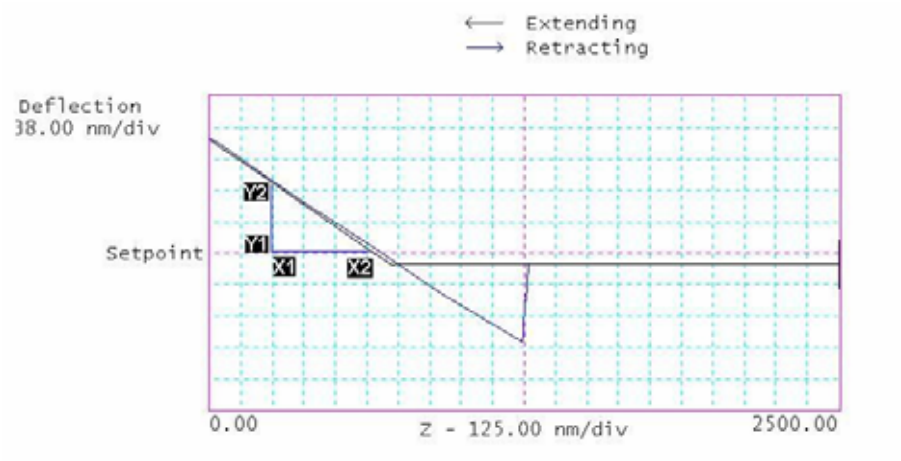

Figure 4. 8: General force distance curves and measuring of (P8)

4.5 Tensile Strength Measurements

4.5.1 Determination of an Adequate Sample Size:

Changes in the elastic properties of wool fibres and loss in tensile strength and elongation behaviour after dyeing are indicative of degradation. Because of this, tensile tests were performed and the results compared to the surface properties obtained from AFM images. Due to the variation in strength of the wool fibres it was important that an adequate number of fibres were tested [2] to ensure that the results are representative of the bulk.

When measuring the tensile strength in single wool fibres, it is therefore important to test a large number of fibres per sample. The quantity of tested fibres for each sample was calculated based on the standard deviation of the results of the pilot study (first sample set), using the statistical analyses method reported in Modern Statistics in Practice [3]. The sample size was calculated to predict an average value within a 95% confidence level and at a precision level (Cp) of 0.62. In this case fifty fibres were considered to produce satisfactory results. This amount of samples is equal to the standard sample amount of the British standard (BS 3411), and higher than the lowest sample size (40) of the US standard (ASTM D 3822), (see appendix D) [4].

4.5.2 Experimental Procedure

The Instron Model 4444 tensile strength tester was used to determine the tensile strength of individual fibres. This instrument is a CRE (Constant Rate of Extension) testing machine. The British Standard 1971 (BS 3411: 1971) tensile test method for single

wool fibres was used [5].

Single wool fibres were attached to a paper with adhesive tape across a rectangular gap as illustrated in Figure 4.9. The ends of the paper frame were clamped in the pneumatic jaws of the tensile tester. The extension rate was set to 10 mm per minute and a load cell with a maximum force of 50 N was used. Before operating the machine, the cardboard was cut across in the middle, which left the fibre clamped in the jaws without support and ready for testing [6, 4]. All measurements were performed in standard atmospheric conditions (a temperature of 20 ± 2ºC and a relative humidity of 65 ± 2%).

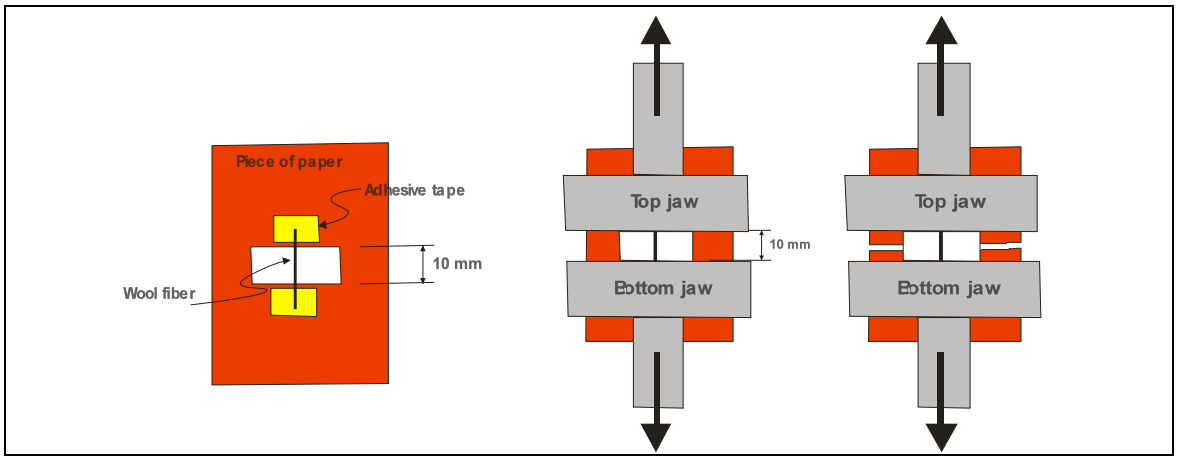

Figure 4. 9: Sample mounting procedure for tensile tests

A complete force extension curve up to the breaking point was obtained for all samples. For each colour a total of at least 50 (for some samples 60) separate fibres were tested. The breaking load, breaking extension, modulus at break, and other tensile properties were recorded.

Some results had to be discarded, based on the following problems [7]:

1) Jaw break: the specimen broke at the edge of the jaws (usually those samples have an elongation of less than 10 %).
2) Specimen slippage: the specimen slipped from between the jaws (usually those samples have an elongation of more than 90 %).
3) Faulty machine operation: the testing machine operated in a faulty manner.
4) Extreme results: the test result was beyond the generally accepted limits of variations. (While fluctuations in test data are expected, the test results should not be extreme, otherwise it is assumed that the specimen is not representative of the fibre being tested, and the result should be discarded.)

4.6 References

1. Veeco Metrology Group, *Digital Instruments, Nanoscope Command Reference Manual*. 1st ed., Digital Instruments /Veeco Metrology Group Inc., 2001. p.14 /25.
2. M. G. Huson, *The Mechanism by Which Oxidizing Agents Minimize Strength Losses in Wool Dyeing.* Textile Res. J., 1992. 62(1): p. 9-14.
3. A. Steyn, C. F. Smit, S. D. Toit and C. Strassheim, *Modern Statistics in Practice*. Academic Press, 1994. p. 393-396.
4. B. P. Saville, *Physical Testing of Textile*. 1st ed., Cambridge England, CRC Press LLC, 2002. p. 139-140.
5. British Standards Institution *BS Handbook 11: 1974, Methods of Test for Textiles*. Section 2. Fibres, London, BSI Publication, 1974. p. 2/35-2/39.
6. P. Mason, *The Fracture Of Wool Fibres Part I: Viscoelastic Nature Of The Fracture Properties.* Textile Res. J. 1964. 34 (9): p. 747-754.
7. A. C. Cohen, *Beyond Basic Textiles*. 1st ed., New York, Fairchild Publications, 1982. p. 26-27.

5 Results and Discussion

Discussions of the obtained results are divided into four main sections:

- Discussion of the surface characteristics of wool fibres obtained from AFM images and the effect of dye on the scale features.
- Discussion of the effect of the dyeing process on the tensile strength and fibre elongation at break.
- Discussion of the effect of dyeing with different colour lightness on the scale features tensile strength and elongation.
- The relationship between the surface changes and the changes in the tensile strength and elongation.

5.1 General Surface Features of Wool Fibre

Merino wool fibres were scanned in tapping mode and the topography images were captured. Several of the AFM images obtained on dyed and undyed wool fibres are depicted in Figures 5.1 to 5.10.

The general structure of an undyed fibre surface is illustrated in Figure 5.1, and the characteristic cuticle scales are resolved clearly. It can be observed that undyed wool has flat scales with well-defined scale edges, which are characteristic for wool. The scales tend to be of equal width. In almost all images the scales stretch across the entire fibre width, and therefore each scale has only two neighbours. Boundaries, which separate the neighbouring cuticular cells, are clearly defined.

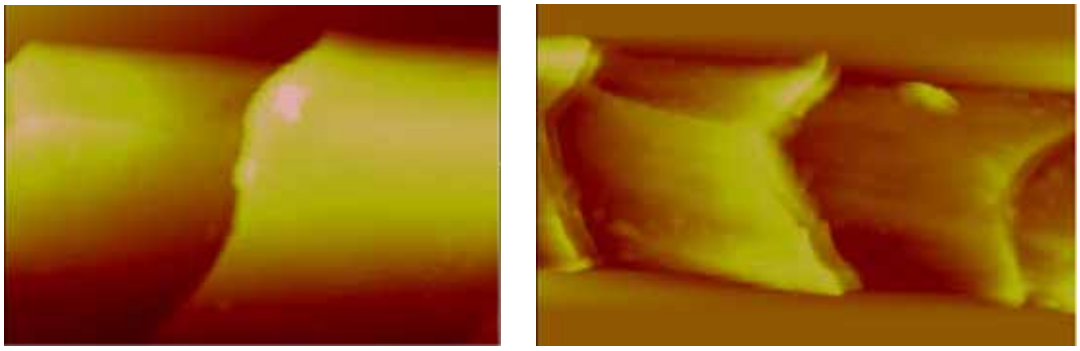

Figure 5. 1: Surface of undyed wool fibres.

Dyed fibres are shown in Figures 5.2 – 5.6. A comparison with the undyed fibres in Figure 5.1 shows clearly the significant morphological changes on the cuticle surface, which means that dyeing had a recognisable effect on the scale structure and in some cases even on the fibre cortex. The surface damage (due to processing) manifests itself mostly in the removal of fatty acids [1]. Also, the cuticular material is considered to be largely amorphous and highly crosslinked, mainly with disulphide bonds, which are highly susceptible to degradation at high dyeing temperatures [2]. The surface damage of the fibres, however, takes place in different degrees.

Pieces can be "chipped" off from the scales during dyeing, as illustrated in Figures 5.2 and 5.3. It is possible that mechanical stress during dyeing caused the chipping of the cuticle scales. The physical damage of the surface decreases the resistance of the surface against chemical attack, which has great impact on the dye uptake [3].

In addition to broken scales, scale edges can be raised or lifted compared to undyed samples, and also surface etching is clearly visible in Figure 5.3, where the fibre surface seems to be rougher.

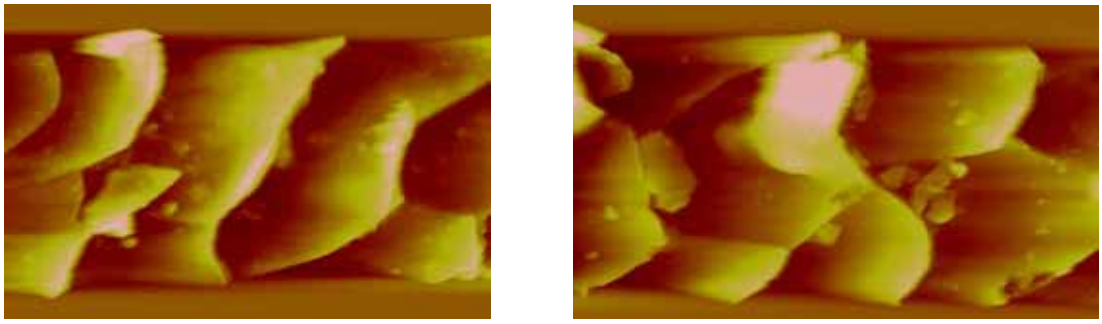

Figure 5. 2: Chipping of fibre scales due to mechanical stress during dyeing.

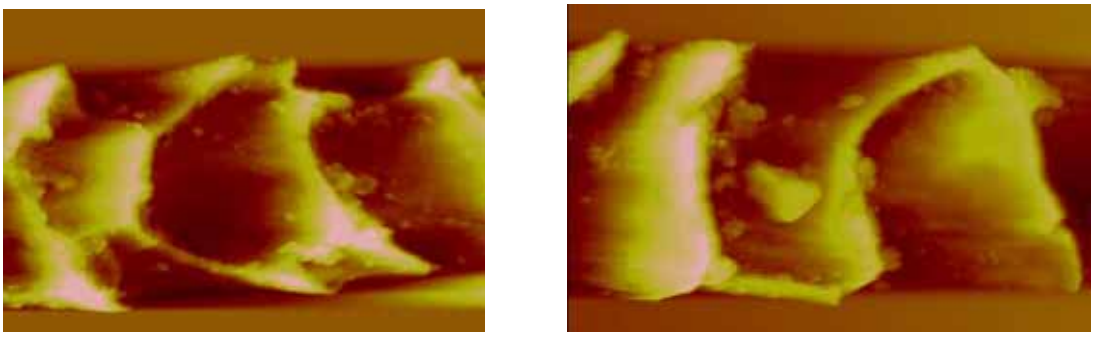

Figure 5. 3: Raised scales edges and severe damage underneath the scales.

Figures 5.4 and 5.5 show that the shape of the cuticular cells of dyed fibres appears to be similar to that exhibited in undyed fibres, but some damage was observed, such as scale "raising" and chipping of the scale edges. Although no stripping or complete removal of cuticular scales is observed in these images, the fibre surface appears to

have less topographical details in Figure 5.5, where the scales seem to be blurred. This might be either due to the dye molecules covering the scale surface or to the fact that part of the surface layer has been removed. The dye molecules cannot be resolved by AFM at this magnification level, therefore it is difficult to decide what exactly causes the surface modification.

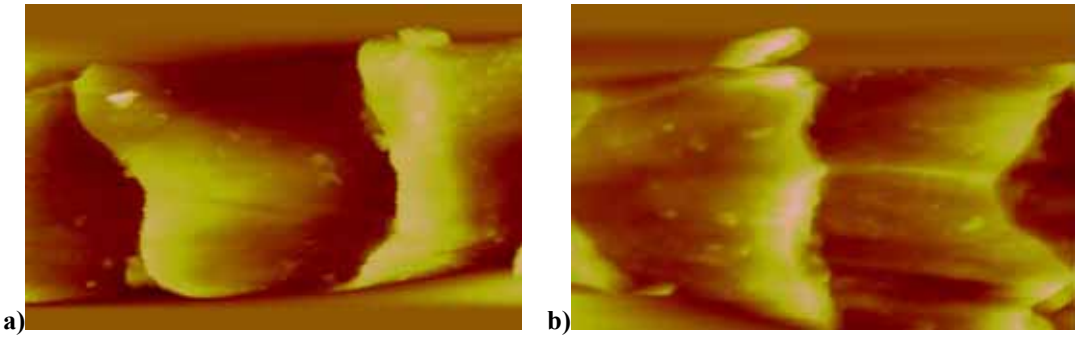

Figure 5. 4: Surface damage of wool fibres after dyeing: a) scale raising and b) scale chipping

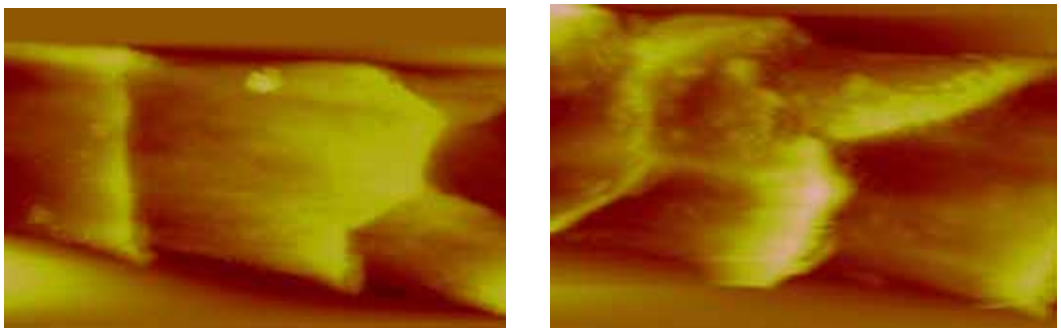

Figure 5. 5: Etched scale surface after dyeing.

"Fluting" of the cells on the scale edges can also be observed as shown in Figure 5.6. The fluting damage could be due to surface etching of the fibre or dissolved proteins from the surface leaving behind a wrinkled surface. The fluting could be related to the natural striations of the surface, which are illustrated in Figure 5.8.

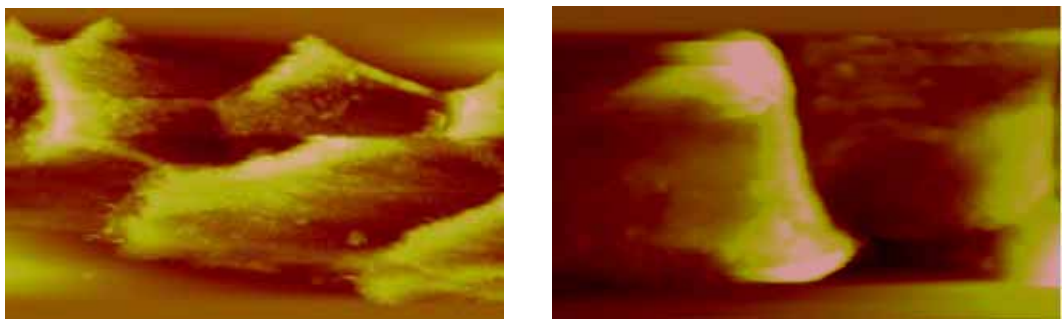

Figure 5. 6: Fluting of the scale surface after dyeing

Figure 5.7 shows severe damage on the surface and even inside the fibre, such as the formation of holes on the fibre, which is called "pitting", as well as scale edge chipping.

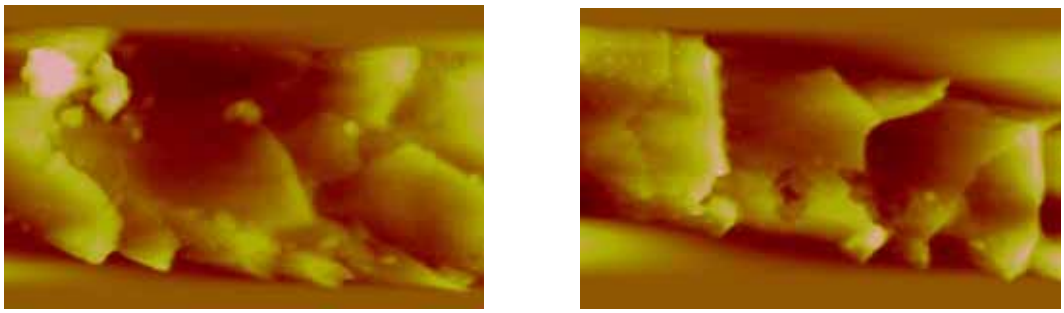

Figure 5. 7: Pitting of the fibre surface after dyeing

Generally images that show a uniform surface free from pitting, suggest that the dye is relatively homogeneously distributed on the fibre surface.

Some scale edges are raised, as can be seen in Figures 5.4 and 5.3. This was found mostly for dark colours. The outside of the scales seems to be more resistant to the dyeing chemicals than the soft underbody of the scale at the point where it is attached to the body of the fibre, which results in raised scales. This means that the scale could eventually be separated from the main shaft or underbody.

The images show that the chemicals used for dyeing could affect and raise the protruding edges of the scales above the main body of the fibre. In other words, the fibre material might be degradated or removed from underneath the scale, which leads to an increase in the scale height. From the AFM images it can also be seen, that dissimilarities exist on the surface of wool fibres at the junctions between overlapping scale cells. Fractions could advance from one of these junctions if there was no crack or notch along the length of the fibre at which the failure had developed earlier. The most apparent surface modifications were chipping, pitting, fluting of the cells and raising of scale edges.

The morphology of the scale surface is better resolved in three dimensional images in Figures 5.8 - 5.10.

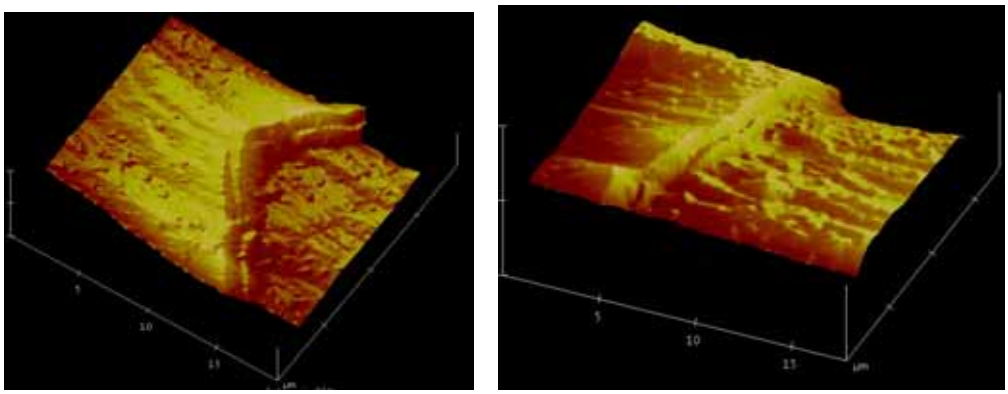

Figure 5. 8: 3D image of undyed wool fibre

Figures 5.8 - 5.10 show fine, uniform striations parallel to the fibre axis especially around the scale edge. The images suggest that the surface has a ridge and groove structure. These ridges have a height in the range of 50-200 nm and a distance of 500-1000 nm. Some of these ridges have a length of more than 5µm. These results agree well with results reported in literature [4, 5].

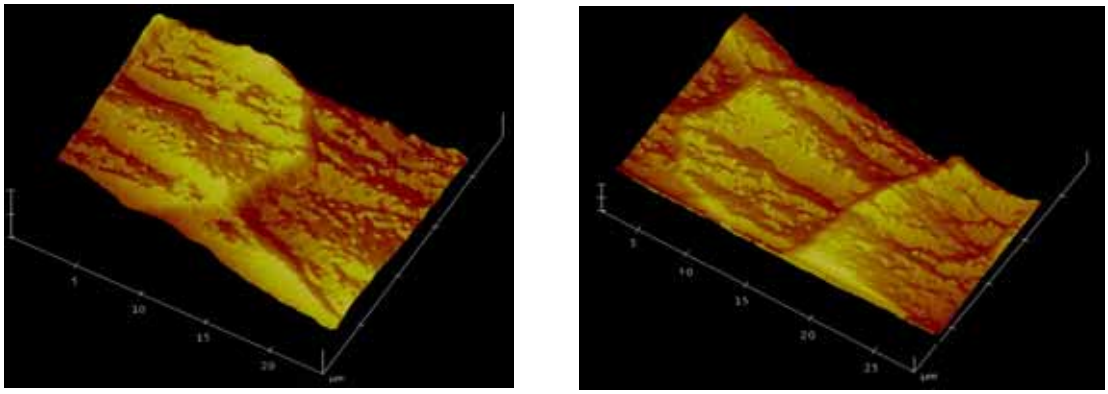

Figure 5. 9: 3D image of blank dyed fibres

Figure 5.9 shows the surface changes for a blank dyed sample. The surface appears to have changed, which could be due to degradation of proteins on the surface as a result of the acid attack, exposure to dyeing liquid in the dye-bath and elevated dye-bath temperature. Indications of fluting can also be seen in these images.

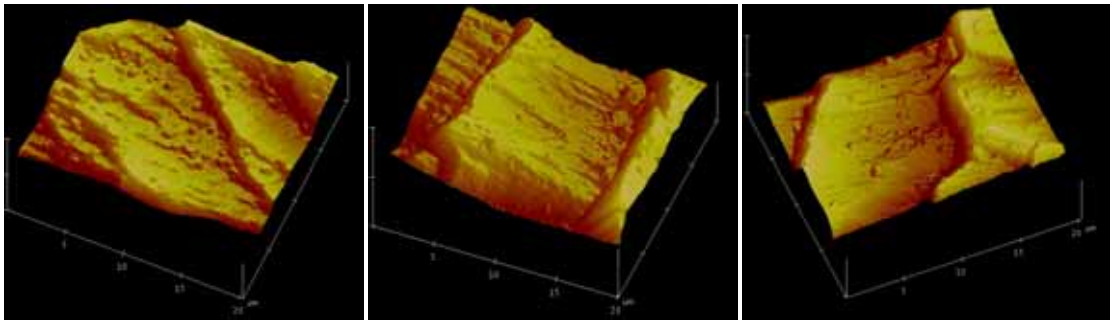

Figure 5. 10: 3D image of dyed wool fibres

Figure 5.10 shows changes in the scale surface after dyeing. A clear separation line in the contact area between the two scales is visible. The change in the height of the ridges, which could be due to dyeing, is accounted for in the surface roughness measurements.

5.2 *Pilot Study (Comparison of the effect of dyeing on two different fibre diameters in the first sample set)*

5.2.1 Surface Characteristics of the Scales of Dyed and Undyed Wool Fibre

From measuring eight different surface parameters (P1-P8) of undyed fibres and fibres dyed black and navy with Lanasol reactive dye, with a diameter of 18.5 and 20 µm respectively, the following results were obtained. All figures illustrate the distribution of the measured parameter based on statistical measurements of twenty images acquired along five different fibres resulting in 100 measurements for each sample.

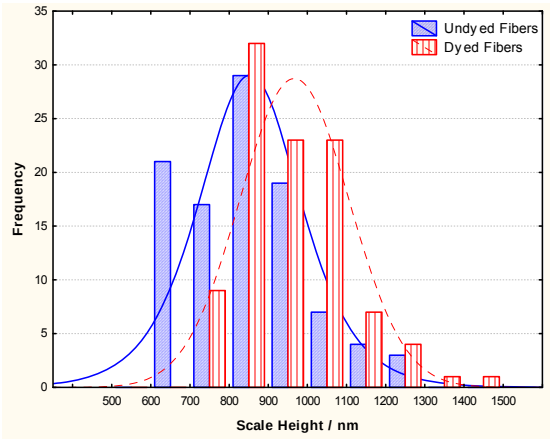

Figure 5. 11: **Cuticle scale height of dyed and undyed fibres with a diameter of 18.5 µm**

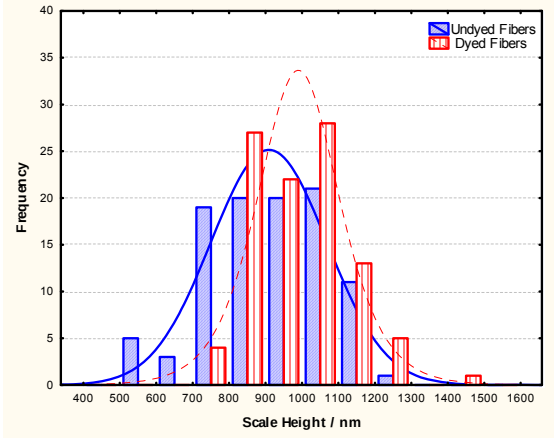

Figure 5. 12: Cuticle scale height of dyed and undyed fibres with a diameter of 20 µm

Figures 5.11 and 5.12 show the distribution of the cuticle scale height of dyed and undyed fibres with a diameter of 18.5 and 20 µm. For both fibre types a slight shift to higher values can be observed after dyeing. The distribution of the 20 µm dyed fibres is narrower than for the undyed fibres in contrast to the 18.5 µm fibres, where dyed and undyed fibres have a similar, fairly narrow distribution. The scale height seems to be increased by the dyeing processes independent of the fibre diameter. This increase could be explained by the deposition of dye molecules on the surface, in addition to damage of the area underneath the scale junction as displayed in Figures 5.29 and 5.20.

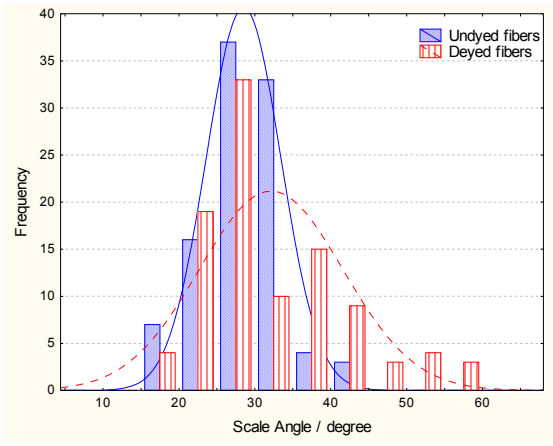

Figure 5. 13: Scale angle of dyed and undyed fibres with a diameter of 18.5 µm

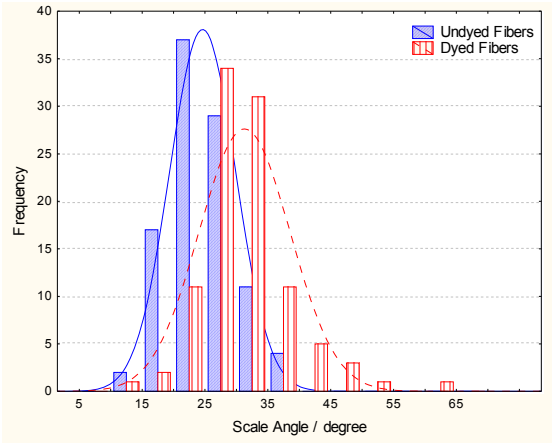

Figure 5. 14: Scale angle of dyed and undyed fibres with a diameter of 20 µm

Figures 5.13 and 5.14 show the distribution of the cuticle scale angle. Generally it seems as if the distribution becomes wider after dyeing, although this is more noticeable for the 18.5 µm fibres. The distribution width corresponds to irregularities in the scale angle, which results from heterogeneous damage to the scale edges. For both samples the average step angle increases after dyeing.

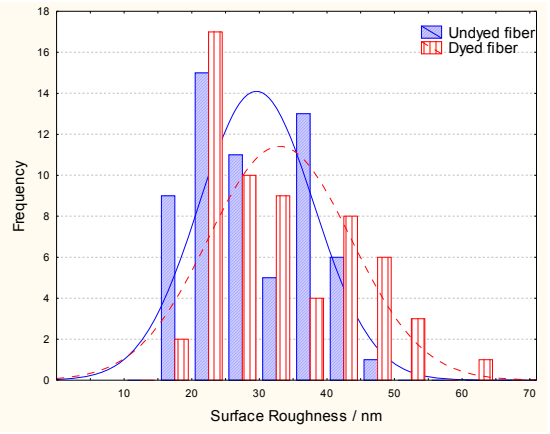

Figure 5. 15: Surface roughness of the cuticle of dyed and undyed fibres with a diameter of 18.5 µm

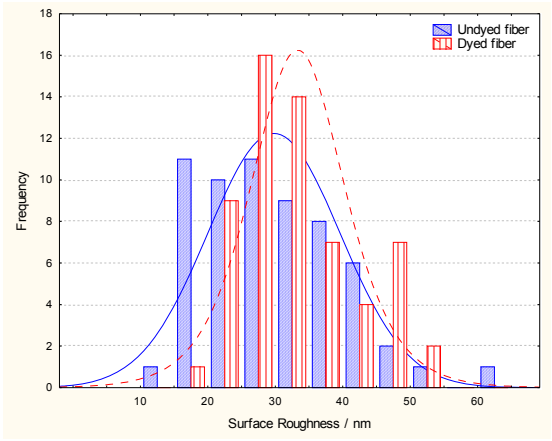

Figure 5. 16: Surface roughness of the cuticle of dyed and undyed fibres with a diameter of 20 µm

The distributions of the surface roughness on the scale top are shown in the Figures 5.15 and 5.16. It appears as if the distribution becomes wider for dyed fibres, especially in the case of the 18.5 µm fibres. The shift of the peaks to higher values after dyeing indicates an increase in the surface roughness of the scale due to damage that occurred during dyeing.

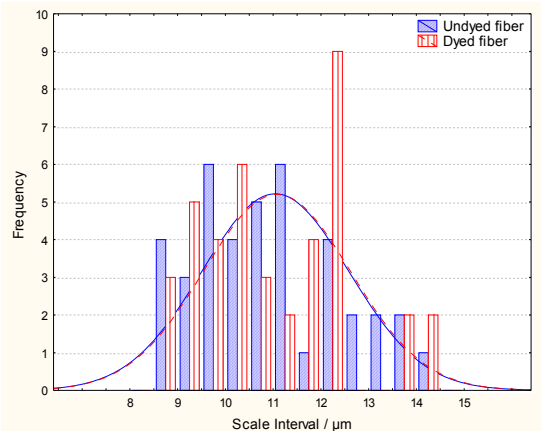

Figure 5. 17: Cuticle scale interval of dyed and undyed fibres with a diameter of 18.5 µm

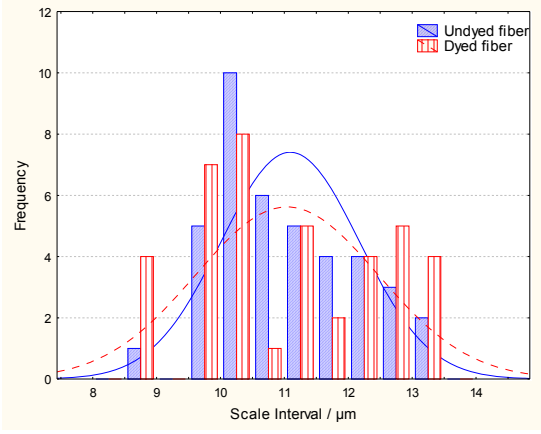

Figure 5. 18: Cuticle scale interval of dyed and undyed fibres with a diameter of 20 µm

Figures 5.17 and 5.18 show the distribution of the cuticle scale intervals for dyed and undyed fibres. There is no change in the distribution of the 18.5 µm fibres after dyeing. In contrast, the distribution becomes wider after dyeing for the 20 µm fibres. In both cases, however, the average value remains almost the same before and after dyeing.

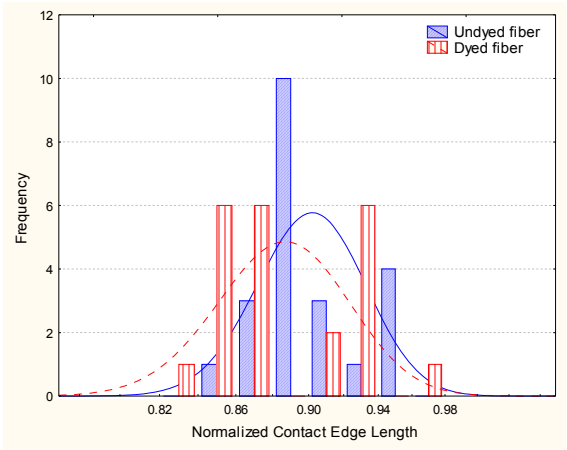

Figure 5. 19: Normalized contact edge length of dyed and undyed fibres with diameter of 18.5 µm

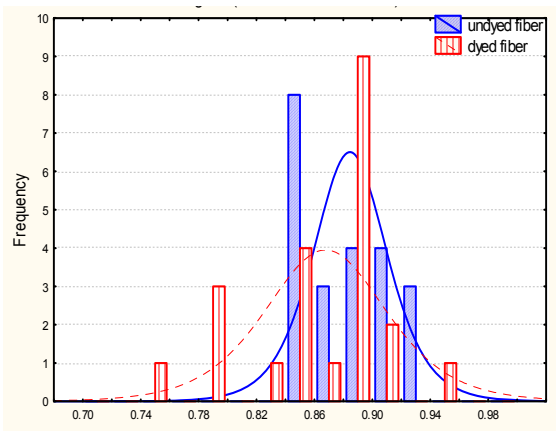

Figure 5. 20: Normalized contact edge length of dyed and undyed fibres with diameter of 20 µm

Figures 5.19 and 5.20 illustrate the distribution of the normalized contact edge length for dyed and undyed fibres. The dyed fibres results show a wider distribution than undyed fibres, especially in Figure 5.19. The average value is shifted slightly to lower values, which indicates that dyeing has a larger effect on the lower edge of the scales (scale edge junction line B in Figure 4.5) than on the top edge of the scale (line A in Figure 4.5). This wear or damage to the junction area indicates that dye molecules diffuse into the wool fibre through the cell edges rather than any other part of the wool surface, which confirms results from Wortmann et al. [4].

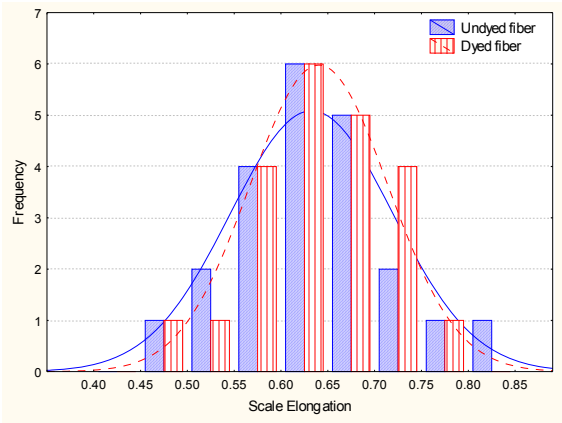

Figure 5. 21: Scale elongation of dyed and undyed fibre with a diameter of 18.5 µm

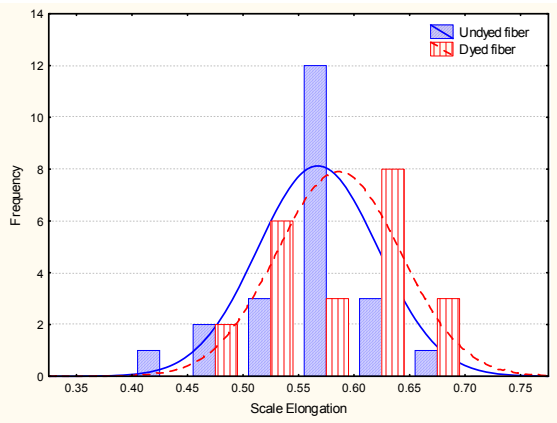

Figure 5. 22: Scale elongation of dyed and undyed fibres with a diameter of 20 µm

The distribution of the scale elongation is illustrated in Figures 5.21 and 5.22. It is almost the same for both fibre diameters, and the average value for 18.5 µm fibres remains the same after dyeing, which means that dyeing has no or little effect on the scale elongation.

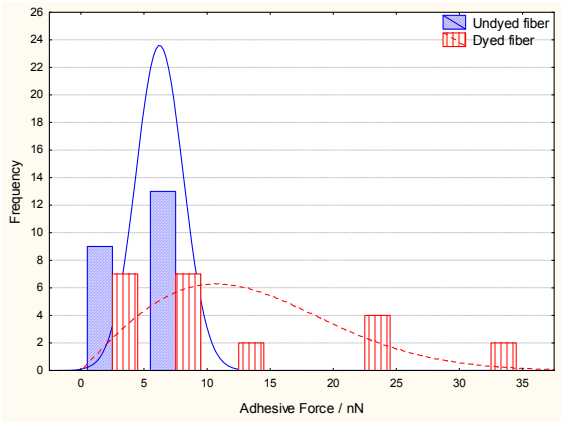

Figure 5. 23: Adhesive force of dyed and undyed fibres with a diameter of 18.5 µm

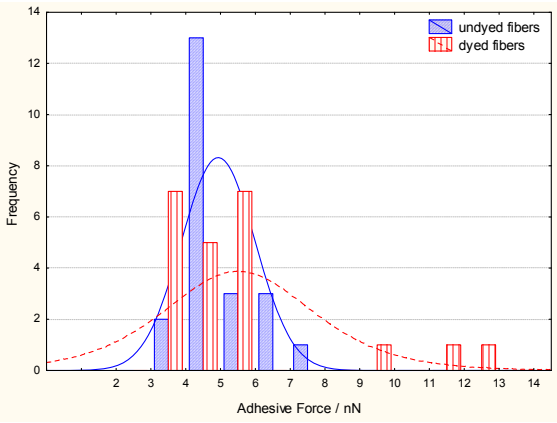

Figure 5. 24: Adhesive force of dyed and undyed fibres with a diameter of 20 µm

Figures 5.23 and 5.24 show there is generally a large change in the distribution of the adhesive force after dyeing. The distribution is narrow before dyeing, which indicates a homogenous chemical surface. This homogeneity is reduced during dyeing and the surface becomes heterogeneous, as can be seen from the broad peaks in the Figures 5.23 and 5.24 of both fibre types after dyeing. The damage in the epicuticle layer (covalent bonds of fatty acids in the top layer of the scale surface) leads to a more hydrophilic surface with less homogeneity. These results confirm the results obtained by Negri [5]. Another possible explanation for the broad distribution is that some of the dye molecules aggregate on the wool surface.

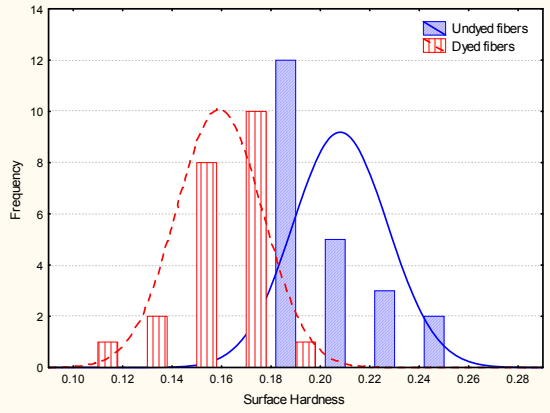

Figure 5. 25: Relative surface hardness of dyed and undyed fibre with a diameter of 18.5 µm

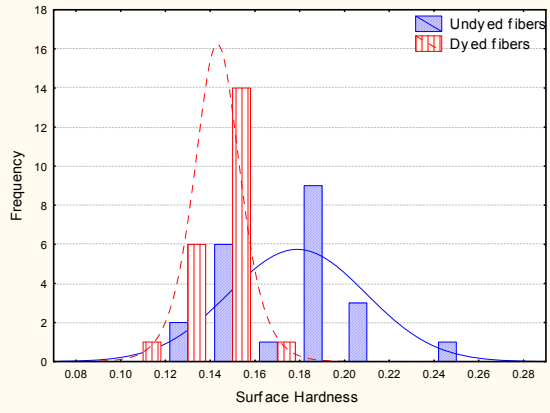

Figure 5. 26: Relative surface hardness of dyed and undyed fibres with a diameter of 20 µm

Figures 5.25 and 5.26 illustrate the distribution of the relative surface hardness of dyed and undyed fibres. It appears that the surface hardness of dyed fibres has a similar distribution to that of undyed fibres for the 18.5 µm fibres. For 20 µm fibres the distribution becomes narrower after dyeing. In both cases the average relative hardness decreases after dyeing, which indicates that the extensive disulfide bonds in the cuticle layer, which are responsible for the high rigidity of the outer layer of wool fibres were damaged. As the relative hardness decreases the depth of the damage ranges deeper into the wool fibre [2].

All the figures above indicate that the surface damage caused by dyeing occurs both in the cuticle layer and deeper in the cortex layer as indicated by Figures 5.7, 5.23 and 5.24. Under dyeing conditions, disulphide bonds can be broken, amide bonds hydrolysed to lower the molecular weight of the peptide chains and the polypeptide chains of the surface and the inner part of the wool fibre are attacked by acetic acid, which is used as solution medium. This can lead to damage of the surface [7-9].

A comparison of the data and the distribution of different surface characteristics of undyed and dyed fibres, which are illustrated in Figures 5.11 – 5.26, shows clearly that the average values of the scale parameters can be used to obtain an indication of the surface damage caused by dyeing. The average values with standard deviations for all these characteristics are illustrated in tables 5.1 and 5.2 in order to make a comparison between dyed and undyed fibres easier.

Table 5.1 shows the average values with standard deviations and the change in the measured parameter as a percentage of the undyed sample (P %) for fibres with a diameter of 18.5 μm, where

$$P\ \% = |P_{undyed} - P_{dyed}| / P_{undyed}$$

Table 5.1: Scale parameters of undyed and reactive dyed fibres with an average diameter of 18.5 μm

Scale Parameters (P)	Undyed	Dyed	P %
Scale Height (P1)	846.4 ± 153.73	963.57 ± 158.1	+13.84
Step Angle (P2)	25.25 ± 3.94	31.9 ± 9.3	+26.33
Roughness of the Scale Top (P3)	29.43 ± 7.827	32.84 ± 10.2	+11.58
Scale Interval (P4)	11.03±1.50	11.05 ± 1.52	+0.18
Normalized Contact Edge Length (P5)	0.902±0.029	0.882 ± 0.035	–2.22
Scale Elongation (P6)	0.631± 0.082	0.634 ± 0.073	+0.43
Adhesive Force (P7)	6.186 ± 1.8	10.9 ± 6.6	+76.20
Relative Surface Hardness (P8)	0.207 ± 0.018	0.158 ± 0.017	–23.67

Table 5.2 shows the average values with standard deviations and the change in the measured parameters as percentage of the undyed sample (P %), for fibres with a diameter of 20μm.

Table 5. 2: Scale parameters of undyed and reactive dyed fibres with an average diameter of 20 μm

Scale Parameters	Undyed	Dyed	P %
Scale Height (P1)	882.58 ± 156.3	986.8 ± 164.1	+11.81
Step Angle (P2)	24.35 ± 5.5	31.1 ± 7.2	+27.6
Roughness of the Scale Top (P3)	29.64 ±9.3	33.14±8.3	+11.81
Scale Interval (P4)	11.064 ± 1.06	11.02±1.40	–0.36
Normalized Contact Edge Length (P5)	0.896 ± 0.029	0.869 ± 0.05	–3.01
Scale Elongation (P6)	0.579 ± 0.053	0.584 ± 0.054	+0.86
Adhesive Force (P7)	4.9 ± 1.03	5.48 ± 2.5	+13.02
Relative Surface Hardness (P8)	0.18±0.028	0.143± 0.011	–20.85

Comparison of the average surface characteristics of 18.5 μm and 20 μm fibres shows that the fibre diameter has no great influence. For example, the increase in % of the average scale height for 18.5 μm fibre is 13.84 %, and for 20 μm fibres 11.81 %.

However there is no clear explanation for the huge increase in the adhesive force for 18.5 μm fibres if compared with 20 μm fibres. The difference could be as a result of the different origin of the 18.5 and 20 μm wool fibres. The standard deviations for 18.5 μm fibres are, however, smaller than for 20 μm fibres in most cases. All dyed samples showed large standard deviations compared to the undyed samples, which indicates heterogeneous changes on the fibre surface.

5.2.2 Tensile Test Results

The tensile strength of individual wool fibres was determined with tensile tests. An average of fifty fibres was measured for each sample and reported as the breaking load. Breaking extension was reported in mm per 10 mm gauge length. The results for undyed and dyed fibres with a diameter of 18.5 μm are illustrated in table 5.3

Table 5. 3: Average breaking load and extension of undyed and dyed fibres with an average diameter of 18.5 μm.

Parameters	Undyed	Dyed	P %
Av. breaking load (N)	0.120 ± 0.035	0.104 ±0.037	–13.33
Av. breaking extension (mm)	5.78 ±2.17	5.091 ±2.22	–11.92

Table 5.4 shows the tensile test results of undyed and dyed fibres with a diameter of 20μm.

Table 5. 4: Average breaking load and extension of undyed and dyed fibres with an average diameter of 20 μm.

Parameters	Undyed	Dyed	P %
Av. breaking load (N)	0.144 ±0.029	0.121 ±0.038	–15.9
Av. breaking extension (mm)	6.09 ±1.38	5.068 ±2.028	–16.8

It is apparent that the thinner fibres show less breaking extension and lower breaking load than the thicker fibres. In both cases the average breaking extension of the fibre as well as the average breaking load decreases after dyeing. These results confirm earlier results by Gullbrandson [7] that wool fibres lose tensile strength after dyeing process. Tables 5.3 and 5.4 show that the breaking load for 18.5μm fibres decreases after dyeing by about 13.33 %, which is less than the decrease percent of the breaking load of the 20μm fibres, which is 15.9 %. Similar to the breaking load the breaking elongation decreases with 11.92 % and 16.8 % for 18.5 μm and 20 μm fibres respectively.

These results indicate that as the fibre diameter increases, the decreases in the breaking load and extension both become more noticeable. The standard deviations for both dyed and undyed fibres are high, which could be the results of variations in the fibre alignment between grips, fibre crimp, pre-tension and fibres cross-section. These and other factors can influence fibre breakage, which results in the high standard deviations.

Figure 5.27 shows the relation of fibre breaking load to breaking elongation for the two different fibre diameters of 18.5 µm (a) and 20 µm (b), before and after dyeing.

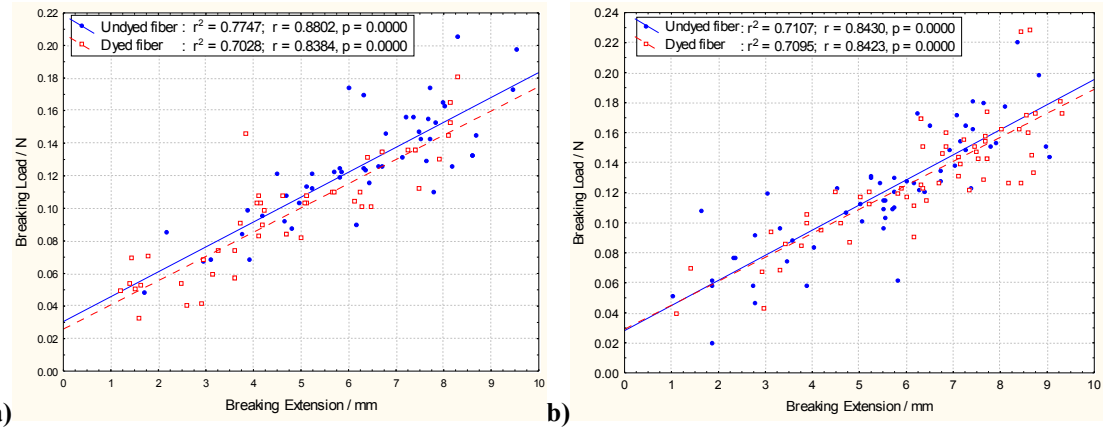

a) b)

Figure 5. 27: **Breaking load as a function of breaking extension for dyed and undyed fibres with. a) 18.5 µm and b) 20 µm diameter.**

The simple correlation coefficient r, which is dimensionless and indicates how strong the variables (in this case breaking load and elongation at break) correlate, is 0.8802 and 0.8384 for undyed and dyed 18.5 µm fibres respectively. For the 20 µm fibres it is slightly lower: 0.843 for undyed fibres and 0.8423 for dyed fibres. It seems as if due to dyeing the correlation between the elongation and the load at break becomes weaker for both fibre types. The results are scattered throughout the range of fibre elongation, indicating surface damage rather as reason for a loss in strength than fibre bulk properties. The effects of surface damage due to the environmental and other external factors such as cleaning and scouring [10] are also noticeable if the two undyed fibres are compared. Environmental effects are involved, exposure of the wool to weathering, moisture, heat, and sunlight (UV). To minimize these effects, only fibres from the same lot with close diameters were investigated.

5.3 Second and Third Sample Sets (Comparison of the effect of dyeing and dye concentration)

5.3.1 Scale Height (P1)

Figure 5.28 shows the changes in the average scale height (P1) for a variety of colours, for both sample sets. The actual scale height distribution for each sample is given in Appendix C.

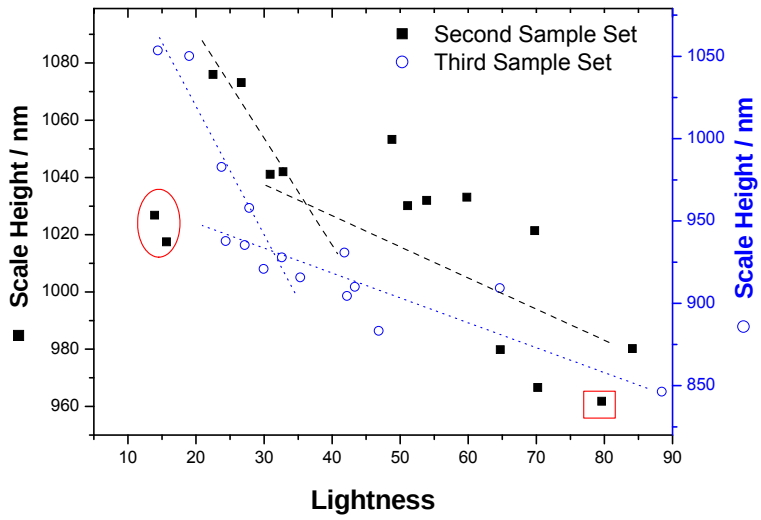

Figure 5. 28: Changes in the scale height as a function of the lightness value

In both sample sets the average scale height of the undyed fibres (samples with lightness values of 88.45 and 84.12) is within the published range of the cuticle scale height for wool fibres [11]. This result is also consistent with reports of Liu et al. [12]. It is apparent that the average scale height generally increases as the colour becomes darker. For both sets a point can be determined within lightness range of 30 to 40 at which the gradient increases drastically. Colours with a lightness value below this point can be expected to show different tensile strength and breaking extension behaviour and could be referred to as "dark" colours.

The increase in P1 can be explained by surface degradation, which breaks the polypeptide structure in the joint area between two scales during dyeing. This area is considered the weakest part in the fibre [13] (Figure 5.29). It can be expected that small cracks or flaws start to grow and as the colour becomes darker, the possibility that this initial crack grows, increases further. This can also be seen in the noticeable change in the tensile strength due to increased damage of the fibre underneath the scale edge.

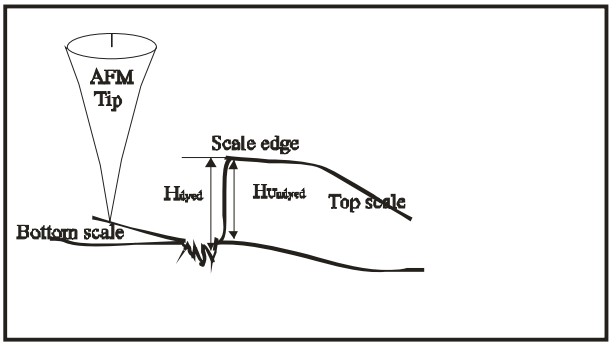

Figure 5. 29: Possible reason for a change in the scale height after dyeing

Another possibility for the increase in P1 could be that the dye molecules cover the top scale (Figure 5.30), and therefore P1 increases even if the joint area has not been degraded. This should, however not be more than a few nanometres, and it is therefore not a suitable explanation for dark colours, where the increase of P1 is about 100 nm.

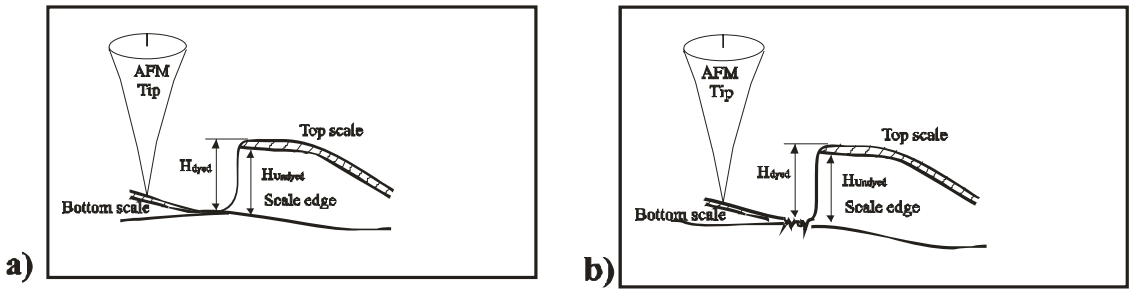

Figure 5. 30: Two other possible explanations for the height changes after dyeing. a) is more likely for light colours and b) is more likely for dark colours.

Figures 5.29 and 5.30 show that the height increases mainly due to severe damage to the soft underbody of the scale at the point where it is attached to the body of the fibre. Therefore, it could be expected that on the fibres dyed with dark colours the scale might eventually be separated and parted from the main shaft or underbody, which could lead to a loss in the elongation properties and fibre strength. This assumption is supported by the literature [14] and by Figure 5.10.

Dye molecules diffusing along the cell membrane complex, between the cuticles, work as catalysts or auxiliary agents to damage the junction regions between the overlapping scales together with acid, heat and water (similar to the way environmental stress cracking works). The degree of damage is also affected by the concentration of the dyestuff in the dye bath: high concentration leads to more surface damage, which is shown by the huge increase in the scale height for samples with dark colours. For

darker colours a higher concentration of dyestuff is needed to diffuse through the cuticle layer into the cortex and with the darkness of the colour the concentration of the dye inside the fibre increases, which results in more damage and therefore a larger change in P1.

Figure 5.28 shows that Lanasol reactive dye (marked by a circle in Figure 5.28) has less effect on the scale height, even though the colour of the two Lanasol dyed samples is darker (15.67, 13.94) than that of Lanaset metal complex dyed fibres. This means that reactive dyes inflict less damage to the wool surface.

Additionally it was found that the second sample set (fibres from the same lot) shows less change in P1 than the third sample set. The large changes in the third sample set could be explained by the variation in fibre surface features due to the fact that the fibres did not originate from the same lot [15].

In some cases it was found that dyeing destroyed surface features, which led to a decrease in P1 as illustrated in Figure 5.31. This describes an abnormal fibre surface, where the scale features show distinct signs of degradation.

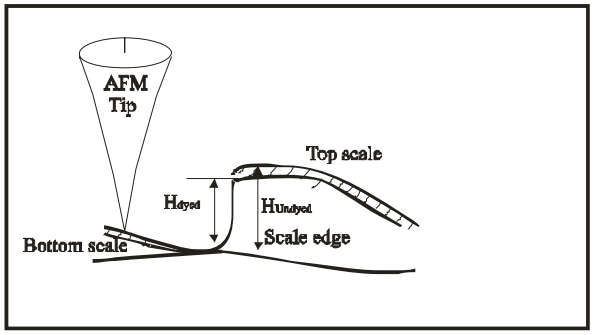

Figure 5. 31: Possible reason for a decrease in scale height after dyeing

For the blank dyed sample (marked by a square in Figure 5.28) with a lightness value of 79.6 and the sample with a lightness of 70.2, the scale height decreased compared to the undyed sample. It seems as if in those cases the top of the scale was etched away and the dye molecules were not distributed evenly on this part of the fibre surface.

5.3.2 Step Angle (P2)

Figure 5.32 shows the change in the average step-angle versus the lightness. Similar to the scale height the step angle increases with increasing depth of shade. Because the scale top is less susceptible to damage than the joint area between the two scales [16],

P2 is increased after dyeing, especially in the case of dark colours, where the step edge is affected by the serious damage in the underbody of the scale at the point where it is attached to the fibre body as explained before.

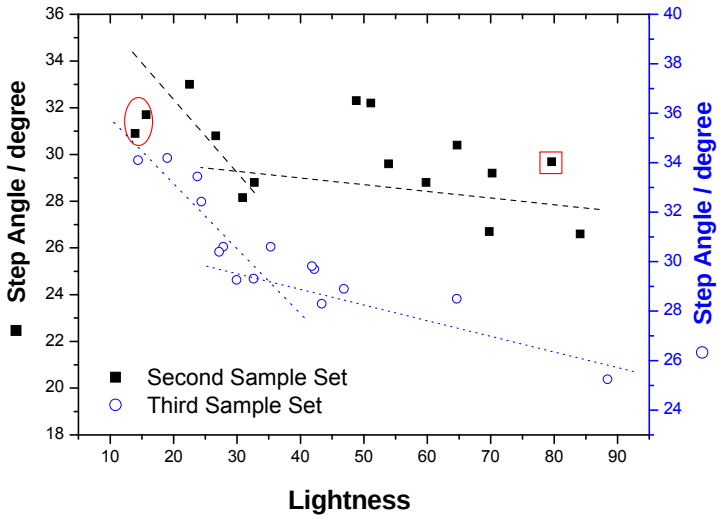

Figure 5. 32: Changes in the step angle as a function of the lightness value

Additionally, the dye molecules diffuse through the scale top (trans-cellular diffusion) into the cortical layer of the fibre, which causes slight damage, and as the colour becomes darker the number of passed dye molecules increases and the damage becomes more noticeable. The change in the step angle will thus be more noticeable for dark colours than for light colours.

For both sets a point can be determined at which the gradient increases drastically. Similar to the scale height this point lies between a lightness value of 30 and 40. Colours with a lower lightness value can be regarded as “dark” and can be expected to show different physical and mechanical properties.

The area underneath the scale edge is not homogenously etched away along the scale edge from bottom to top and along the fibre width, which leads to variations in the step angle from one sample to another and also to a high variation in the step angle, within the same sample (see Appendix C).

As for the scale height, Lanasol reactive dyes (marked by a circle) show less effect on the scale angle than Lanaset dyes, which confirms the earlier observation that reactive dyes cause less damage to the wool surface. This result is consistent with Parton`s findings [17]. The lower damage caused by Lanasol reactive dye could be due to the additional crosslinks, which are produced by the reactive dyes. This also indicates that

the changes in the parameters P1 and P2 depend more on the dye types than on the other materials in the dye bath, such as the softening solution or carrier solution.

5.3.3 Surface Roughness of the Scale Top (P3)

The third surface property measured as a function of the lightness degree, was the surface roughness of the scale top. AFM images reveal a large variation of P3, as illustrated by the changes in the ridge and wrinkle heights in Figures 5.7- 5.9, which result in large deviations from the average value of the surface roughness. Generally the surface roughness of the fibre increases after dyeing. The effect of the surface etching is obvious, the fibre surface becomes rougher and some scale edges are raised. The increase in the surface roughness could be due to two reasons: the dyeing chemicals are etching or eroding the surface and due to mechanical effects [3]. By taking only the surface roughness of the scale top into account mechanical effects can be eliminated. P3 versus the lightness is shown in Figure 5.33.

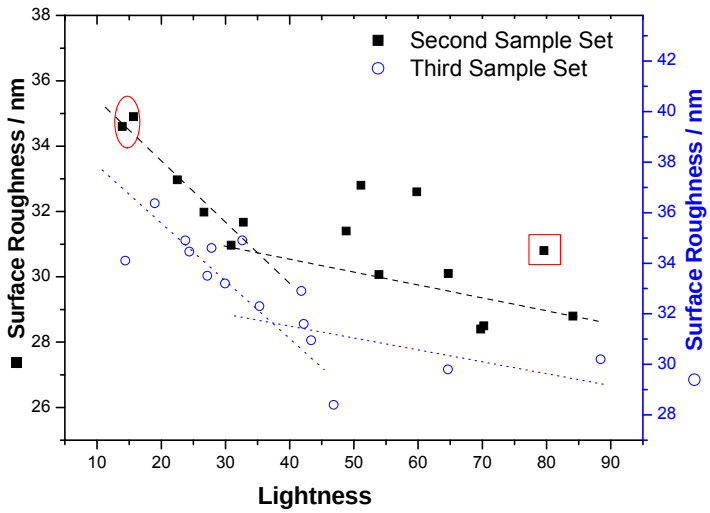

Figure 5.33: Changes in the surface roughness as a function of the lightness value

Generally lighter colours showed a smoother surface than fibres dyed with darker colours. The mechanism of the change in P3 can be explained by the chemical and mechanical wear of the fibre surface, resulting in chipping or stripping of some of the scales from the fibre surface. Also, the dye molecules can diffuse into the wool fibre through the cuticle layer, which damages the surface slightly and increases P3. As the colour becomes darker the number of passed dye molecules increases and the damage becomes more noticeable. P3 is therefore clearly affected by the concentration of the dyestuff in the dye bath. A higher concentration leads to more surface damage as is

clear from the huge increase in P3 for darker colours.

It can also be noticed that some samples with lighter colours have a lower surface roughness than the undyed fibres. This could be because of the chipping or the etching of the surface during dyeing. As small pieces chip away from the scale edges, a fresh cuticle surface is revealed that is relatively smooth, even when it is covered with dye molecules. Because there are less dye molecules in the dye bath for lighter colours, the possibility of the dye molecules to react with the polypeptide on the surface that has been formed during the dyeing process, is less and therefore the fresh surface will stay smooth as it is.

It is also clear that P3 for Lanasol dyed samples follows the same trend of Lanaset dyed samples, which indicates that the change in the surface roughness does not depend on the dye type, as was found for P1 and P2.

5.3.4 Scale Interval (P4)

The fourth parameter that was measured and plotted versus the lightness degree is the scale interval. The average values of the undyed fibres from both sample sets are very close to the value of 10.1µm published by Robson et al. [18]. P4 as a function of colour lightness is shown in Figure 5.34.

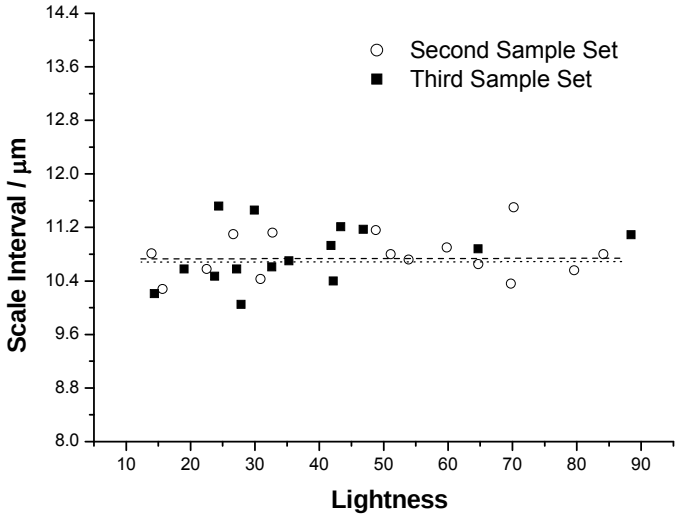

Figure 5.34: Changes in the scale interval as a function of the lightness value

Generally P4 does not change much after dyeing, and it can be used to ensure that the observed scales are in the same range, because along the fibre length the scale height

could vary with the scale interval by more than 20 %, depending on the scale interval, which can vary from 4 to 18 µm along the fibre [14]. By acquiring images only of scales with an average scale interval of 9 – 13 µm the variation in scale height can be minimized to less than 5%.

5.3.5 Normalized Contact Edge Length (P5)

Figure 5.35 shows the change in the average normalized contact edge length for each scale edge in the acquired images versus the lightness value.

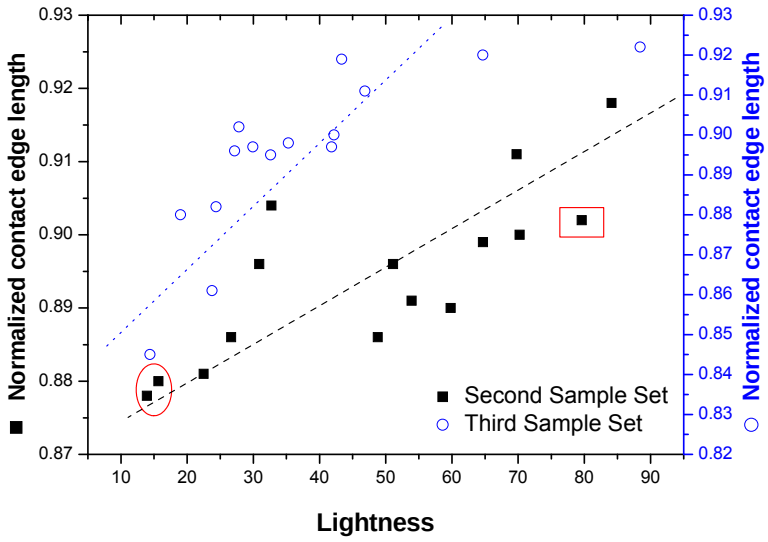

Figure 5.35: Normalized Contact Edge Length as a function of the lightness value

Generally P5 decreases as the colour becomes darker, which confirms the assumption that the scale height increases after dyeing, especially for dark colours. P5 confirms that the underbody of the scale edge is more susceptible to degradation than the rest of the surface, which leads to an increase in the scale height and a decrease in the length of the scale edge junctions and section width of the scale top. Because the decrease in the length of the scale edge junctions is larger than that of the section width (due to the huge damages in the junction area) P5 always decreases.

Once again neither P5 of the blank dyed sample (marked by square) or the Lanasol dyed samples (marked by circle) show specific changes compared to the Lanaset dyed samples.

5.3.6 Scale Elongation (P6)

This parameter describes the ratio between the length of the scale along the fibre axis and width of the scale across the fibre axis.

Generally the scale elongation has a value between 53 % and 63 %, as it is illustrated in Figure 5.36. The scale elongation does not change much with colour lightness. In fact the changes of this value are not related to the dyeing material but to the mechanical stress during the fibre processing before and during the dyeing process.

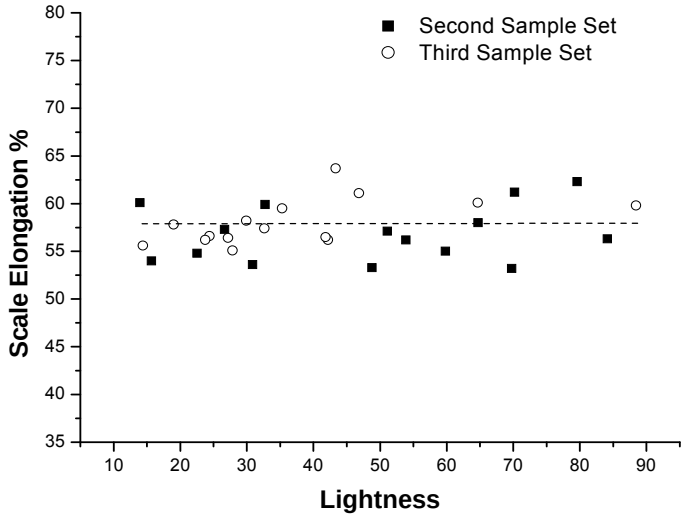

Figure 5.36: Changes in the scale elongation as a function of the lightness value

The consistent results indicate that the fibres have not been elongated as a result of mechanical stress during dyeing, which would effect the elongation of the fibre in the tensile test results and lead to a decrease the fibre extension.

5.3.7 Adhesive Force (P7)

Two physical properties were calculated from force distance curves: the adhesive force, or surface energy (P7) of the fibre surface and the relative surface hardness (P8). The changes in the average adhesive force as a function of lightness are presented in Figure 5.37.

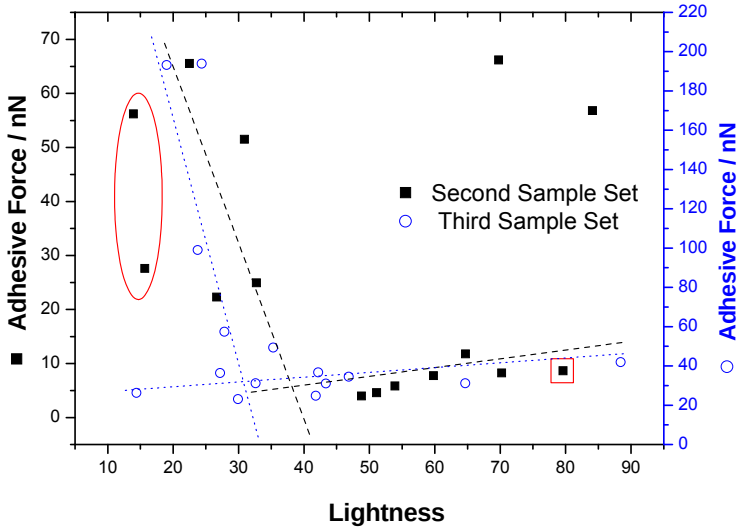

Figure 5.37: Adhesive force as a function of the lightness value

Figure 5.37 shows large changes in the adhesive force after dyeing with dark colours. P7 is related to the chemical structure of the fibre surface [19], which is changed during dyeing. As can be seen in Figure 5.37, P7 is almost constant for light colours up to a lightness value of 30 – 40, where it increases more as the colour becomes darker, which can be explained by the increasing surface damage.

This is confirmed by results from Andrew et al. [1], who pointed out that the surface damage caused by the processing is due to the removal of fatty acids, which leads to a decrease in surface resistance, and therefore to damage in the epicuticle layer (fatty acid layer in the scale top), which again leads to a more hydrophilic and a less homogeneous surface. This is illustrated in Figures 5.24 and 5.25.

Figure 5.37 shows clearly that the gradient of P7 changes in the lightness range of 30-40, which could be related to a change in dye diffusion into the fibre and the damaged layer, as demonstrated by Wortmann [4]. Therefore the changes in P7 can be used as an indication of how deep the damage reaches into the endocuticle layer.

From the above it can be concluded that P1, P2, P3 and P5 change in the lightness range between 30 and 40, which could indicate that the dye molecules enter another layer (most likely the cortex). This might lead to a different diffusion rate because the cortex layer has a lower crosslinking density and more functional groups, which makes the diffusion of the dye molecules easier and increases the ability of the cortex layer to interact with the dye molecules and thus more damage will occur to the wool surface.

The change of the gradient in the region between 30 – 40 in Figure 5.37 can be referred to as the physical separation between light (less surface damage, only in the epicuticle layer) and dark colours, where the damage reaches deeper into the endocuticle layer.

The surface damage is also demonstrated by measuring the adhesive force of a film of the dyestuff, which was used for the laboratory dyeing. For this film P7 is found to be approximately 10.78 nN, which is in the range of the adhesive force measured for light colours of the second sample set (lightness higher than 30). Therefore the increases in P7 can not be explained only by the dye molecules on the surface, but also by damage or removal of the surface layer, especially in the case of dark colours.

Figure 5.37 shows that Lanasol reactive dye (marked by a circle) has almost a similar effect on P7 as Lanaset dyes.

5.3.8 Surface Hardness (P8)

The gradient of the force/distance curve of the contact region is proportional to the relative surface hardness of the fibre. The change in P8 due to dyeing is illustrated in Figure 5.38.

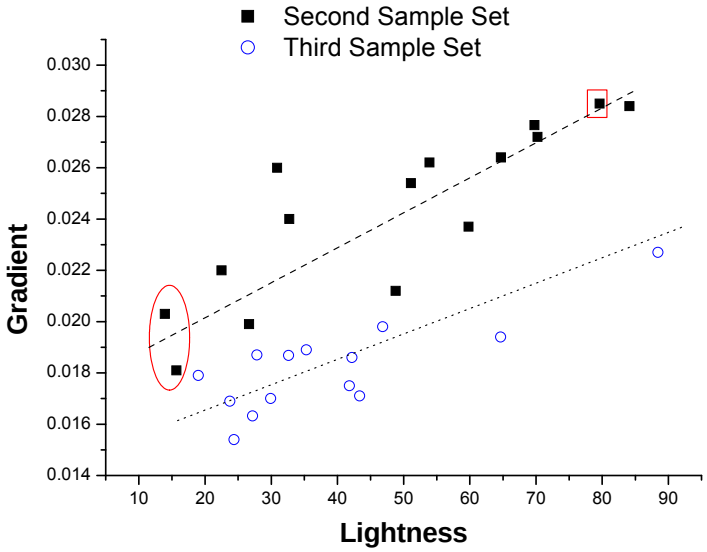

Figure 5.38: Gradient of the F/D curve, representing the relative surface hardness of the fibre as a function of the lightness value

P8 decreases generally with darker colours. This decrease in P8 indicates that the extensive disulfide bonds in the cuticle layer were damaged, which are responsible for the high rigidity of the outer layer of undyed fibres [2]. As P8 decreases the damage goes deeper into the fibre and affects the bulk properties, which results in a loss of the fibre strength. It is also clear that P8 follows the same trend for Lanasol and blank dyed samples, which indicates that the surface hardness is independent from the dye type.

It seems not to matter if the fibres are from the same lot or not, the behaviour of the surface parameters as a function of lightness follows the same trend. This is probably because the AFM determines only surface characteristics, which are mainly influenced by the dye and are independent of the fibre diameter and wool type.

5.3.9 Results of the Tensile Tests

The tensile test results are shown in Figure 5.39. Only seven force extension curves are shown as examples for the tested fibres each sample for: undyed, blank dyed, light colour dyed and dark colour dyed samples.

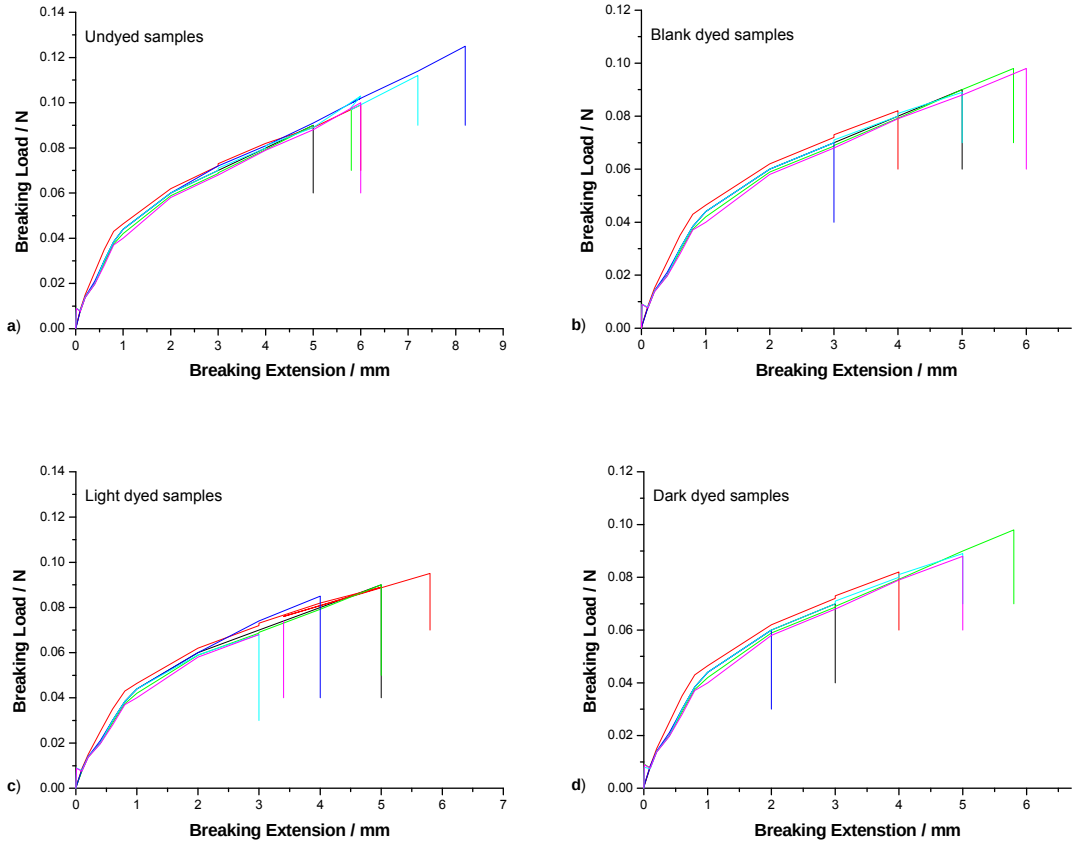

Figure 5.39: Mechanical behaviour of wool fibres extended at a constant rate, a) undyed samples, b) blank dyed samples, c) light dyed samples, d) dark dyed samples.

Generally most of the force extension curves had the same general form (Figure 5.39). The curves can be divided into three regions. They start with a stiff initial region, called the Hookean region. The fibre deforms more easily throughout the short yield region that follows. Finally it becomes less easily extensible (but it is still easier than the Hookean region) in the post yield region.

The curves of undyed fibres are closer to each other than the curves of dyed fibre

samples. They vary, however, in the breaking point, e.g. the maximum elongation and maximum load. For example, the standard deviation of the breaking load rises from 0.029 to 0.038 after dyeing (see Appendix E). This variation could be explained by either the varying degree of damage of the fibres or the difference in cross-section areas, as the fibre diameter could not be controlled exactly for the 50 wool fibres in each sample, even if the fibres were from the same lot.

It also seems as if the surface damage caused by dyeing has little effect on the shape of the load-elongation curves, but the breaking point is on average shifted to values of lower breaking elongation. This indicates that dyeing causes little or no change to the internal fibre structure, especially with regard to performance properties such as fibre strength, but rather that the damage is concentrated on localised parts on the fibre surface. The effect of the above on the tactile properties and fabric handle was not investigated in this study and could be a subject for further investigation.

Broken disulphide bonds and hydrolysis of amide bonds lead to damage and form flaws and microcracks on the surface, therefore lower values of the breaking load and low elongation can be expected for these fibres. From the AFM images of dark colours it can be seen that most of the surface degradation occurs at the junction regions between overlapping cuticle scales.

Malformation or degradation in the form of cracks or holes, which appear to extend into the fibre cortex, may be of significance in reducing the fibre strength and extension at break.

Figure 5.40 shows the results of tensile tests, where the relation of the fibre breaking load to the breaking elongation is illustrated for the second group. Four samples are shown as an example: an undyed, a blank dyed, a light colour dyed and a dark colour dyed sample.

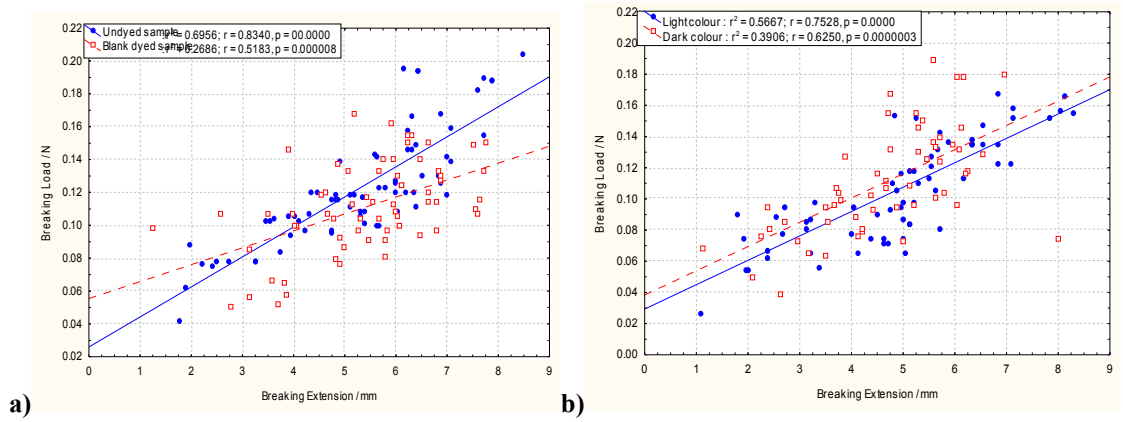

Figure 5.40: Scatter plot of the breaking load as a function of the breaking elongation for a) undyed and blank dyed fibres, b) light and dark colour dyed fibres

Figure 5.40 shows clearly that the breaking load is scattered throughout the range of fibre elongation, which might be caused by surface damage. Generally the simple correlation coefficient (r) becomes smaller after dyeing. This effect is more pronounced for dark colours.

The breaking load and extension are plotted as a function of lightness in the Figures 5.41 and 5.42. Each point represents an average of 50 tested fibres (the actual values of breaking load and elongation and standard deviations are given in Appendix E). The average elongation at break for different lightness values is illustrated in Figure 5.41.

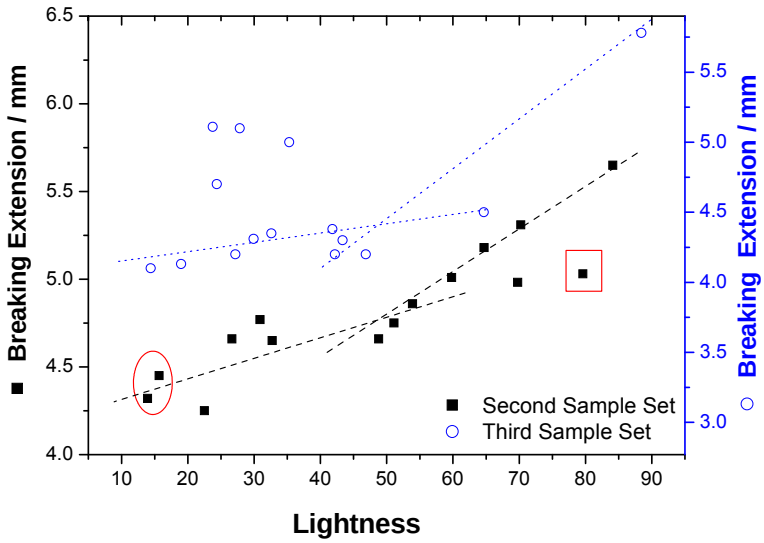

Figure 5.41: Average breaking extension as a function of the lightness value

The average load at break for different lightness values is illustrated in Figure 5.42.

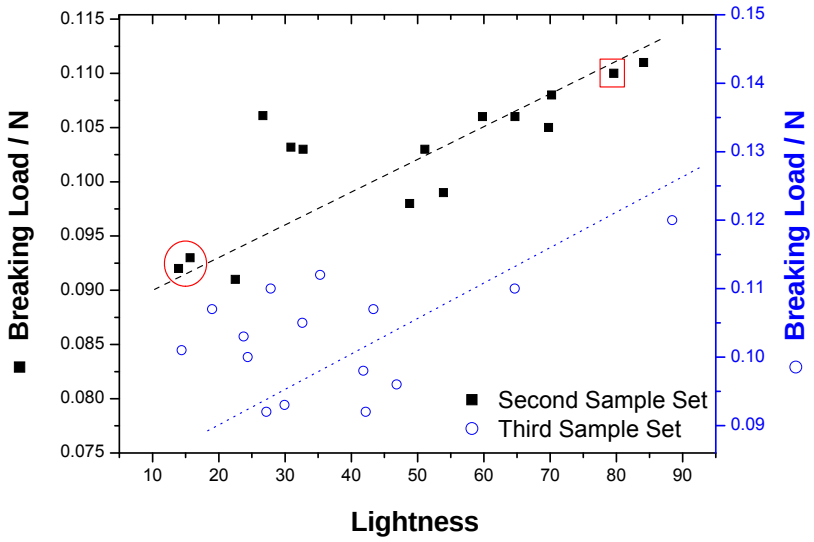

Figure 5.42: Average breaking load as a function of the lightness value

From Figures 5.41 and 5.42 one can see that the tensile test results vary considerably for both sample sets, but more for the third set. It can be observed that the fibre extension and load decrease after dyeing. This confirms AFM results that for darker colours more damage occurs to the fibre surface, as well as earlier studies by Gullbrandson [7] and Brack [1]. It is clear that as the darkness of the colour increases the breaking load and the breaking extension decrease, which indicates that the fibre damage increases as the dye concentration increases. This reduction in these mechanical properties could be related to the conversion of cystine to lanthinine (Figure 5.43), as was demonstrated by Houff et al. [20], and might be related as well to breakage of the sulphur bonds in the cystine links in the peptide chain (Figure 5.44).

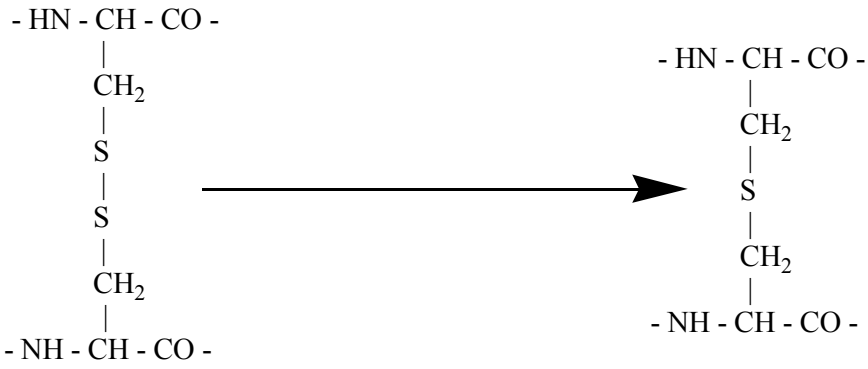

Figure 5. 43: Conversion of cystine to lanthinine during dyeing.

These bonds consist of two sulphur atoms and are the prime linkage, which connect the threads into networks. When these sulphur bonds are broken, wool becomes weak and breaks at small elongation.

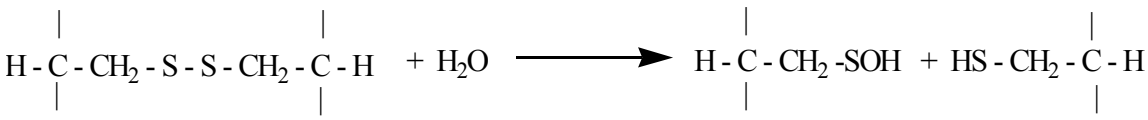

Figure 5. 44: Breakage of the cystine links in the peptide chain results in a reduced crosslinking density

An additional oxidation reaction might occur during dyeing to form cysteic acid as is illustrated in Figure 5.45:

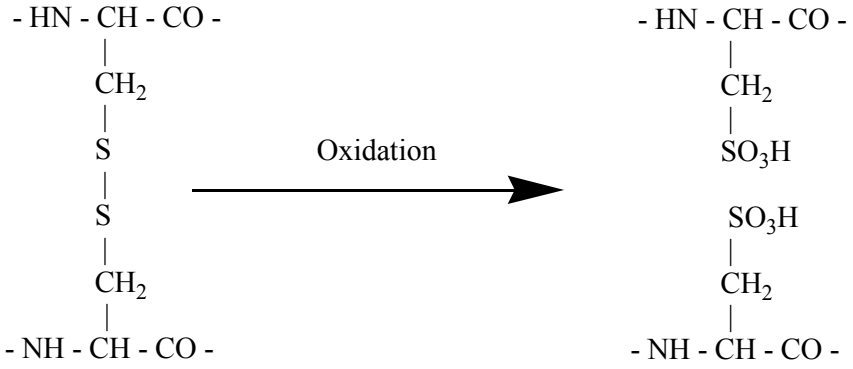

Figure 5. 45: Oxidation reaction of the cystine to form cysteic acid and reduce the crosslinking density in the fibre

Figure 5.41 shows that the elongation at break first decreases steeply as the colour becomes darker. The gradient changes in a lightness range of 40 – 50 and the decrease becomes less steep. Figure 5.42 shows that the breaking load decreases uniformly over the entire colour range.

The change in the mechanical properties as the colour becomes darker could be a result of cuticle damage that occurred during dyeing. The dye concentration during dyeing must be high in order to achieve the desirable colour darkness. As the darkness increases the dye molecules diffuse into the wool fibre increasing, which causes more damage and leads to more flaws (micro-cracks or crazes) and weak spots where fractures can start if the fibre undergoes any stress. This makes the fibres easier to break under less stress or force and with less elongation.

The Lanasol dyed samples (marked by a circle) follow the same trend as Lanaset dyed samples for the elongation and the load at break.

Tensile results follow a recognizable trend if the fibres are from the same batch. Fibres from different batches (third sample set) show the same trend but with a rather large distribution of results. This points out that the tensile results are not only influenced by

the surface properties and therefore the dye, but rather by the bulk fibre morphology. Tensile results depend on the entire fibre morphology: the cortex layer as well as the cuticle layer, and therefore it is not the best way to characterise the influence of dyeing on the fibre surface.

5.4 Correlations of Tensile Test and AFM Results

The AFM results illustrated that the surface of dyed fibres shows the following types of damage: wearing away of the surface scales, transverse cracks (which often coincide with the edge of the overlapping scale) large and deep cracks, holes, other types of damage such as an increase in the depth of the junction line between two scales (which is indicated by an increase in P1 and a decrease in P5) and wearing off of the bottom scale edge (this indicated by an increase in P2). It was expected that these forms of damage should lead to a decrease in the elongation and strength of the fibre. By combining AFM and tensile test results, the relation between the surface changes and loss in the fibre strength and breaking extension can be presented more clearly.

Figures 5.46 and 5.47 show the relation between the scale height changes and the breaking load and elongation for the second and the third sample set. It appears that the increase in P1 correlates well with the decrease in the breaking load and elongation. This could be used as evidence to prove that fractions initiate at the junction between the overlapping cuticle scales. The breaking load and elongation decreases with increasing P1, the relations are, however, non-linear except for breaking load of the second sample set.

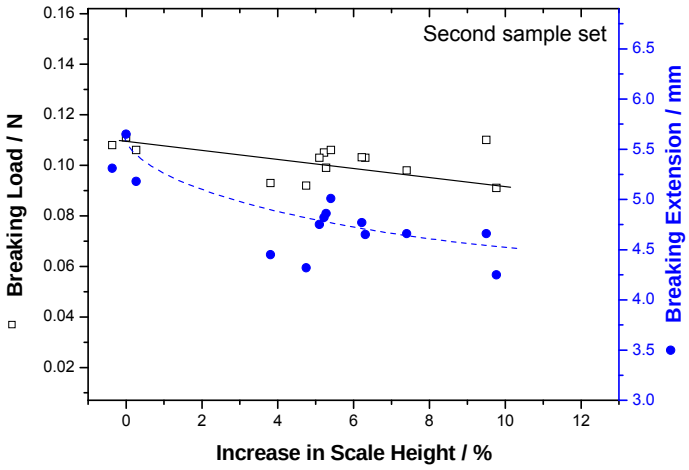

Figure 5.46: Maximum tensile stress and the maximum elongation as a function of the increase in scale height.

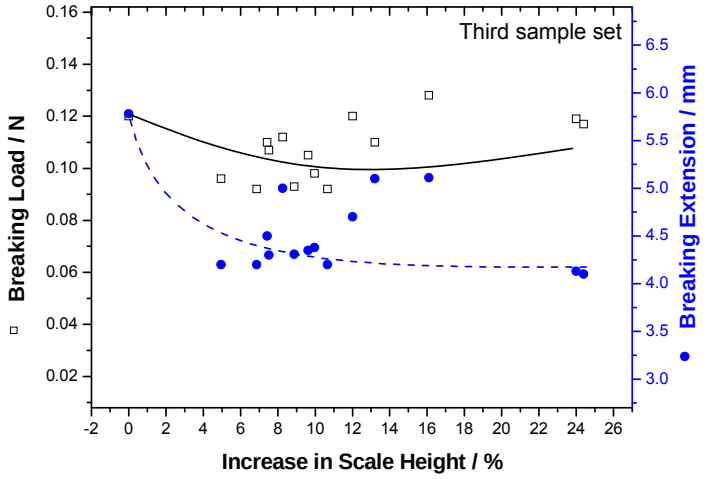

Figure 5.47: Maximum tensile stress and the maximum elongation as a function of the increase in scale height.

It is well known that the fibre strength depends on the cortex layer and the cell membrane complex (crosslinking density and the degree of crystallinity) more than on the cuticle layer. The stress strain behaviour, however, indicates fibre changes in the bulk in addition to surface damage [21]. Therefore, an increase in P1 could be used as an indication for a potential loss in fibre strength and elongation due to surface damage if the fibres are from the same lot. On the other hand, this is not possible for fibres from different lots as shown in Figure 5.47. This can be explained by the variation in the morphology of the cortex layer either in the type of crystal (α-keratin and β-keratin) or in the chemical structure of this layer (para-cortex and ortho-cortex) [22].

From the above one can conclude that tensile tests can be used to characterise surface damage of the tested fibres, as long as the tested fibres came from the same lot.

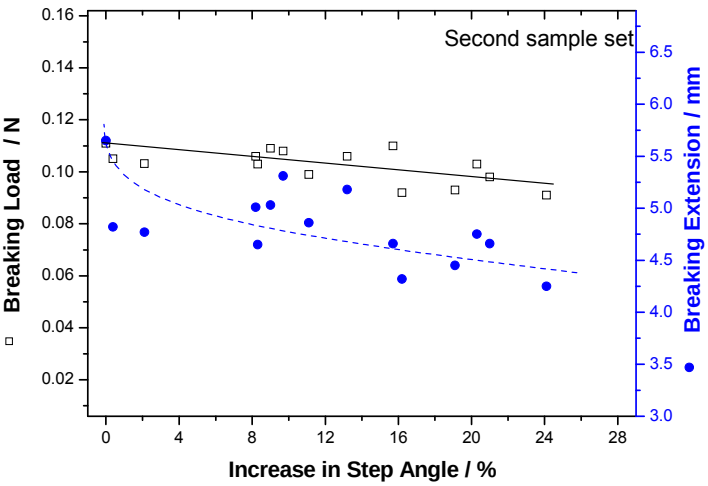

Figure 5.48: Maximum tensile stress and the maximum elongation as a function of the increase in step angle.

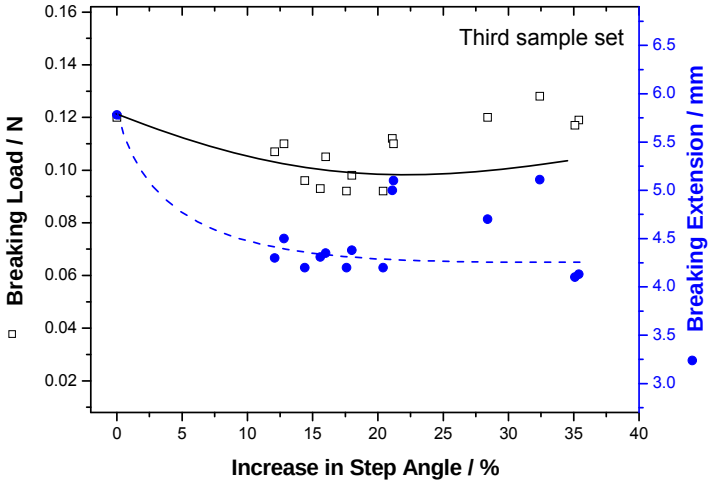

Figure 5.49: Maximum tensile stress and the maximum elongation as a function of the increase in step angle.

The same conclusions can be drawn from Figures 5.48 and 5.49, which illustrate the relation between increasing step angle and the breaking load and breaking elongation for samples from the same lot and different lots, respectively. It seems that the increase in the step angle leads to a concentration of the stress in the junction area during tensile testing, which causes the sample to break at lower elongations and with less stress. For the second sample set the relationship between the increase in the P2 and decrease in the breaking load is linear, in contrast to the non-linear relationship with the fibre elongation at break.

Similar to P1 the effect of the sample history is obvious when comparing the second sample set to the third.

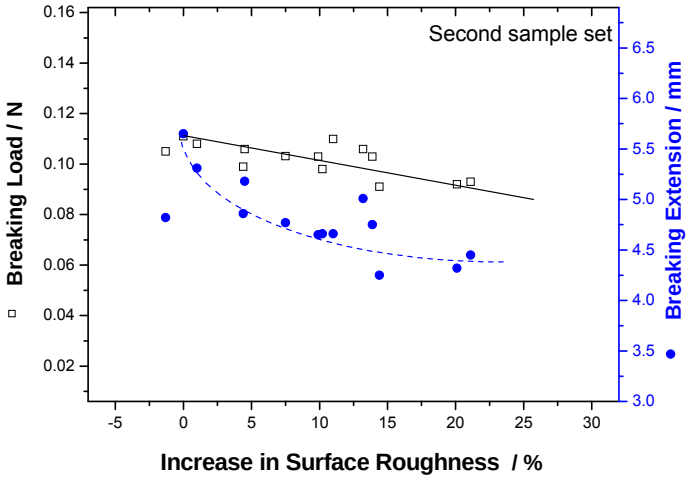

Figure 5.50: Maximum tensile stress and the maximum elongation as a function of the increase in surface roughness.

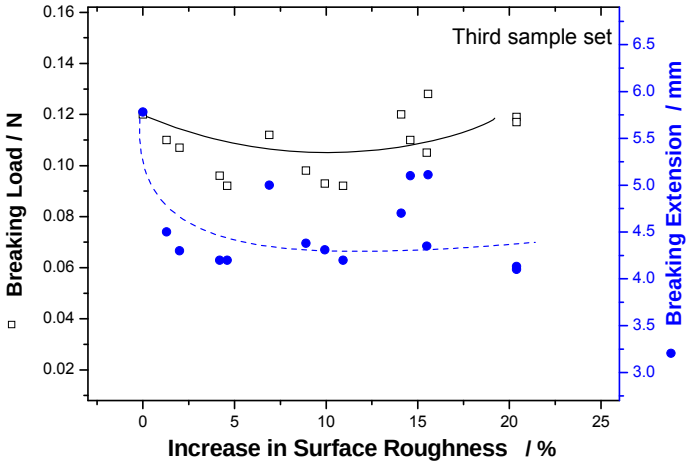

Figure 5.51: Maximum tensile stress and the maximum elongation as a function of the increase in surface roughness.

Figures 5.50 and 5.51 show the fibre strength and the elongation at break as a function of increasing surface roughness for the second and third sample set.

Clearly the relation between these parameters is more regular for the second sample set than the third, which, again, can be explained by variations in the fibre bulk morphology in the third sample set. Generally, the relation between P3 and the strength of the fibres and the elongation at break is similar to P1 and P2 and for all of them the decrease in the elongation is steeper for light colours (less surface changes) than for dark colours.

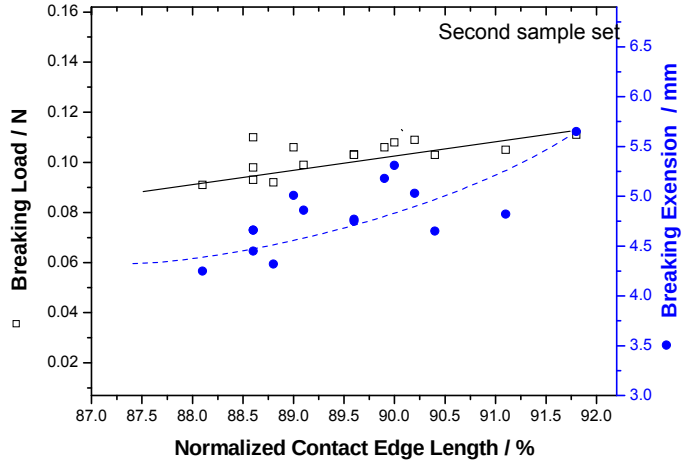

Figure 5.52: Maximum tensile stress and the maximum elongation as a function of the normalized contact edge length.

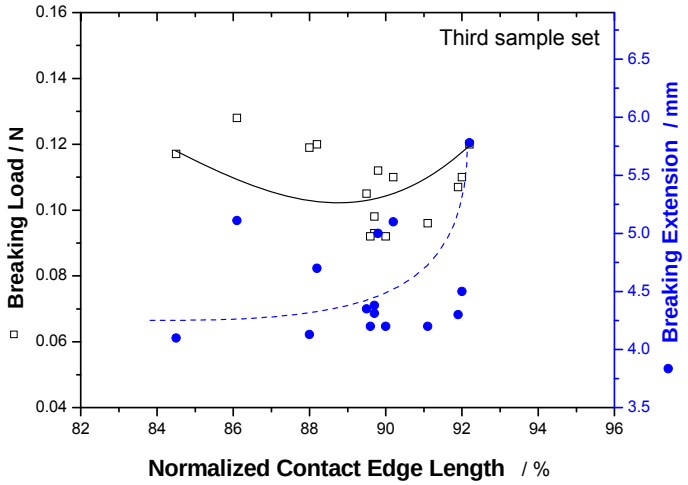

Figure 5.53: Maximum tensile stress and the maximum elongation as a function of the normalized contact edge length.

Figure 5.52 shows the relation between the change in the normalized contact edge length and the breaking load and elongation for the second sample set. Generally the load and elongation increase with increasing P5. It appears as if there is a good linear relation for P5 and the load and a non-linear relation with the fibre elongation at break. This relation is not quite clear for samples from different lots as is illustrated in Figure 5.53 This could be a result of the variation in the morphology of the cortex layer of the wool fibre in the third sample. Therefore, a decrease in P5 can be used as indication for the loss in fibre strength and extensibility due to dyeing only for fibres from the same lot.

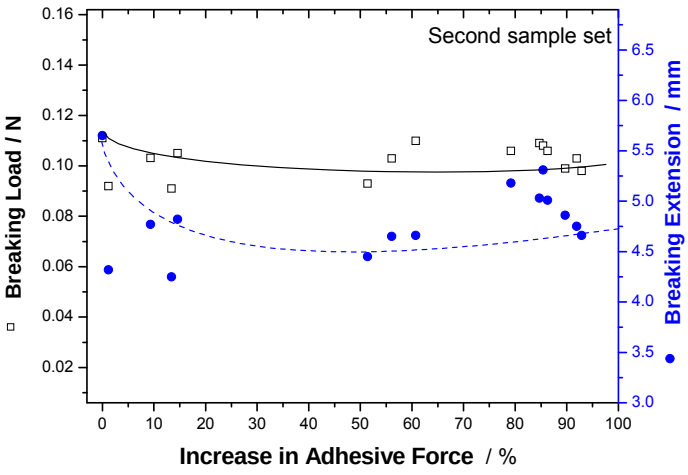

Figure 5.54: Maximum tensile stress and the maximum elongation as a function of the increase in adhesive force

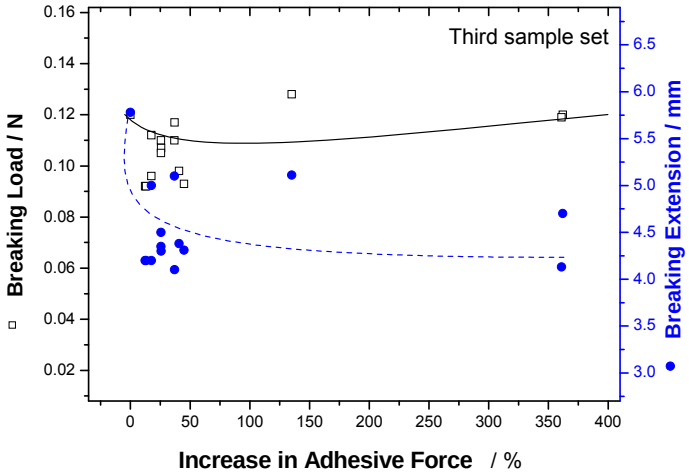

Figure 5.55: Maximum tensile stress and the maximum elongation as a function of the increase in adhesive force

The loss in fibre strength and extension as a function of increasing adhesive force for the second and third sample sets is illustrated in Figures 5.54 and 5.55. Both show clearly a decrease of the load and elongation with increasing P7. It seems that dyeing leads to a removal or damage of the epicuticle layer, which is indicated by the change in the adhesive force. This result is consistent with reports by Negri [5]. The change depends greatly on the diffusion of dye into the wool fibre. As the concentration increases, the damage reaches deeper and has a large effect on the tensile strength as well as the elongation at break, especially for dark colours. This is probably due to two reasons: either the damage reaches into the cortex layer or the morphology of the fibres has been changed. It appears from the figures that there is non-linear relationship between P7 and the elongation or load at break for both sample sets, which could be the result of varying levels of surface damage.

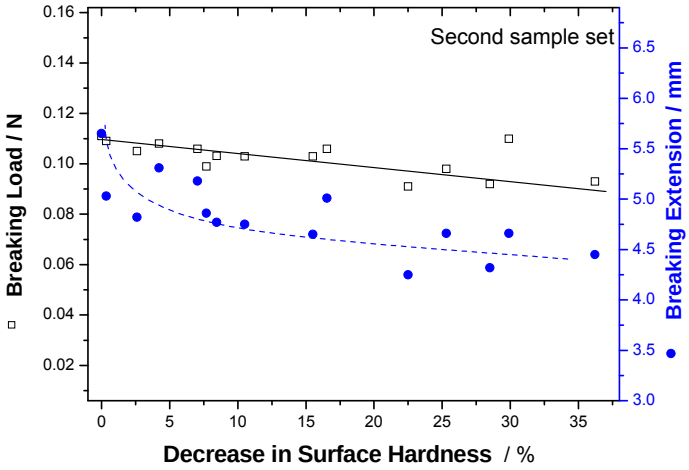

Figure 5.56: Maximum tensile stress and the maximum elongation as a function of the decrease in surface hardness

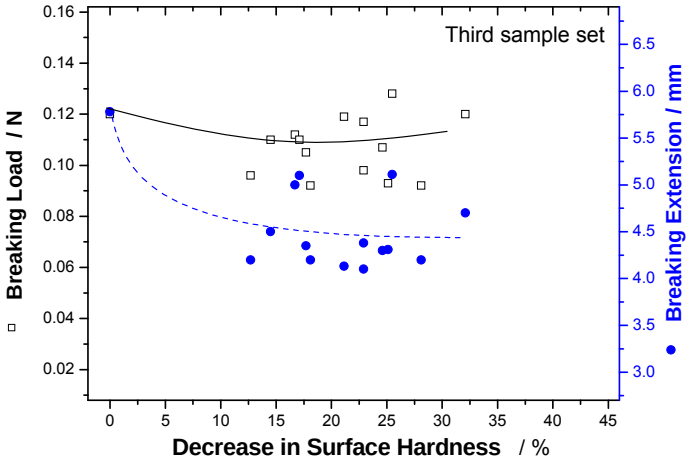

Figure 5.57: Maximum tensile stress and the maximum elongation as a function of the decrease in surface hardness.

Figure 5.56 and 5.57 show the changes in the fibre strength and the elongation, as a function of decreasing surface hardness, which is related to different degrees of damage in the cuticle layer of the wool fibres.

The load and elongation at break decrease with decreasing P8. The relationship is non-linear, except for the fibre breaking load of the second sample set, which has a linear relationship.

Figure 5.56 and 5.57 show that damage of the cuticle layer can cause a loss in tensile strength and elongation at break for wool fibres, even if in some cases (especially in the load at break) this loss is quite small. This loss can be related to the loss in the relative hardness which is a result of the surface damage.

5.5 References

1. N. Brack, R. N. Lamb, D. Pham, T. Philips and P. Turner, *Effect of Physical Processing on the Wool Fibre Surface.* Textile Res. J., 2001. 71: p. 911-915.
2. J. A. A. Crossley, C. T. Gibson, L. D. Mapledoram, M. G. Huson, S. Myhra, D. K. Pham, C. J. Sofield, P. S. Turner and G. S. Watson, *Atomic Force Microscopy Analysis of Wool Fibre Surfaces in Air and Under Water.* Micron, 2000. 31(6): P. 659-667.
3. R.R. Mather, *AFM Characterization of the Natural Yarns,* Department of Materials Science and Engineering, University of Surrey, Guildford, UK, "http://www.surrey.ac.uk/MME/Research/SPM/6-1.html".
4. F. –J. Wortmann, G. Wortmann and H. Zahn, *Pathways for Dye Diffusion in Wool Fibres*. Textile Res. J., 1997. 67(10): p. 720-724.
5. A. P. Negri, H. J. Cornell and D. E. Rivett, *Effect of Processing on the Bond and Free Fatty Acid Levels in Wool.* Textile Res. J., 1992. 62: p. 381-387.
6. A. N. Parbhu, W. G. Bryson, and R. Lal, *Disulfide Bonds in the Outer Layer of Keratin Fibers Confer Higher Mechanical Rigidity: Correlative Nano-Indentation and Elasticity Measurement with an AFM*. Biochemistry, 1999. 38(36): p. 11755-11761.
7. B. Gullbrandson, *Fibre Damage in the Stock-Dyeing of Wool.* Textile Res. J., 1958. 28(11): p. 965-968.
8. T. Leksophee, S. Supansomboo and N. Sombatsompop, *Effect Of Crosslinking Agents, Dyeing Temperature and ph on Mechanical Performance and Whiteness of Silk Fabric.* J. Appl. Polym. Sci, 2004. 91(2): p. 1000-1007.
9. R. S. Asquith, *Chemistry of Natural Fibre*. 1st ed., New York. 1977. p. 327-330.
10. C. Popescu, J. Chelaru, C. Magrini, S. Pall and V. Corneanu, *Influence of Technological Processes on Tear Strength of Finished Wools*. Textile Res. J. 1985. 55: p.72-74.
11. F.-J Wortmann, and W. Arns, *Quantitative Fibre Mixture Analysis by Scanning Electron Microscopy, Part I; Blends of Mohair and Cashmere with Sheep's Wool.* Textile Res. J., 1986. 56: p. 442-446.
12. X. Liu, L. Wang, and X. Wang, *Resistance to Compression Behaviour of Alpaca and Wool.* Textile Res. J. 2004. 74(3): p.265-270.
13. P. A. Tucker, *Scale Height of Chemically Treated Wool and Hair Fibres*. Textile Res. J. 1998. 68(3): p. 229-230.
14. T. L. Phillips, T. J. Horr, M. G. Huson and P. S. Turner, *Imaging Wool Fibre Surfaces with a Scanning Force Microscope.* Textile Res. J., 1995. 65: p. 445-453.
15. H. P. Lundgren, *Highlights of Papers on Physical and Protein Chemistry.* Textile Res. J., 1956. 26: p. 372-376.
16. J. D. Leeder, *Comments on "Pathways for Aqueous Diffusion in Keratin Fibres".* Textile Res. J., 1999. 69(3): p. 229.
17. K. Parton, *Fibres to Finished Fabrics Proceedings*. Fibre Science/ Dyeing and Finishing Groups Joint Conference 8 & 9 December 1998. p 93-103.
18. D. Robson, P. J. Weedall, and R. J. Harwood, *Cuticular Scale Measurements Using Image Analysis Techniques.* Textile Res. J., 1989. 59: p. 713-717.
19. H. Zahn, H. Messinger, and H. Hocker, *Covalently Linked Fatty Acids at the Surface of Wool: Part of the "Cuticle Cell Envelope".* Textile Res. J., 1994. 64(9): p. 554-555.
20. W. H. Houff, C. J. Wills, and R. H. Beaumont, *Chemical Damage in Wool Part II: Effects of Alkaline Solutions.* Textile Res. J., 1957. 27: p. 196-199.

21. K. Slater, *Textile Degradation.* Textile Progress 1989-91. 20-21(1-2): p. 7-8.
22. M. Feughelman and A. R. Haly, *The Mechanical Properties of the Ortho-and Para-like Components of Lincoln Wool Fibres.* Textile Res. J., 1960. 30(11): p. 897-900.

6 Conclusions and Recommendations

6.1 Conclusions

An atomic force microscope proved to be a viable tool with which to investigate the surface structure of wool fibres in an ambient environment (air, at atmospheric pressure), with almost no sample preparation and without any modifications to the fibre surface. AFM makes it possible to image the fibre topography on a micrometer scale and to understand how different product treatments affect the cuticle structure of fibres. Undyed and dyed fibres can easily be imaged with the non-contact mode of the AFM. Statistical analysis of the images resulted in the identification of fibre surface modifications with great accuracy by measuring several characteristic properties of the cuticle scales of the fibres.

Harsh dyeing conditions seem to damage not only the cuticle surface but in some case the entire wool fibre. Surface damage that occurred during dyeing, particularly with Lanasol reactive dyes and Lanaset metal complex dyes, was investigated and classified according to its severity into four different forms, namely scale raising (lifting), scale chipping, fluting (surface etching) and pitting (hole formation).

The following surface characteristics were found to change due to dyeing: scale height, scale edge angle, scale surface roughness, normalized contact edge length, adhesive force between the AFM tip and the fibre surface and surface hardness. The scale interval and the scale elongation on the other hand, seemed to be unaffected by dyeing. AFM can be used successfully to measure these characteristics and properties of the fibre surface on a micro-scale and relate them to the damage caused by dyeing.

Scale height and scale edge angle measurements indicated the scale raising. The surface roughness of the scale could be related to fluting, and the normalized contact edge length indicated the scale edge chipping.

The effect of different dyes with specific reference to the colour lightness, on the wool surface, was investigated. Generally, it was found that dark colours caused greater damage than light colours. It was also possible to distinguish between areas of different lightness, which could be regarded as "*light"* and "*dark"* area.

Fibres from the second sample set, which came from the same lot, showed more regular results than fibres from varying lots, which can be expected and explained by environmental effects and the history of the wool fibres. Nevertheless the behaviour of all surface parameters as a function of colour lightness followed the same trend even if the fibres came from different lots. This is because the AFM determines only surface characteristica, which are mainly influenced by the dye process.

The results obtained by AFM describing the surface features were compared to results obtained from the single fibre tensile tests, which describe the mechanical behaviour of the entire fibre. This was done in order to investigate the effect of dyeing and the cuticle damage on the fibre strength and extension properties. The comparison demonstrated that the tensile results follow a recognizable trend only if the fibres were from the same lot. Fibres from different lots showed a trend, but with a rather large distribution of results. This points out that the tensile test results are mainly influenced by the fibre morphology (cortex layer as well as cuticle layer) and not so much by surface characteristics. Therefore tensile tests are not the optimum choice to characterise the influence of dyeing on the wool fibre surface.

Findings from the current study confirm earlier results [1, 2] that wool fibres loose tensile strength and elongation properties after dyeing. It was shown that the diffusion of dye molecules into the wool fibre most likely causes the change in the scale characteristics after dyeing. The dye diffusion along the cell membrane complex between the cuticle scales (intercellular diffusion) can be used to explain the change of the scale height, the scale angle and the normalized contact length edge.

The weakest point of the fibre (the joint area of two scales) was examined, where the measured characteristics of the surface illustrated increases in the scale height and scale angle, which indicate damage in the joint area. The cuticle scales were in some cases abnormal but not completely absent after dyeing, but these changes would not be expected to influence the mechanical properties of the fibres significantly. The fact that some fibres were malformed or seriously degraded (some having holes and cracks), which appeared to extend into the fibre cortex, may be of more significance to reduce the fibre strength and extension at break.

The strength of wool fibres might have been influenced by damage that occurred in both components of the cortex layer e.g. the Para and Ortho-cortex, but no clear picture

emerged. All dyed samples showed large standard deviations compared to the undyed samples, which indicates heterogeneous changes on the fibre surface, especially for the adhesive force results.

In summary, this research has met its main objectives. The results gained from this work provide useful information about the surface modification of merino wool due to processing, which could be used to obtain optimum processing conditions that cause less damage to the fibre surface, and might encourage the development of new less destructive dyes.

6.2 Recommendations

Different dye types, assistants, carriers and other dye bath components may have additive effects to the change in the mechanical properties of the fibres, either by acting upon the fibre structure or by damaging the surface. However, no significant conclusion seems to be possible without knowing the exact chemical structure of the used dyes and without the possibility of changing the dyeing conditions, especially the temperature and time, or the dyeing procedure. The investigation of these parameters and their effect on the fibre properties would be recommended. A separation of the process factors which cause the surface damage would be interesting in order to identify the reason for the different forms of damage.

The high resolution of the AFM is important in order to investigate the changes in the contact area between two scales and to determine if the scale was separated from the main fibre body or not. Furthermore the changes in the ridge and wrinkle height could be investigated more conclusively with high resolution.

The strength of wool fibres is mainly influenced by the proportion of the different components of the cortex layer and the structural changes due to dyeing associated with the loss of fibre strength and breaking elongation require further study. Detailed studies including transmission electron microscopy and chemical analysis would be needed to determine the nature and extent of internal structural changes in weak fibres due to experimental dyeing treatments. The effect of dyeing could be examined in even greater detail by using a tensile stage in a scanning electron microscope. This allows regions of the fibre to be examined as the fibre is slowly extended, and the progressive changes in the fibre surface can be recorded on video.

The information obtained in this project does not cover different wool types, the experiments were only carried out on merino wool fibres with maximum diameter of 20 μm. Other types of wool fibres, as well as fibres with other diameters, could be investigated using the same set of characteristics to determine surface changes.

6.3 References

1. B. Gullbrandson, *Fibre Damage in the Stock-Dyeing of Wool.* Textile Res. J., 1958. 28(11): p. 965-968.
2. N. Brack, R. N. Lamb, D. Pham, T. Philips and P. Turner, *Effect of Physical Processing on the Wool Fibre Surface.* Textile Res. J., 2001. 71(10): p. 911-915.

Appendices

Appendix A: Laboratory Dyeing Procedure and Factory Dyeing Conditions

A.1 Laboratory Dyeing Procedure

Laboratory dyeing was carried out on samples of 2 g each, taken from the same original lot that the samples of second set came from, in a Pyrotec 2000 series infrared exhaust dyeing machine. The liquor goods weight ratio was 25:1 and the weight-percent of the dye in relation to the weight of the wool fibres was 0.00, 0.08, 0.10, 0.30, 0.50, 0.80 and 1.00 respectively. The general dyeing cycle is shown in Figure A.1.

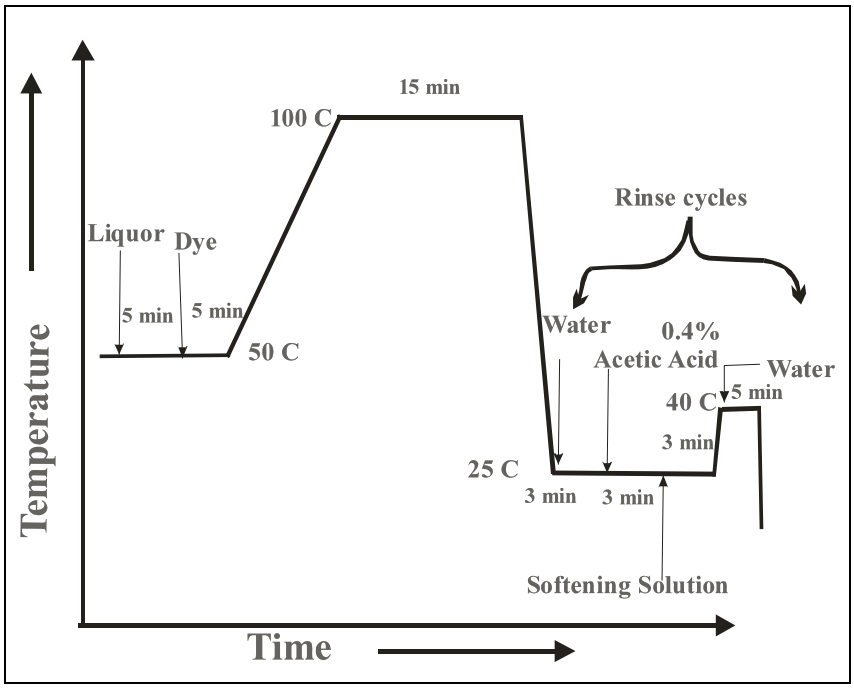

Figure A.1: General dyeing cycle of blue Lanaset dye.

The dyeing conditions (standard time, maximum temperature, acetic acid concentration, pH and the concentration of the auxiliaries) were similar to those in the factory. All fibres were put in a solution of water and auxiliaries (Miralan and Rucowet) at 50 ºC and held there for 5 min. Then the blue Lanaset dye was added to the mixture and after 5 min the solution was inserted into the dyeing machine at the same temperature. The temperature was then gradually increased at 1 ºC/min to 100 ºC, where it stayed for 15 min before the solution was cooled down to room temperature. The fibres were then washed and rinsed, first with water and then with a diluted solution of acetic acid (0.4%), followed by a softening solution (Duran and Belsoft). After draining, the fibres were left to dry in atmospheric conditions (20 ± 2 ºC and 65 % RH).

A.2 Factory Dyeing Conditions

A.2.1 Lanasol dyeing process

All samples were taken from bulk dyed in the Hextex dyehouse under the following conditions:

1. Temperature
   The starting temperature was 50ºC and the maximum temperature 100 ºC.

2. pH
   The concentration of the acetic acid was 2 %. The fibres were subsequently washed in a diluted solution of 0.4 % acetic acid. Dyed fibres were then rinsed with a solution of 3 g/l ammonia.

3. Dyeing time
   The total dyeing process took four hours and 33 min (273 min) to complete.

A.2.1 Lanaset dyeing process

Factory dyeing with metal complex dyes (Lanaset) was carried out under the following conditions:

1. Temperature
   The starting temperature was 50ºC and the maximum temperature 100 ºC.

2. pH
   The concentration of the acetic acid was 2 %. The fibres were then washed in a diluted solution of 0.4 % acetic acid.

3. Dyeing time
   The total dyeing process took two hours and 58 min (178 min) to complete.

Appendix B: Colorimeter Results

For each sample the fibre lightness was measured three times with a colorimeter and the average value was used in this work. The values for the first sample set are illustrated in Table B.1, for the second sample set in Table B.2 and for the third sample set in Table B.3.

Table B.1 Lightness Values for the First Sample Set

Sample name	First measurement	Second measurement	Third measurement	Average value
18.5 µm undyed	88.92	88.02	88.41	88.45
18.5 µm dyed	14.65	14.44	13.41	14.16
20 µm undyed	87.92	87.88	87.44	87.74
20 µm dyed	15.45	14.56	13.45	14.50

Table B.2 Lightness Values for the Second Sample Set

Sample colour	First measurement	Second measurement	Third measurement	Average value
Un-dyed	84.9	84.6	83.12	84.12
Yellow	69.8	68.89	70.9	69.86
Green	32.87	31.98	33.5	32.79
Grey I	30.98	30.64	31.2	30.89
Blue	26.77	26.54	26.66	26.66
Grey II	22.56	22.45	22.81	22.52
Black I	16.02	15.65	15.34	15.67
Black II	13.98	13.48	14.18	13.94
Blank	80.1	78.3	79.5	79.6
Blue 1	69.5	70.9	70.4	70.2
Blue 2	63.5	65.1	64.8	64.7
Blue 3	60.2	59.1	59.8	59.8
Blue 4	54.7	53.8	53.9	54.5
Blue 5	50.1	52.8	51.6	51.1
Blue 6	48.9	49.9	48.6	48.8

Table B.3 Lightness Values for the Third Samples Set

Sample colour	First measurement	Second measurement	Third measurement	Average value
Un-dyed	88.92	88.02	88.41	88.45
Lt-blue green	64.62	64.52	64.78	64.69
Ginger	45.65	47.5	47.4	46.86
Dkl-taupe	42.98	44.01	43.06	43.35
Olive	42.22	42.56	41.76	42.18
De-petrol	41.99	40.98	42.55	41.84
Tobacco	36.4	35.21	34.32	35.31
Khaki	32.26	33.1	32.47	32.61
Brown I	29.65	29.99	30.15	29.93
Brown II	27.38	28.12	27.99	27.83
Grey	27.39	27.12	27.09	27.20
Blue-grey	24.45	24.69	24.03	24.39
Dr-grey	22.98	24.13	24.23	23.78
Olive-green	19.23	19.56	18.51	19.10
Brown III	14.65	14.44	14.41	14.50

Appendix C: Fibre Surface Characteristics Obtained from AFM Measurements

C.1 Scale Height (P1):

The following figures show the distribution of the scale height for all samples. Each graph shows three samples.

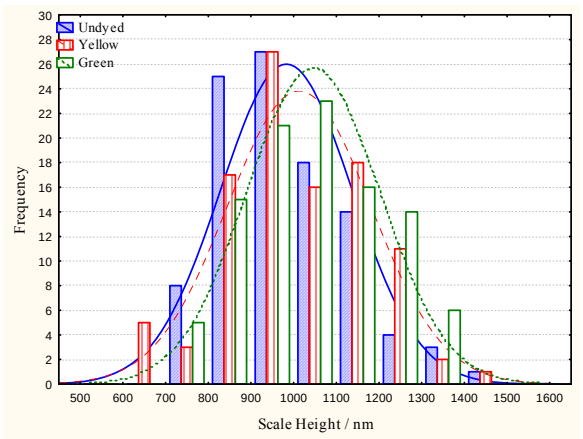

Second Set

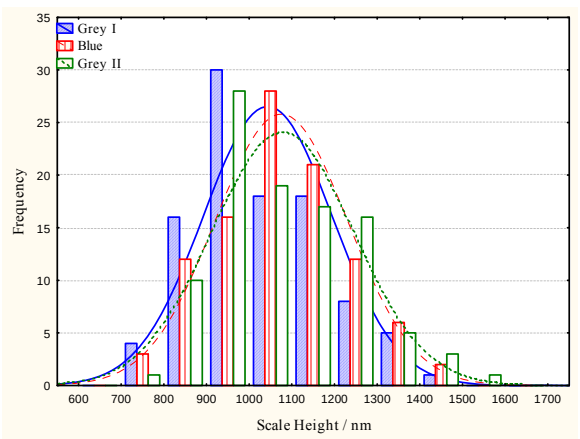

Second Set

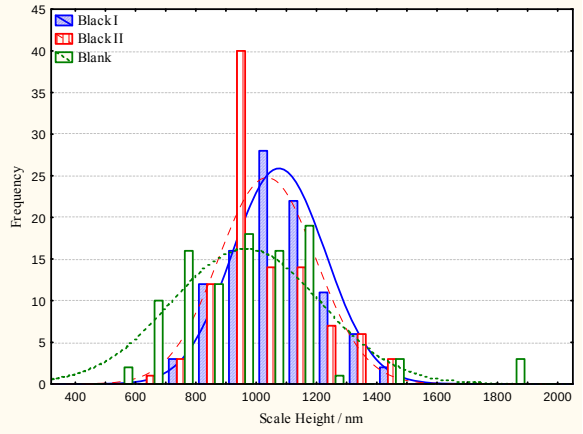

Second Set

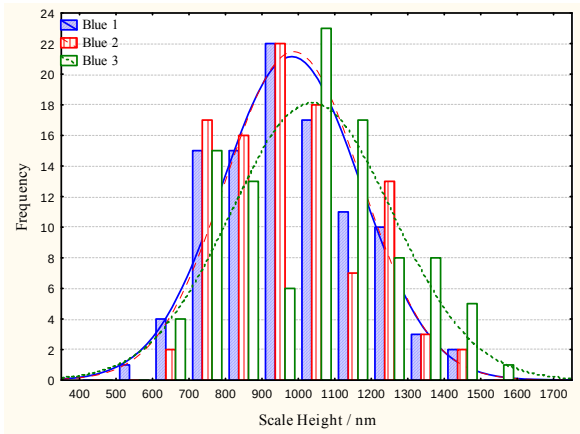

Second Set

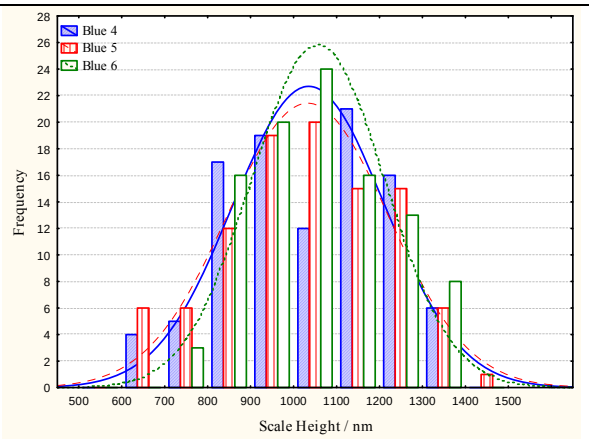

Second Set

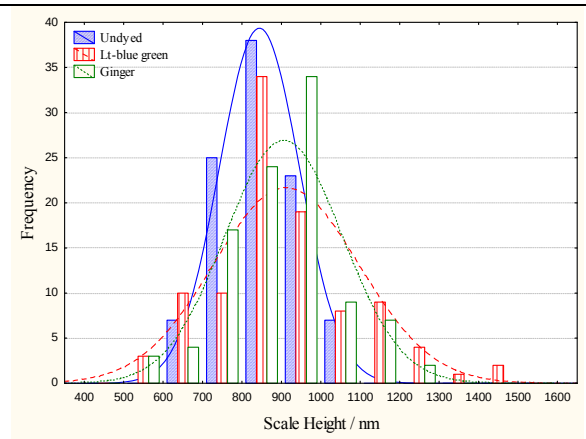

Third Set

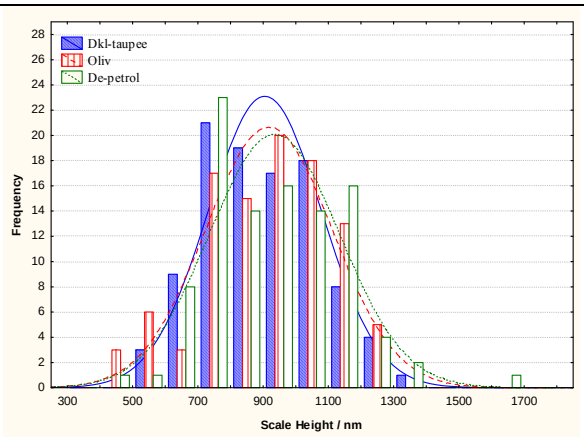

Third Set

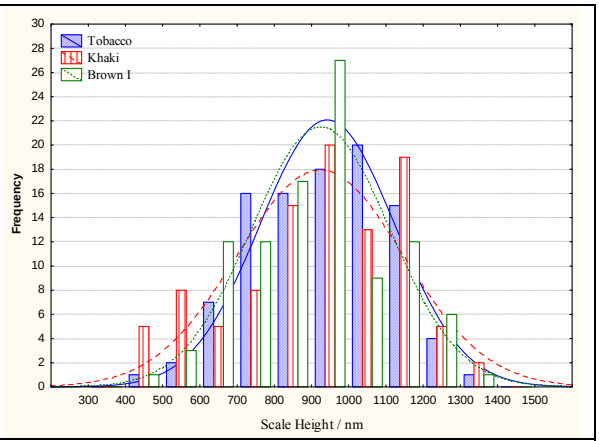

Third Set

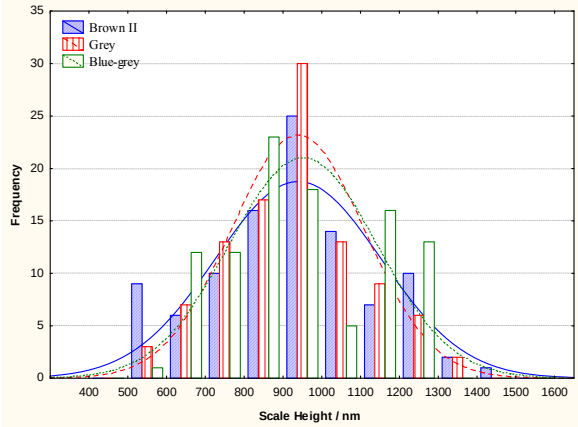

Third Set

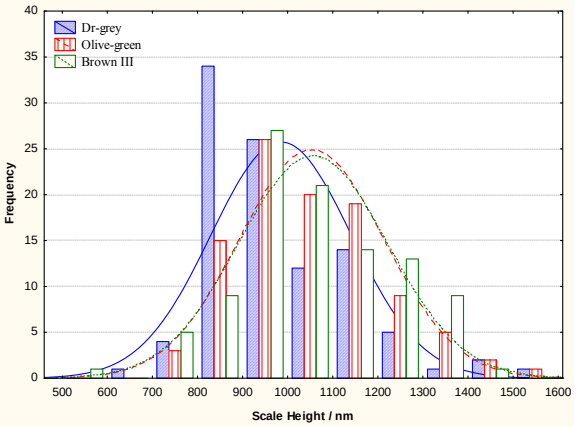

Third Set

C.2 Scale Angle (P2)

The following figures show the distribution of the scale angle for all samples. Each graph shows three samples.

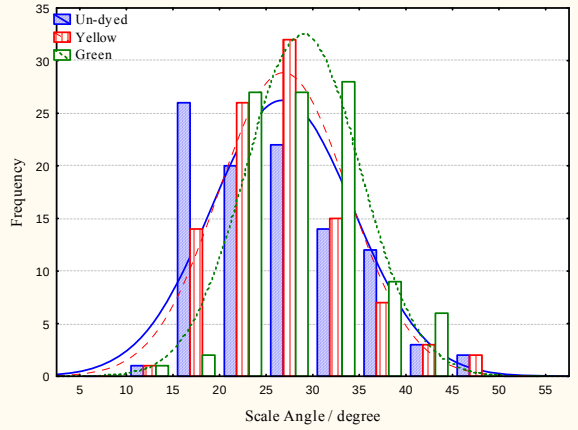

Second Set

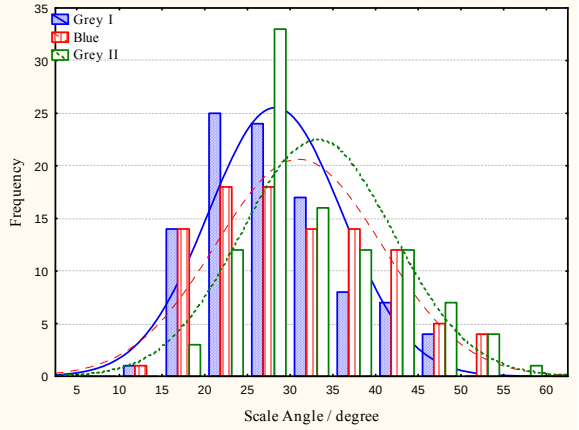

Second Set

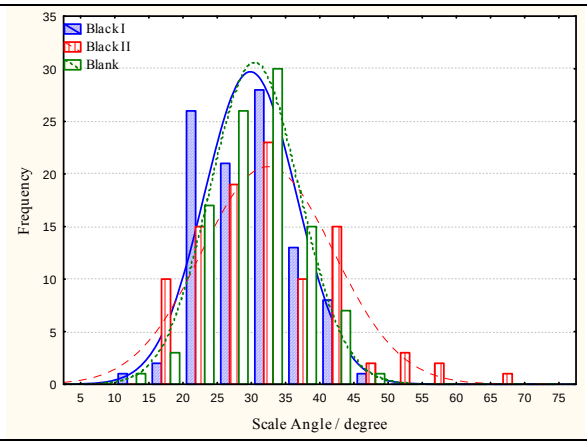

Second Set

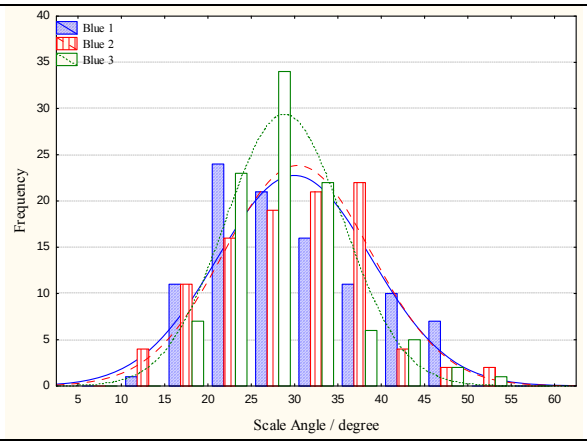

Second Set

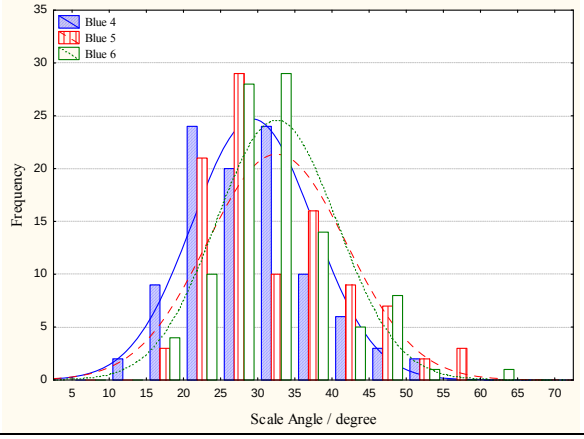

Second Set

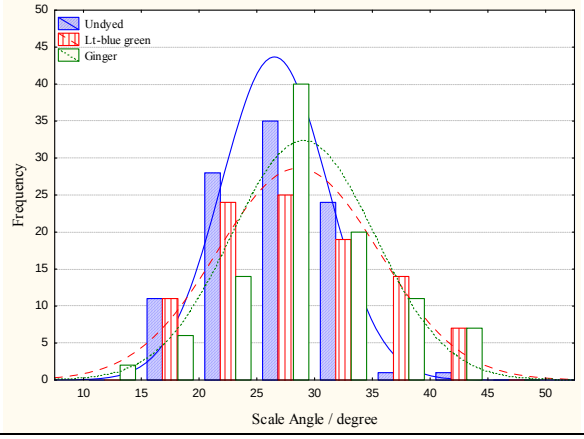

Third Set

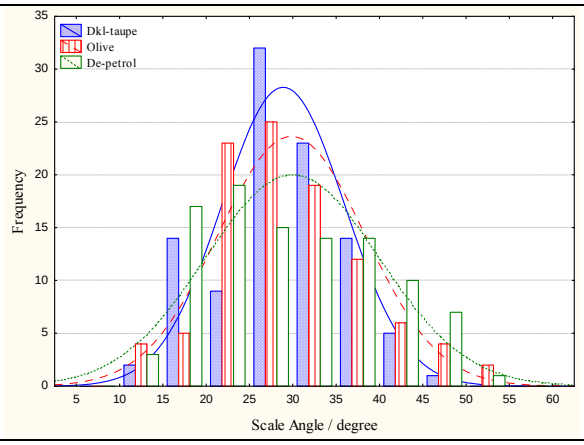

Third Set

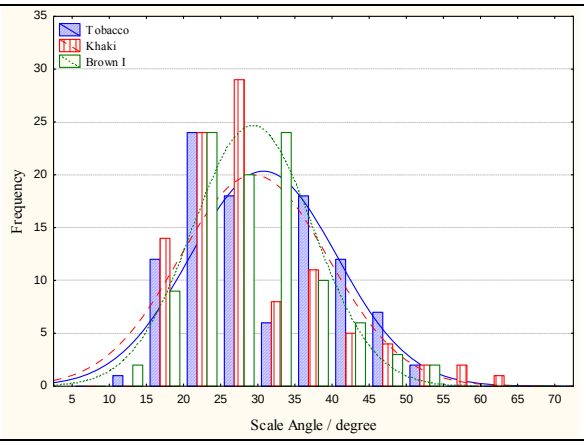

Third Set

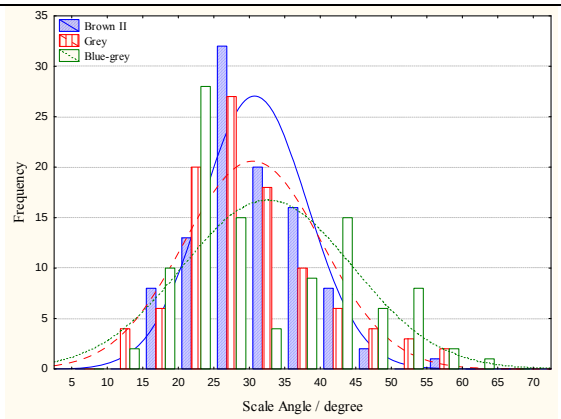

Third Set

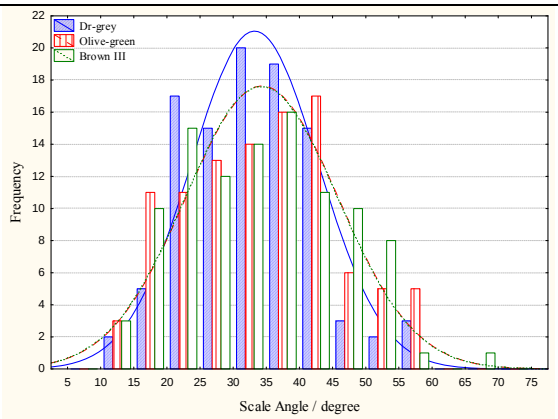

Third Set

C.3 Surface Roughness (P3)

The following figures show the distribution of the surface roughness for all samples. Each graph shows three samples.

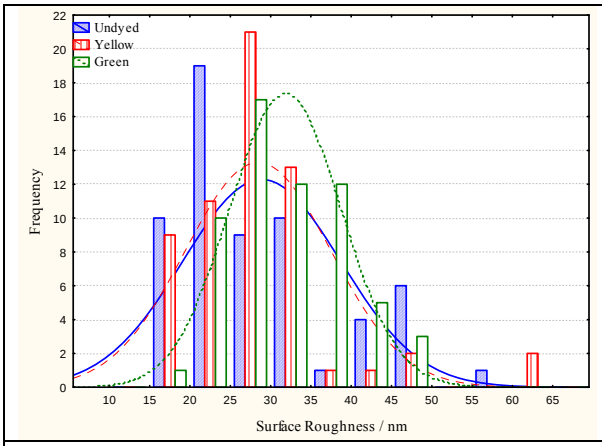

Second Set

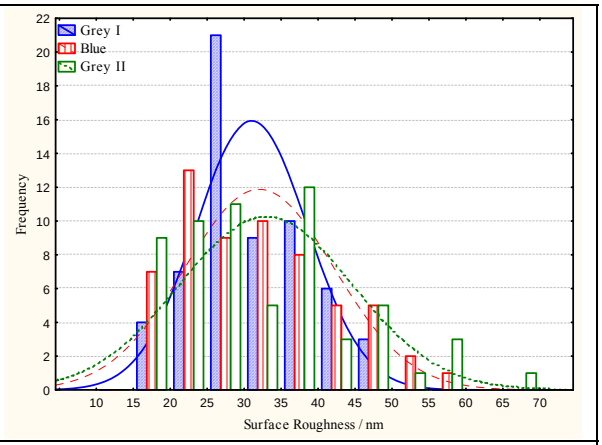

Second Set

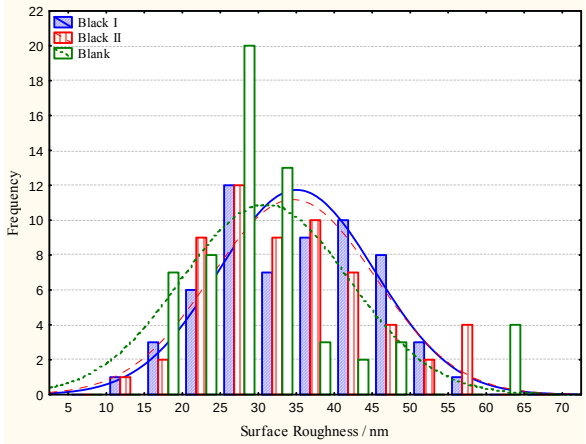

Second Set

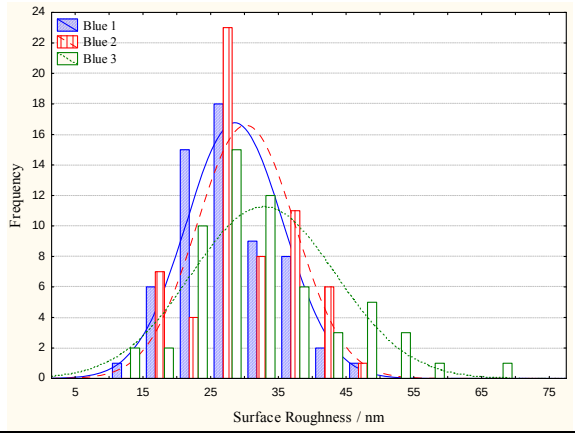

Second Set

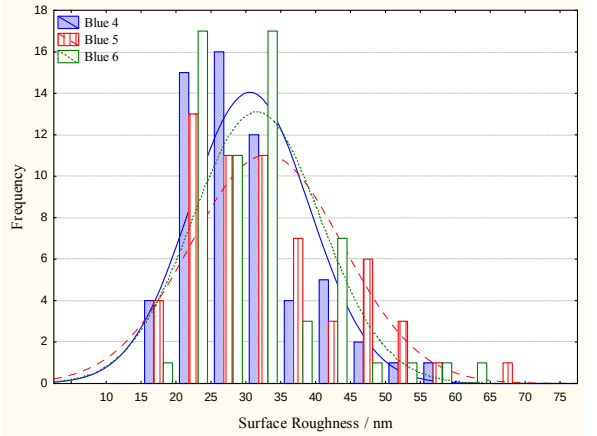

Second Set

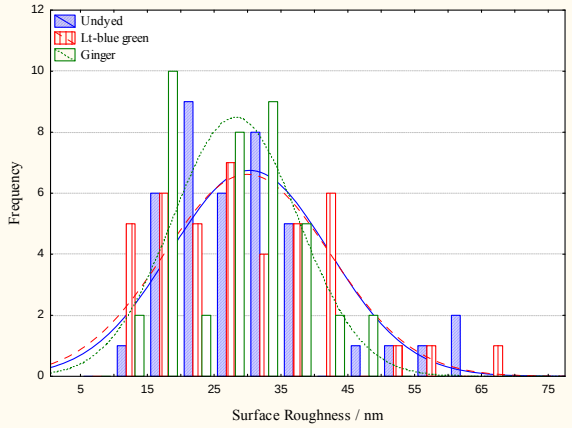

Third Set

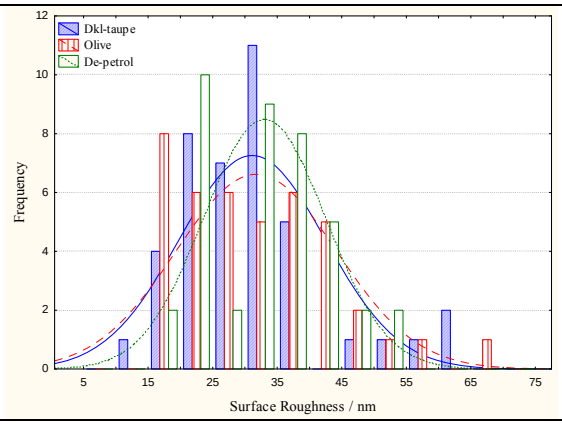

Third Set

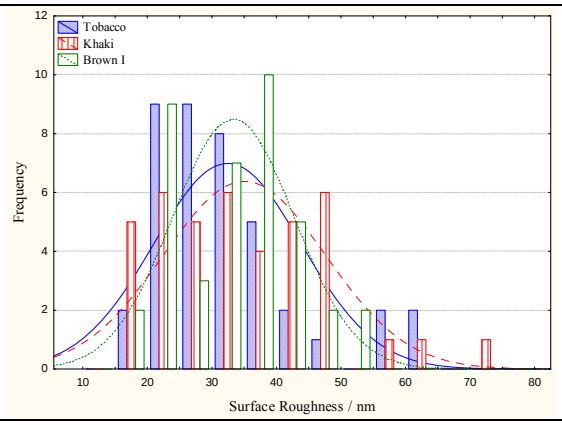

Third Set

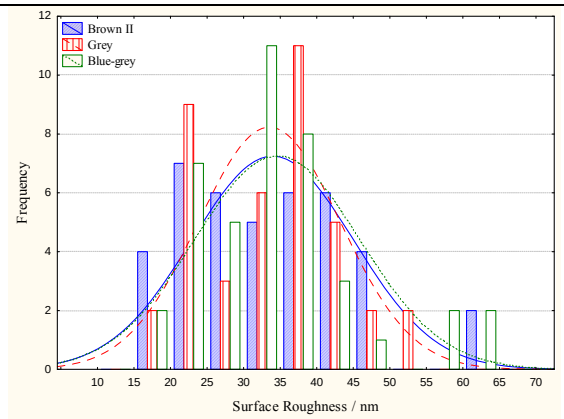

Third Set

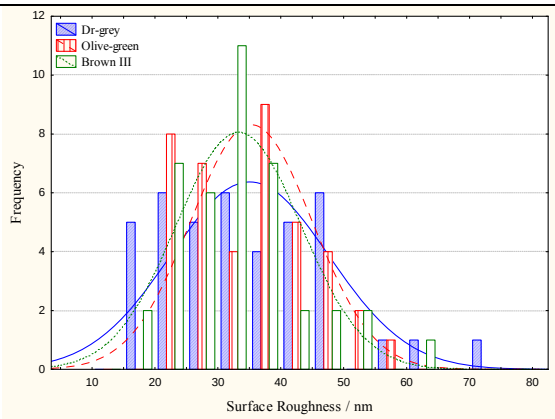

Third Set

C.4 Scale Interval (P4)

The following figures show the distribution of the scale interval for all samples. Each graph shows three samples.

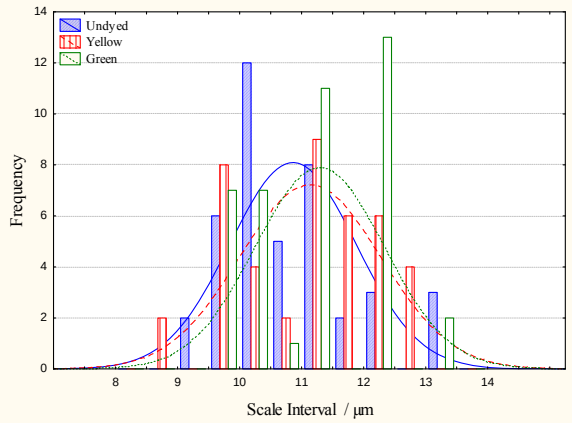

Second Set

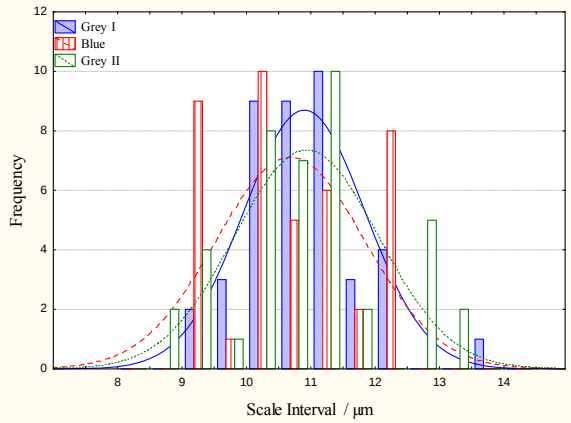

Second Set

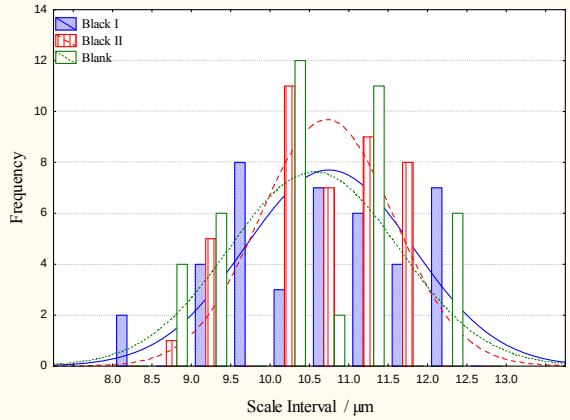

Second Set

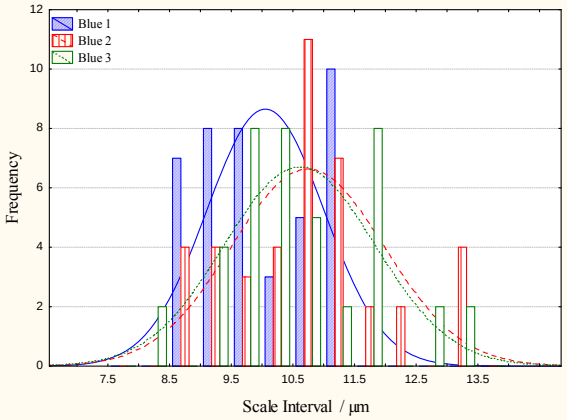

Second Set

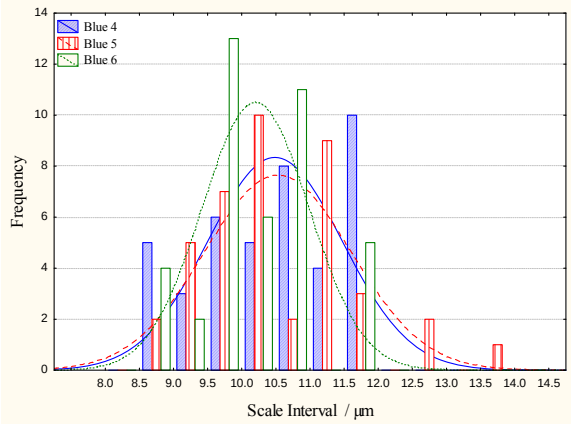

Second Set

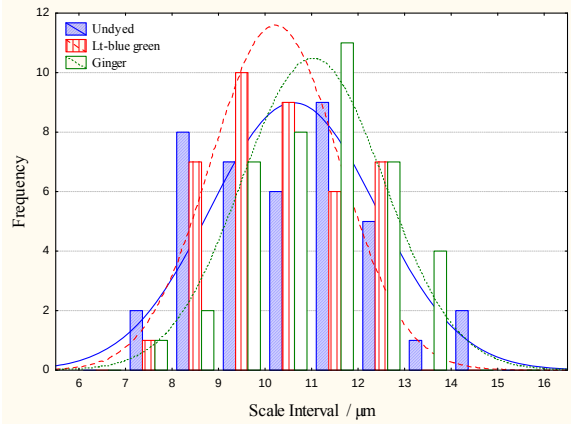

Third Set

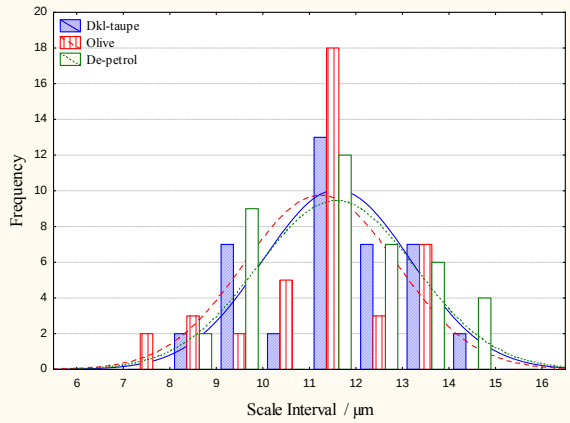

Third Set

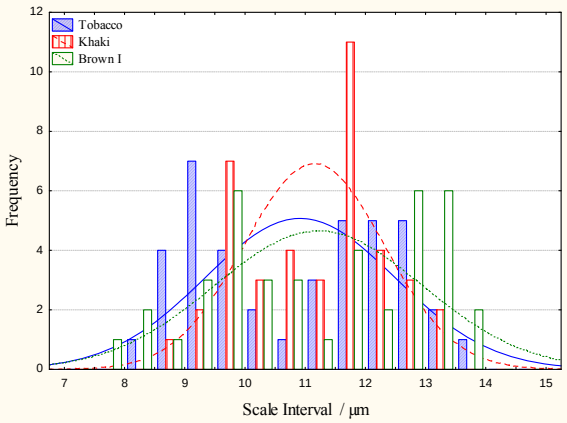

Third Set

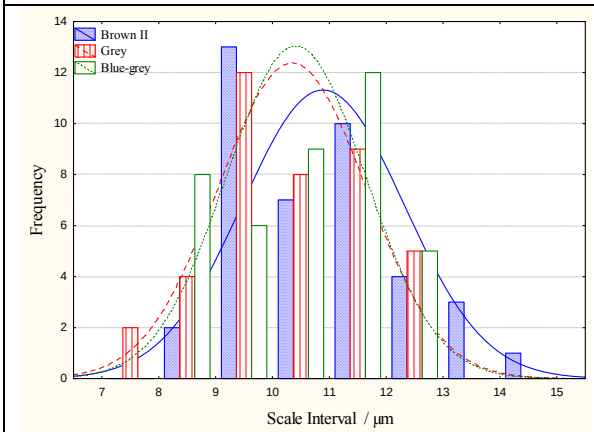

Third Set

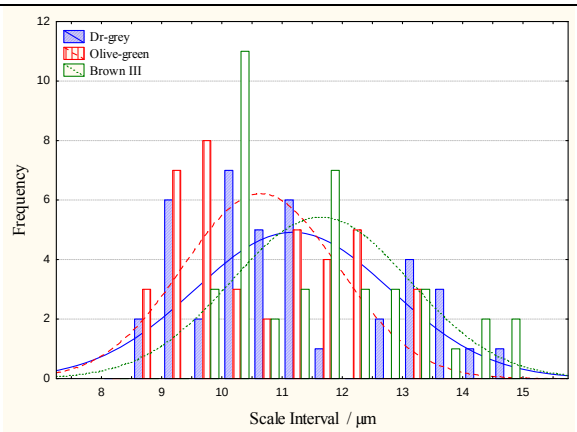

Third Set

C.5 Normalized Contact Edge Length (P5)

The following figures show the distribution of the normalized contact edge length for all samples. Each graph shows three samples.

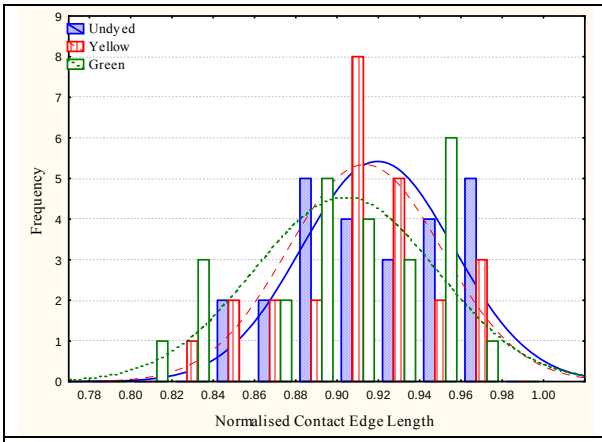

Second Set

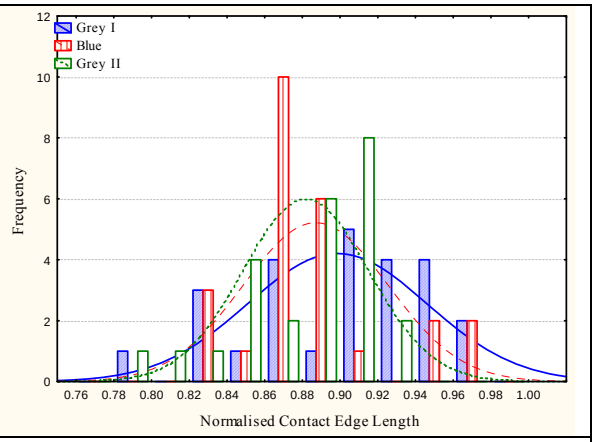

Second Set

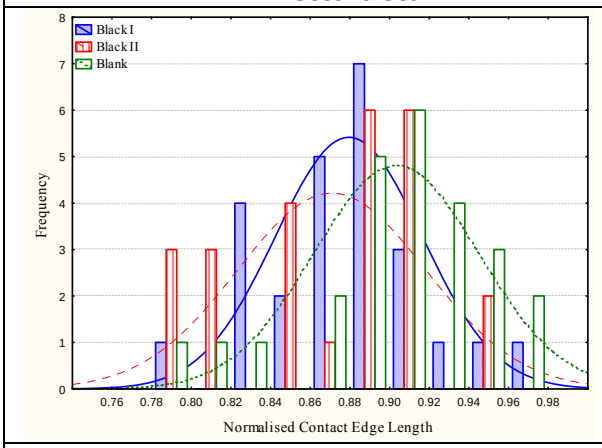

Second Set

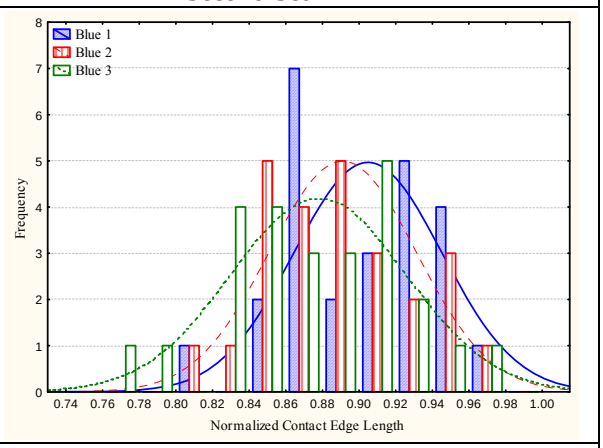

Second Set

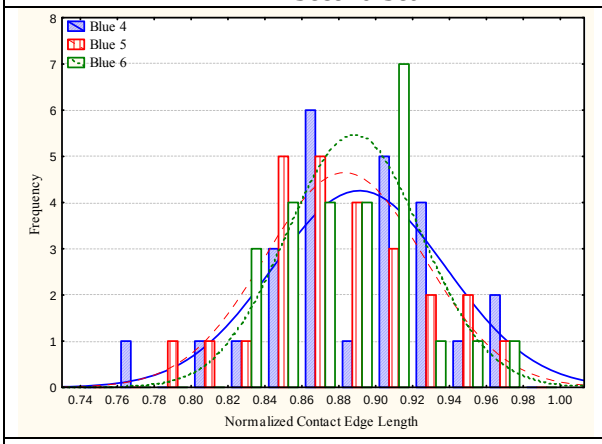

Second Set

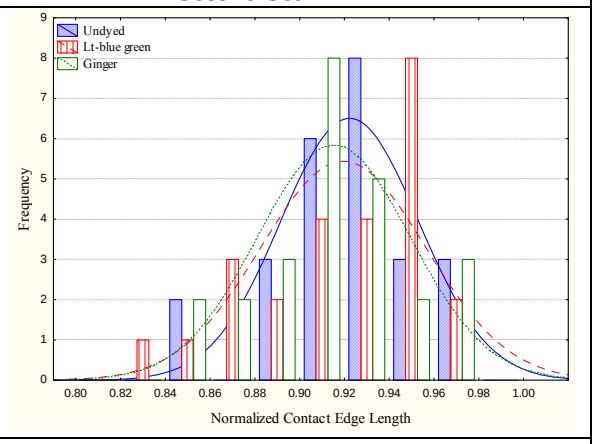

Third Set

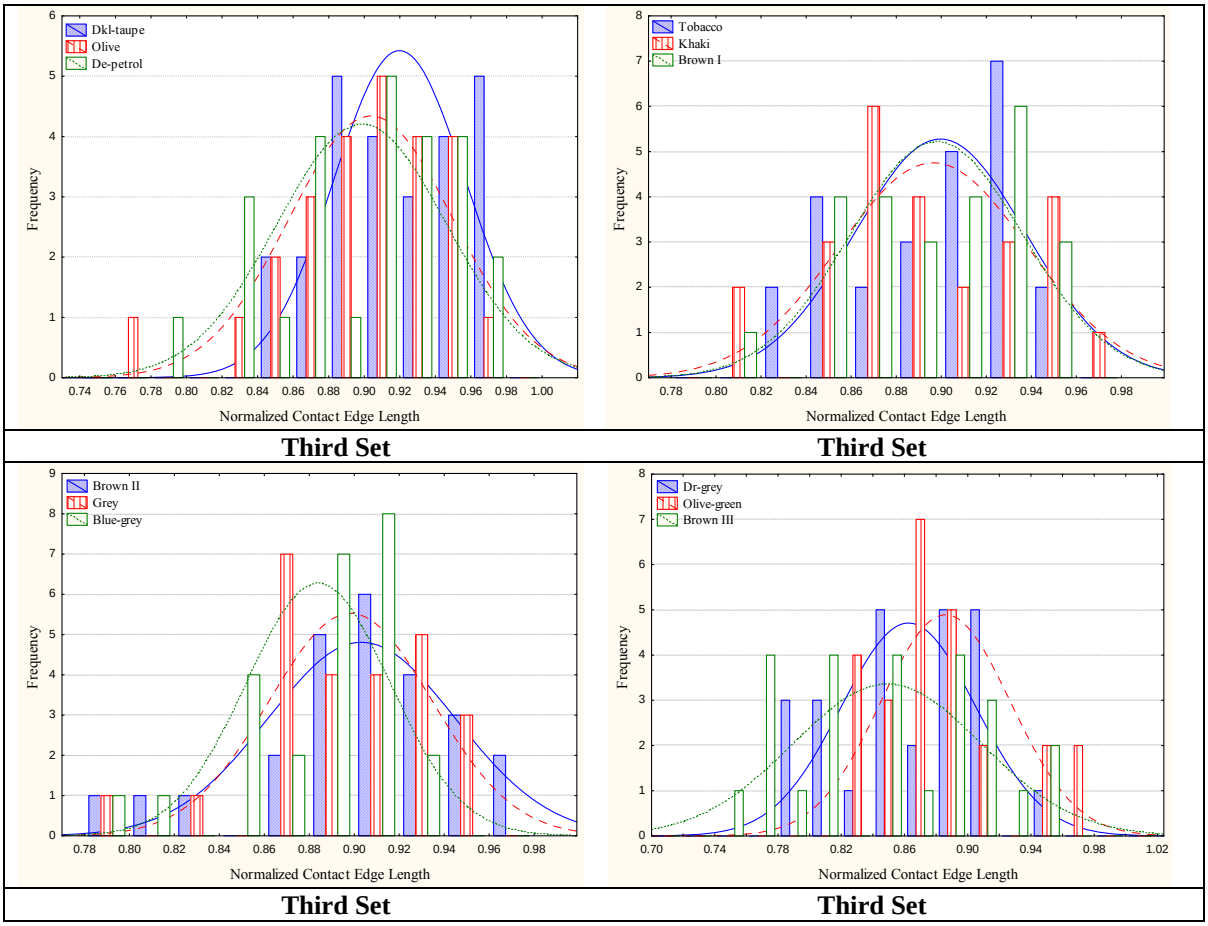

C.6 Scale Elongation (P6)

The following figures show the distribution of the scale elongation for all samples. Each graph shows three samples.

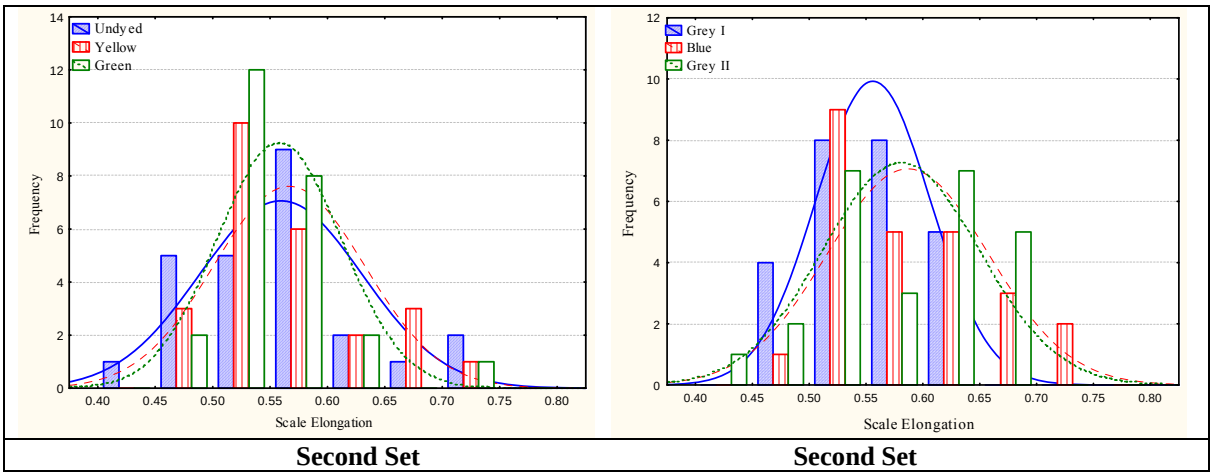

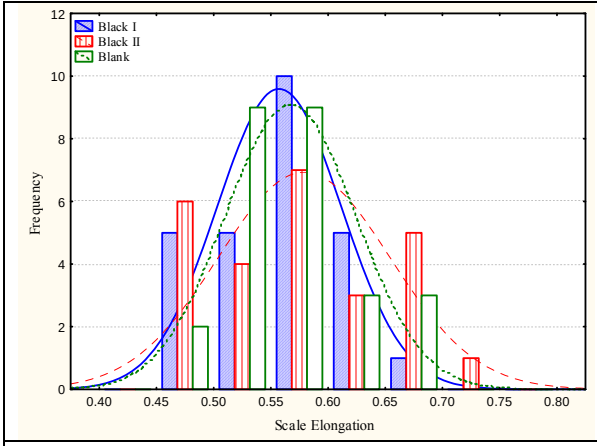

Second Set

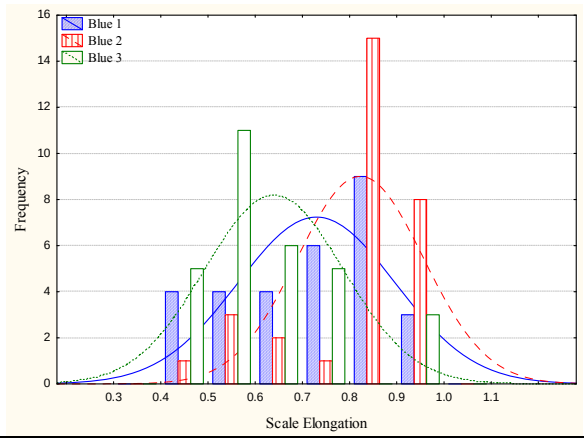

Second Set

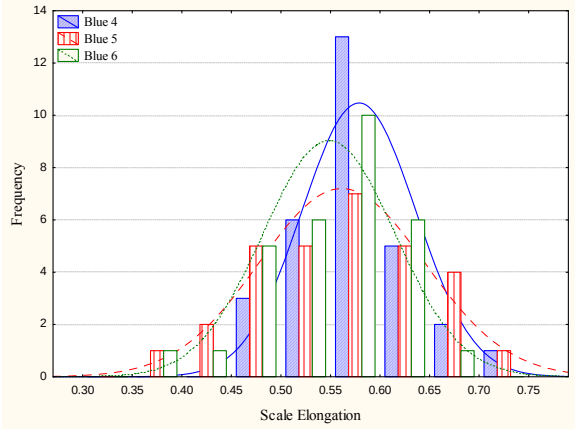

Second Set

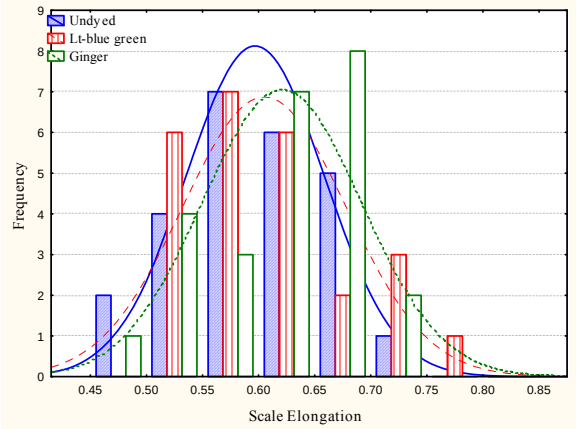

Third Set

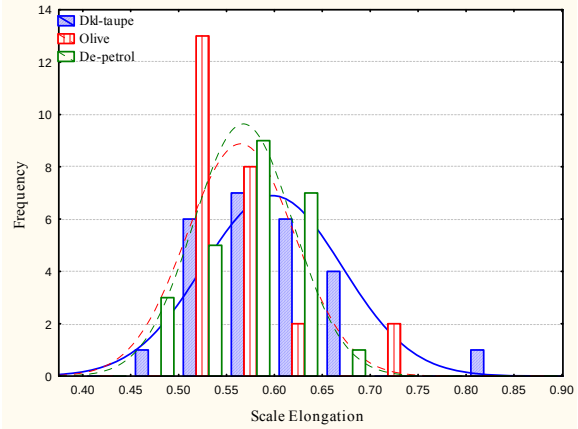

Third Set

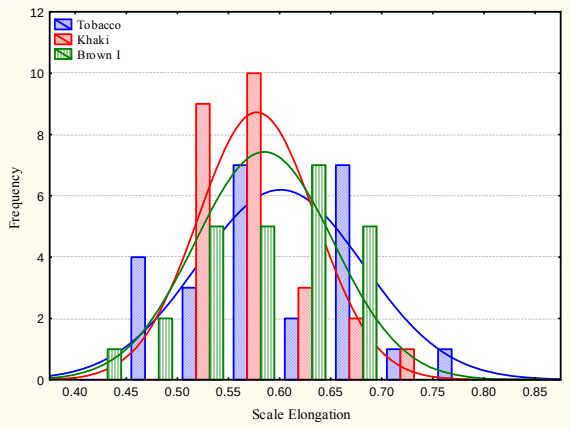

Third Set

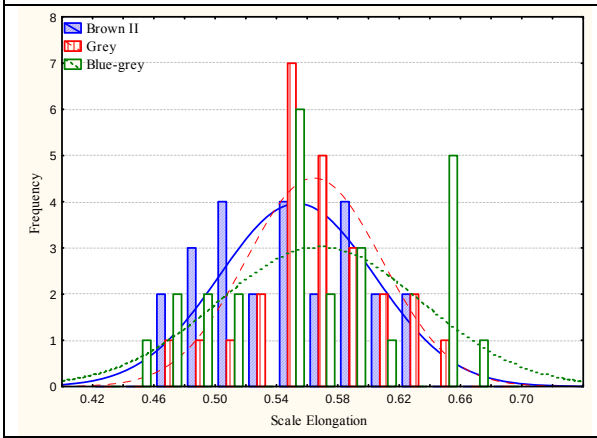

Third Set

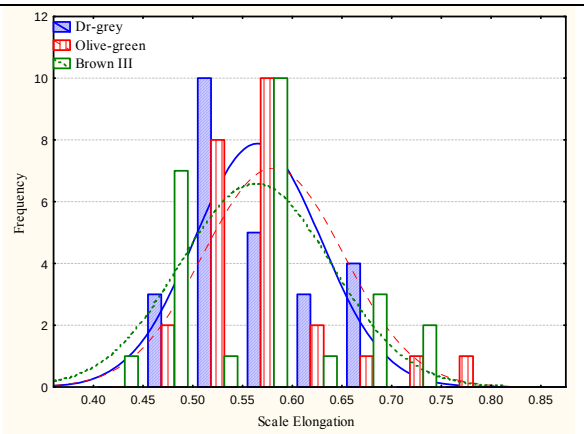

Third Set

C.7 Adhesive Force (P7)

The following figures show the distribution of the adhesive force for all samples. Each graph shows three samples.

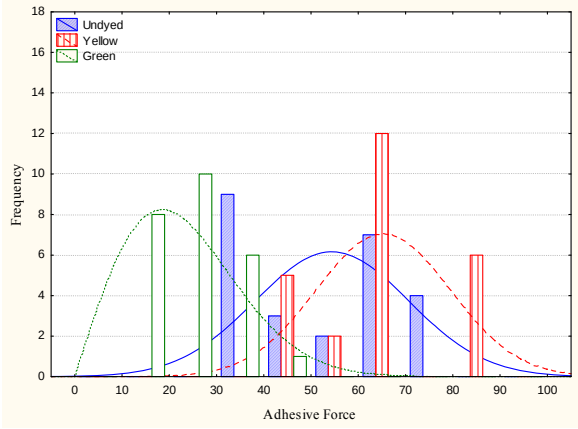

Second Set

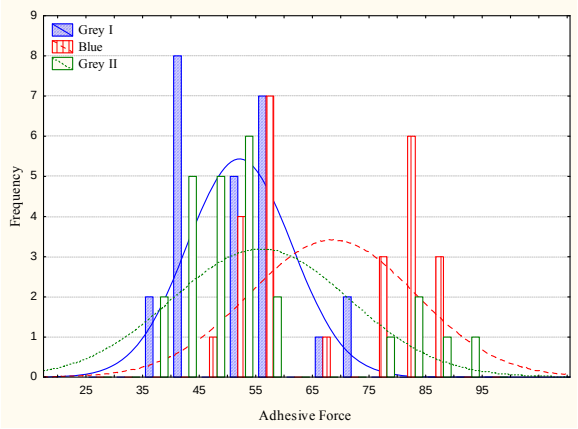

Second Set

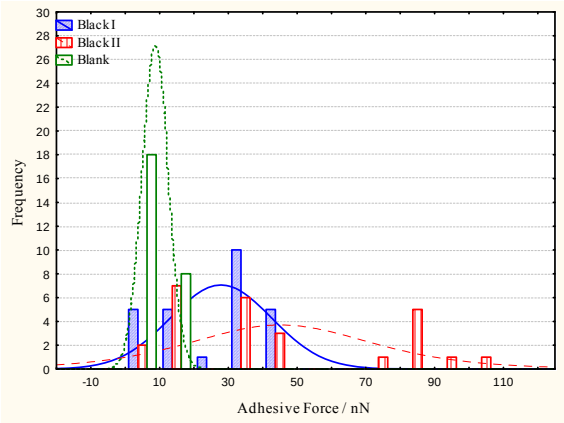

Second Set

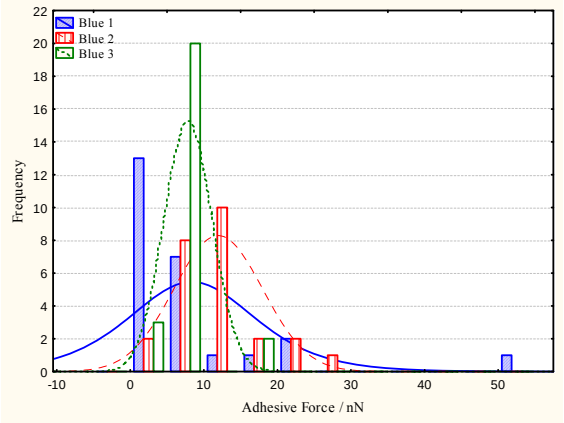

Second Set

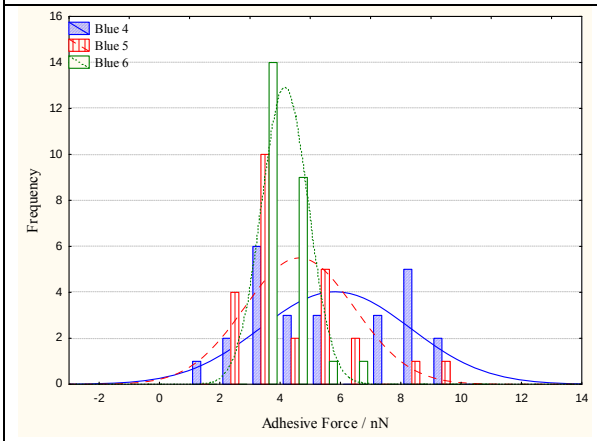

Second Set

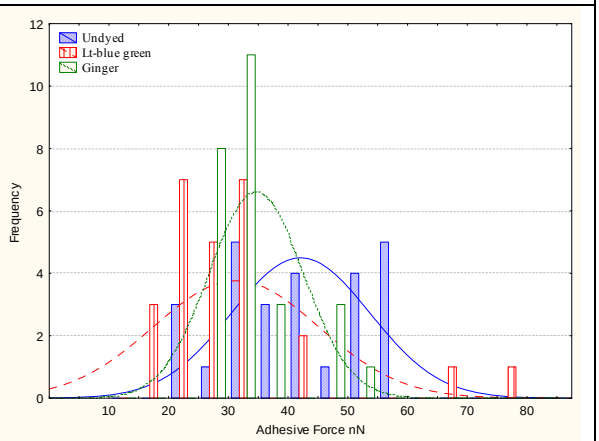

Third Set

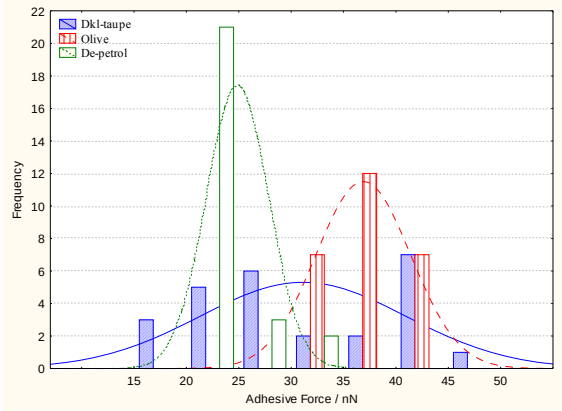

Third Set

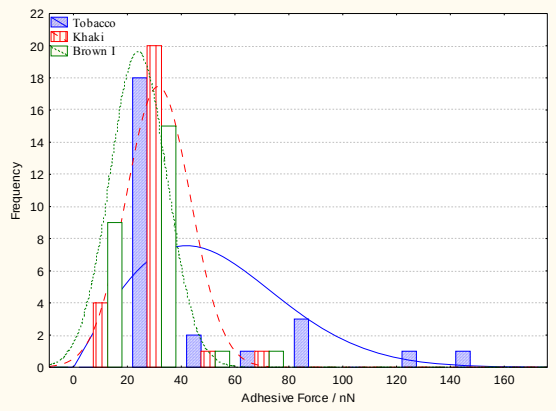

Third Set

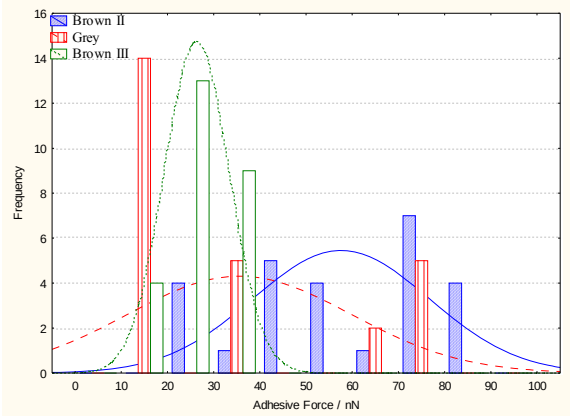

Third Set

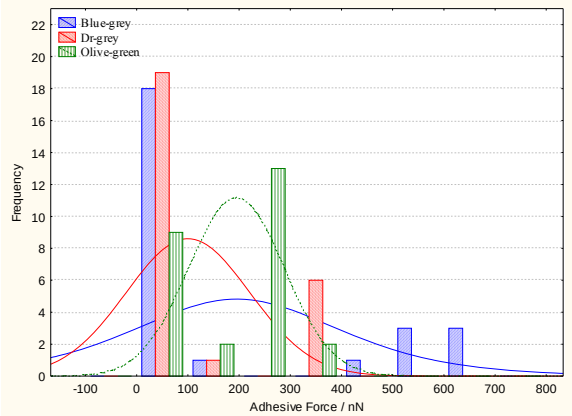

Third Set

C.8 Surface Hardness (P8)

The following figures show the distribution of the surface hardness for all samples. Each graph shows three samples.

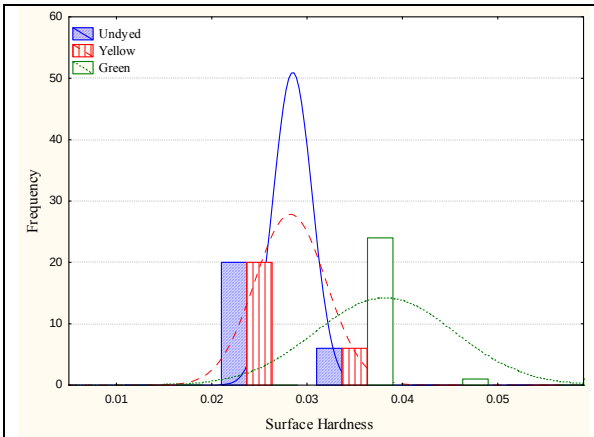

Second Set

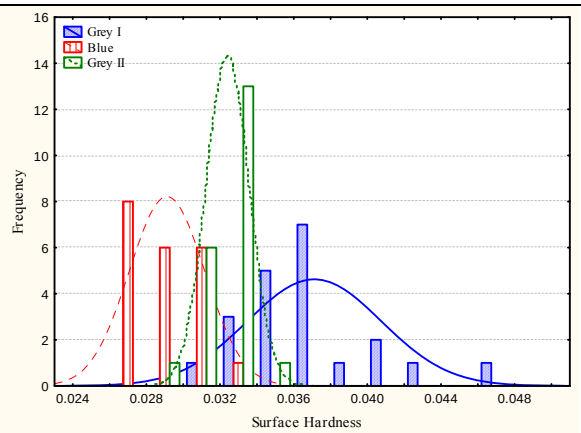

Second Set

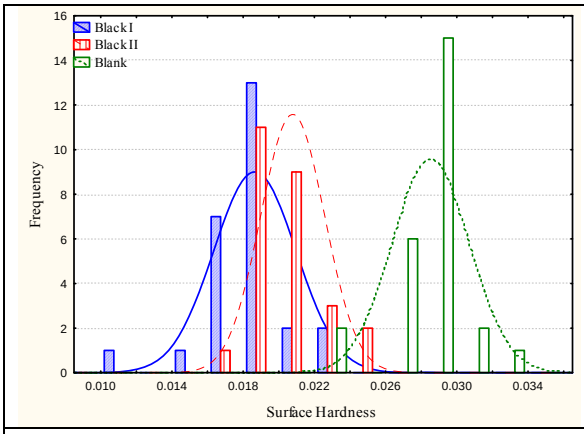

Second Set

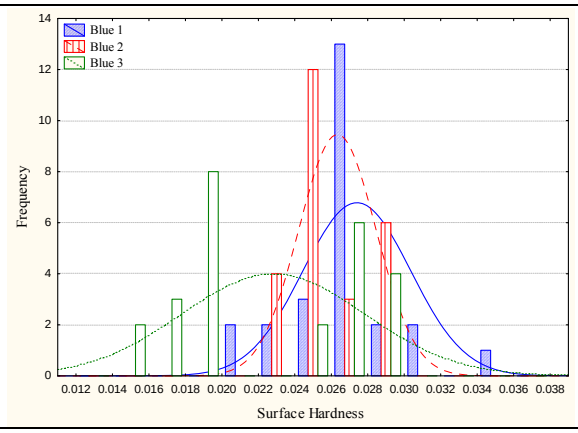

Second Set

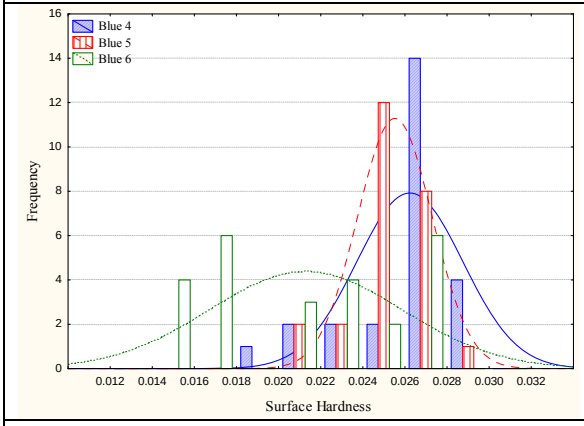

Second Set

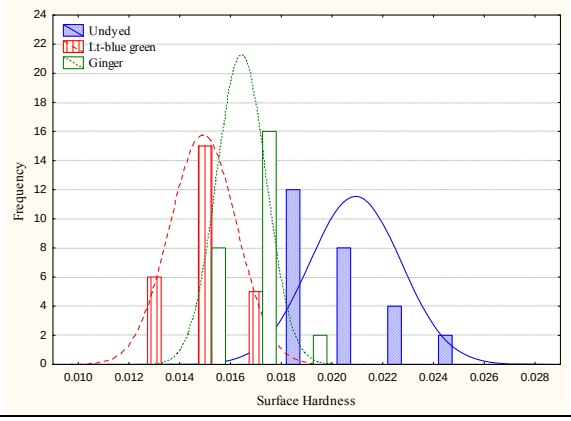

Third Set

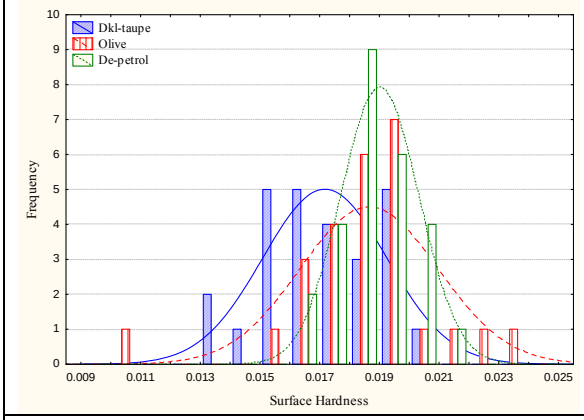

Third Set

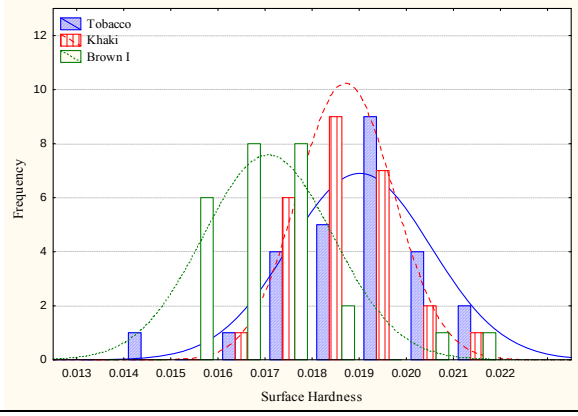

Third Set

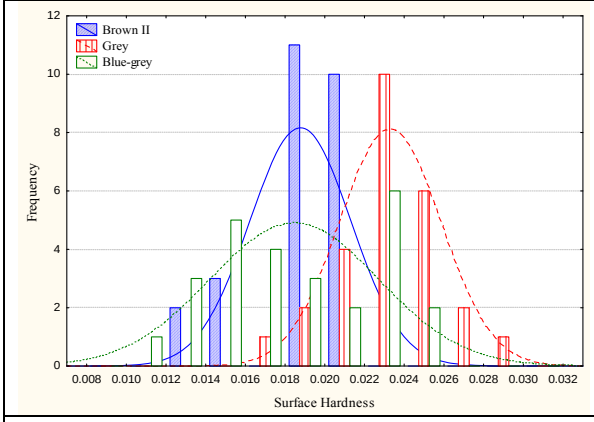

Third Set

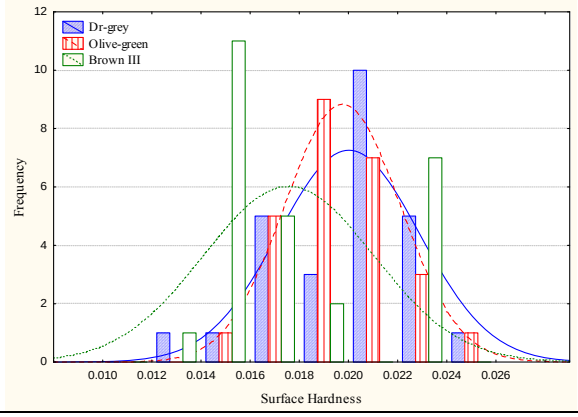

Third Set

C.9 Standard Deviations and Percentage Increase and Decrease of the Scale Parameters

Sample	Sd.P1	P1%	Sd.P2	P2%	Sd.P3	P3%	Sd.P4	P4%	Sd.P5	P5%	Sd.P6	P6%	Sd.P7	P7%	Sd.P8	P8%
Un-dyed	139.9	0.0	7.64	0.0	7.82	0.0	1.3	0.0	0.029	91.8	0.062	0.0	0.0	0.0	0.022	0.0
Yellow	145.5	5.22	6.96	0.38	7.79	-1.3	1.52	2.5	0.030	91.1	0.067	0.8	16.4	14.6	0.04	2.6
Green	148.8	6.31	6.16	8.30	7.23	9.9	1.49	3.4	0.033	90.4	0.068	1.2	15.18	56.1	0.008	15.5
Grey I	149.6	6.22	7.55	2.10	7.33	7.5	1.35	-2.3	0.034	89.6	0.07	-2.5	5.89	9.33	0.037	8.45
Blue	156.3	9.5	8.44	15.7	8.35	11	1.49	4.4	0.032	88.6	0.096	1.5	8.84	60.7	0.021	29.9
Grey II	152.4	9.77	9.59	24.1	8.43	14.4	1.46	-2.6	0.033	88.1	0.095	1.6	14.7	13.4	0.011	22.5
Black I	150.9	3.81	8.18	19.1	8.23	21.1	1.56	1.7	0.033	88.6	0.06	0.2	17.4	51.4	0.012	36.2
Black II	152.6	4.75	7.91	16.2	8.69	20.1	1.54	-2.4	0.034	88.8	0.043	0.9	2.8	1.2	0.024	28.5
Blank	188.5	-1.87	9.48	9.00	8.52	63.9	1.48	4.4	0.035	90.2	0.056	1.6	4.4	84.7	0.013	0.35
Blue 1	167.0	-0.36	8.9	9.70	7.89	1.0	1.46	-1.4	0.034	90.0	0.086	2.6	3.5	85.4	0.025	4.22
Blue 2	166.2	0.27	9.08	13.2	7.91	4.5	1.53	3.5	0.034	89.9	0.082	4.5	5.6	79.2	0.025	7.04
Blue 3	169.3	5.4	7.37	8.20	8.56	13.2	1.52	-5.2	0.035	89.0	0.076	6.7	16.3	86.3	0.0414	16.55
Blue 4	169.6	5.28	9.6	11.1	8.45	4.4	1.53	1.3	0.036	89.1	0.084	-2.3	4.3	89.7	0.028	7.70
Blue 5	170.3	5.1	9.48	20.3	8.96	13.8	1.54	-3.4	0.035	89.6	0.065	0.68	6.6	91.9	0.023	10.50
Blue 6	162.3	7.4	9.4	21.0	9.16	10.2	1.48	2.5	0.033	88.6	0.089	1.0	17.2	92.9	0.033	25.3
Un-dyed	134.9	0.0	4.94	0.0	7.69	0.0	1.68	0.0	0.032	92.2	0.056	0.0	1.18	0.0	0.018	0.0
Lt-blue green	156.9	7.43	6.96	12.8	7.19	-4.69	1.56	6.6	0.033	92	0.066	1.5	1.99	25.6	0.012	14.5
Ginger	148.5	4.95	6.16	14.4	7.89	3.85	1.82	4.2	0.033	91.1	0.067	2.1	1.137	17.6	0.0096	12.7

Sample	Sd.P1	P1%	Sd.P2	P2%	Sd.P3	P3%	Sd.P4	P4%	Sd.P5	P5%	Sd.P6	P6%	Sd.P7	P7%	Sd.P8	P8%
Dkl-taupe	160.8	7.52	7.05	12.1	8.56	6.04	1.69	-1.6	0.032	91.9	0.067	-1.22	1.416	25.9	0.020	24.6
Olive	155.3	6.86	8.44	17.6	8.66	10.40	1.66	4.5	0.034	90	0.066	-1.80	0.653	12.4	0.022	18.1
De-petrol	149.6	9.97	9.9	18	8.23	8.38	1.65	-1.6	0.034	89.7	0.075	3.52	0.43	40.8	0.011	22.9
Tobacco	139.4	8.26	9.8	21.1	8.36	17.11	1.77	5.7	0.033	89.8	0.065	0.79	5.85	17.6	0.014	16.7
Khaki	135.9	9.62	9.9	16	8.45	11.4	1.74	1.4	0.034	89.5	0.080	1.89	1.04	25.6	0.0099	17.7
Brown I	165.5	8.88	8.08	15.6	8.26	16.10	1.75	6.5	0.033	89.7	0.076	1.22	0.88	44.9	0.013	25.1
Brown II	142.7	13.2	7.37	21.2	8.23	12.41	1.66	1.6	0.035	90.2	0.081	-1.21	2.75	36.8	0.025	17.1
Grey	137.4	10.66	9.68	20.4	8.24	15.63	1.81	1.1	0.034	89.6	0.083	-3.21	3.48	13.2	0.025	28.1
Blue-grey	162.5	12	11.9	28.4	7.96	17.11	1.78	1.2	0.033	88.2	0.097	-2.50	33.1	362	0.0414	32.1
Dr-grey	172.0	16.1	9.6	32.4	8.88	22.04	1.88	3.2	0.033	86.1	0.081	-0.64	17.4	135	0.028	25.5
Olive-green	189.3	24	11.48	35.4	8.54	21.04	1.85	0.8	0.033	88	0.078	1.30	13.4	361	0.023	21.14
Brown III	194.6	24.4	11.4	35.1	8.61	3.85	1.89	2.9	0.036	84.5	0.076	-0.25	1.02	37	0.033	22.9

Appendix D: British Standard Tensile Testing Method of Individual Textile Fibres (BS 3411: 1971)

1. Introduction

This British standard describes the determination of the tensile properties of all individual fibres with constant rate of extension machines. Provision is made for the use of a gauge length of 10mm, 20mm or 50mm, with either pre-tensioned or slack specimens.

2. Apparatus

The following is required for measurements:

a. A tensile testing machine, which is linked to a computer to record the results.

b. A constant rate of extension machine. The rate of increase in the distance between the clamps should not vary by more than 5%, after the first two sections.

c. Means to place single fibres in the clamps without damage.

d. Atmospheres for conditioning and testing as defined in BS 1051 i.e. an atmosphere with a relative humidity of 65 ± 2 % and a temperature of 20 ± 2 ºC.

3. Test Specimens

a. **Sampling.** The test samples were selected as described in chapter 4 and the sample size were are chosen from the laboratory samples to be representative of this set.

b. **Length of specimen.** It is recommended that for general purposes, the gauge length be 10 mm, and that the actual length be recorded with an accuracy of ± 1 %.

c. **Number of tests.** The number of tested samples should not be fewer than 50 test specimens.

d. **Preparation of specimens.** Individual straight fibres should be mounted between the jaws without damaging them as follows:

   A rectangular hole, with the length of the gauge, is cut in thin cardboard, and the fibre is mounted across the hole with adhesive tape. The ends of the card are clamped in the jaws of the tensile tester. Before operating the machine the cardboard is then cut across in the middle, which leaves the fibre clamped into the tensile tester without support and ready for testing.

4. Test Procedure

a. Set the jaws to the required or specified distance.

b. Clamp the cardboard, so that the fibre lies along the axis of extension of the instrument.

c. Cut the cardboard across, so that the fibre is free and adjust the instrument to zero load.

d. Put the travelling clamp in motion and extend the specimen to the point of rupture (using the series IX computer programme).

e. Note jaw breaks, i.e. breaks in which one of the broken ends is not visible, and exclude results of such specimens.

f. For each sample the load and gauge length are set to zero before measurement.

5. Calculation and Expression of Results

In addition to the load extension curves the following quantities are calculated:

a. The mean breaking load and standard deviation.

b. The mean breaking extension with standard deviation.

Appendix E: Tensile Test Results

E.1 Maximum Fibre Strength and Elongation for the First Sample Set (Pilot Study)

18.5 µm Undyed		18.5 µm Dyed		18.5 µm Undyed		18.5 µm Dyed		20 µm Undyed		20 µm Dyed		20 µm Undyed		20 µm Dyed	
B. L.*	**B. E.****	**B. L.**	**B. E.**	**B. L.**	**B. E.**	**B. L.**	**B. E.**	**B. L.**	**B. E.**	**B. L.**	**B. E.**	**B. L.**	**B. E.**	**B. L.**	**B. E.**
0.087	4.80	0.132	8.62	0.103	4.95	0.053	2.51	0.159	6.83	0.096	3.31	0.226	8.44	0.083	4.04
0.120	5.22	0.084	4.68	0.068	3.3	0.073	3.27	0.139	7.14	0.057	3.86	0.159	8.61	0.119	3.03
0.095	4.18	0.135	7.39	0.174	7.73	0.089	4.21	0.105	1.10	0.057	2.74	0.099	4.61	0.106	4.73
0.067	2.93	0.145	8.00	0.120	4.48	0.119	8.49	0.120	8.94	0.173	6.25	0.158	7.78	0.127	6.01
0.084	3.75	0.052	1.65	0.093	3.12	0.110	5.67	0.184	9.26	0.131	5.25	0.142	8.07	0.123	7.38
0.123	6.34	0.073	3.60	0.069	1.42	0.110	5.69	0.122	7.33	0.134	6.72	0.185	9.17	0.150	7.81
0.065	1.16	0.134	6.71	0.153	7.82	0.049	1.20	0.111	6.17	0.167	1.62	0.084	2.77	0.138	7.03
0.154	7.67	0.103	5.10	0.142	7.72	0.153	8.14	0.116	5.99	0.096	5.51	0.173	8.44	0.165	7.27
0.115	6.43	0.071	1.77	0.169	6.32	0.115	7.13	0.106	5.02	0.076	2.32	0.124	5.65	0.165	6.51
0.128	7.64	0.165	8.16	0.110	7.81	0.110	6.25	0.085	3.41	0.057	1.85	0.060	1.25	0.108	5.52
0.197	9.55	0.205	8.29	0.146	6.78	0.103	5.07	0.185	9.35	0.122	6.26	0.102	2.44	0.120	6.38
0.174	6.01	0.146	3.84	0.119	5.81	0.103	4.09	0.181	8.72	0.076	2.34	0.075	2.91	0.126	5.44
0.173	9.45	0.091	3.73	0.099	3.88	0.135	7.24	0.150	6.36	0.121	4.18	0.170	6.54	0.220	8.36
0.122	5.70	0.118	5.50	0.038	1.11	0.053	1.38	0.151	6.84	0.126	6.16	0.150	7.01	0.154	7.14
0.126	8.18	0.140	6.29	0.068	3.30	0.130	7.92	0.144	7.10	0.131	5.76	0.121	5.39	0.179	7.64
0.048	1.69	0.068	2.94	0.174	7.73	0.112	7.48	0.123	5.90	0.115	5.51	0.149	7.78	0.127	6.74
0.089	6.17	0.099	4.22	0.120	4.48	0.108	5.82	0.126	8.44	0.091	2.76	0.052	1.19	0.179	7.88
0.124	6.30	0.103	4.14	0.093	3.12	0.049	1.20	0.181	9.28	0.123	4.51	0.168	6.27	0.149	5.93
0.162	8.04	0.107	4.11	0.069	1.42	0.153	8.14	0.171	8.55	0.061	5.83	0.154	5.49	0.108	5.69
0.145	8.67	0.051	0.52	0.153	7.82	0.115	7.13	0.162	8.42	0.036	1.79	0.060	1.25	0.208	9.40
0.142	7.53	0.081	4.99	0.142	7.71	0.110	6.25	0.228	8.63	0.162	7.40	0.102	2.44	0.051	1.03
0.112	5.22	0.059	3.13	0.169	6.42	0.049	1.21	0.173	8.75	0.143	9.05	0.075	2.91	0.103	5.55
0.131	7.12	0.107	5.13	0.123	5.68	0.153	8.15	0.173	9.33	0.130	5.23	0.170	6.54	0.110	5.74
0.126	6.69	0.057	3.62	0.122	5.98	0.110	6.26	0.150	7.44	0.073	3.45	0.228	8.63	0.088	3.58
0.147	7.49	0.083	4.10	0.155	7.21	0.131	6.41	0.106	3.88	0.177	8.09	0.132	4.69	0.061	1.85
Average Value				**0.100**	**5.08**	**0.104**	**5.09**	**Average Value**				**6.09**	**0.144**	**5.068**	**0.12**
Standard Deviation				**0.035**	**2.17**	**0.037**	**2.22**	**Standard Deviation**				**1.38**	**0.029**	**2.028**	**0.038**

*** B. E. = Breaking Extension, ** B. L. = Breaking Load.**

E.2 Maximum Fibre Strength and Elongation for the Second and the Third Sample Sets

E.2.1 Results of breaking load and breaking extension for the second set (fibres from the same lot)

Undyed		Yellow		Green		Grey I		Blue		Grey II		Black I		Black II	
B. L.	**B. E.**	**B. L.**	**B. E.**	**B. L.**	**B. E.**	**B. L.**	**B. E.**	**B. L.**	**B. E.**	**B. L.**	**B. E.**	**B. L.**	**B. E.**	**B. L.**	**B. E.**
0.097	6.78	0.087	5.01	0.167	6.89	0.159	5.60	0.123	5.69	0.124	4.79	0.110	4.59	0.085	4.59
0.058	3.85	0.065	3.21	0.143	5.57	0.079	4.28	0.118	6.27	0.072	1.86	0.077	3.51	0.087	5.46
0.137	7.58	0.056	3.36	0.108	5.32	0.075	3.52	0.135	5.94	0.046	1.12	0.100	4.11	0.055	3.16
0.099	6.07	0.076	1.67	0.146	6.23	0.112	6.58	0.179	6.96	0.110	5.52	0.087	4.26	0.059	3.22
0.064	3.81	0.089	1.79	0.189	7.70	0.087	5.42	0.076	4.11	0.135	6.68	0.093	5.06	0.081	4.48
0.077	5.18	0.151	7.11	0.157	6.21	0.060	3.73	0.116	4.48	0.198	6.18	0.083	5.91	0.084	4.98
0.089	3.02	0.155	8.30	0.146	6.29	0.096	4.47	0.178	6.03	0.146	6.32	0.103	5.31	0.067	3.28
0.077	4.92	0.134	6.55	0.204	8.46	0.149	6.71	0.096	3.66	0.091	3.42	0.106	4.78	0.064	2.48
0.104	6.29	0.077	3.99	0.051	2.61	0.100	5.19	0.068	1.13	0.059	2.42	0.103	4.14	0.104	6.08
0.063	5.01	0.135	6.32	0.139	7.07	0.092	5.63	0.092	4.40	0.131	6.78	0.092	6.38	0.095	5.72
0.118	7.56	0.087	3.19	0.042	2.01	0.138	6.88	0.088	4.08	0.067	2.71	0.059	1.84	0.100	4.55
0.057	3.49	0.127	5.55	0.154	7.70	0.127	5.19	0.065	3.17	0.076	4.01	0.124	5.13	0.182	7.56
0.038	1.04	0.034	1.21	0.138	4.91	0.135	6.66	0.102	4.36	0.093	4.02	0.060	3.55	0.103	2.29
0.079	5.01	0.165	6.53	0.149	6.38	0.107	5.45	0.107	4.66	0.132	6.21	0.104	5.17	0.118	5.25
0.150	7.77	0.038	2.48	0.167	6.32	0.089	3.26	0.116	6.21	0.146	6.25	0.120	6.29	0.139	5.61
0.112	5.94	0.100	5.28	0.142	5.64	0.119	5.11	0.130	5.29	0.083	3.87	0.088	4.94	0.119	2.85
0.132	5.68	0.116	4.92	0.126	6.89	0.092	4.34	0.072	2.97	0.061	1.68	0.068	4.63	0.128	3.26
0.196	6.88	0.061	4.12	0.196	6.15	0.130	5.84	0.095	3.52	0.107	4.44	0.060	3.98	0.083	4.36
0.127	6.88	0.120	6.51	0.159	7.08	0.158	7.66	0.085	2.71	0.136	7.49	0.076	5.31	0.079	3.85
0.108	6.00	0.120	6.80	0.146	7.61	0.059	1.97	0.189	5.57	0.119	5.71	0.112	6.48	0.108	5.45
0.052	3.68	0.143	6.71	0.115	5.08	0.135	5.48	0.131	4.77	0.112	5.41	0.076	2.32	0.053	3.05
0.114	6.62	0.048	2.72	0.097	2.91	0.153	7.05	0.155	4.71	0.079	3.73	0.068	2.32	0.040	1.91
0.115	7.62	0.064	4.12	0.135	7.24	0.138	6.74	0.167	4.77	0.112	4.89	0.072	2.89	0.056	3.21
0.149	7.50	0.120	5.54	0.140	5.43	0.072	4.22	0.107	3.72	0.072	3.31	0.067	2.92	0.065	3.75
0.154	6.21	0.095	2.69	0.130	6.52	0.083	4.88	0.103	5.79	0.128	5.76	0.053	2.17	0.061	3.03
0.140	6.46	0.075	4.99	0.122	5.95	0.106	5.59	0.072	5.00	0.092	4.65	0.063	3.30	0.069	4.52
0.056	3.12	0.083	5.12	0.154	7.26	0.067	3.48	0.076	2.25	0.076	4.55	0.033	2.96	0.037	2.01
0.119	6.63	0.080	3.13	0.052	2.14	0.073	1.70	0.095	4.87	0.033	1.09	0.042	1.16	0.056	2.65
0.132	7.71	0.026	1.10	0.116	5.34	0.186	5.99	0.080	2.43	0.178	6.67	0.083	4.81	0.079	2.69

0.096	5.82	0.104	5.64	0.118	7.01	0.112	5.99	0.136	5.59	0.107	6.17	0.076	4.87	0.075	2.80
0.091	5.45	0.092	4.74	0.102	3.45	0.103	5.43	0.085	3.55	0.071	3.47	0.089	3.24	0.085	3.53
0.114	6.81	0.088	2.55	0.120	6.00	0.123	6.27	0.108	5.12	0.095	5.15	0.100	4.44	0.084	3.21
0.132	6.84	0.055	1.95	0.075	2.42	0.104	1.65	0.178	6.18	0.073	3.21	0.074	3.46	0.068	3.26
0.103	5.65	0.122	7.09	0.041	1.77	0.021	1.21	0.095	2.38	0.088	5.13	0.171	6.65	0.139	5.93
0.087	4.97	0.081	2.38	0.087	5.87	0.073	3.74	0.075	8.00	0.112	6.42	0.143	5.29	0.127	5.69
0.114	5.54	0.142	5.69	0.096	4.21	0.049	2.33	0.063	3.50	0.075	3.79	0.044	3.21	0.151	6.48
0.126	5.28	0.153	4.82	0.104	3.61	0.103	5.27	0.158	3.54	0.048	2.37	0.150	6.39	0.107	5.47
0.140	5.94	0.151	5.24	0.102	4.11	0.104	6.08	0.132	5.63	0.046	1.84	0.154	7.18	0.051	1.28
0.124	6.11	0.075	4.36	0.084	3.74	0.103	4.61	0.145	5.31	0.083	4.06	0.068	2.23	0.061	6.74
0.079	4.84	0.134	6.34	0.100	5.40	0.142	6.06	0.145	6.13	0.091	2.13	0.166	6.21	0.112	5.62
0.153	7.31	0.065	5.03	0.077	3.26	0.096	2.55	0.154	5.26	0.075	3.48	0.065	4.55	0.154	6.06
0.150	6.22	0.112	6.18	0.124	6.42	0.128	5.79	0.128	6.54	0.188	7.46	0.031	2.23	0.130	5.83
0.124	6.11	0.157	8.06	0.115	4.75	0.091	5.05	0.127	3.89	0.114	6.22	0.088	4.19	0.064	2.48
0.106	6.01	0.083	1.95	0.073	5.63	0.092	4.21	0.049	2.07	0.087	4.53	0.093	4.14	0.038	3.41
0.091	5.79	0.118	5.22	0.106	5.31	0.075	4.02	0.079	4.21	0.057	2.35	0.103	4.75	0.134	5.43
0.162	5.89	0.131	5.67	0.130	6.50	0.095	3.54	0.106	6.63	0.105	5.81	0.140	4.91	0.039	1.40
0.093	6.49	0.136	5.88	0.077	2.5	0.079	4.14	0.096	6.06	0.069	4.07	0.110	3.58	0.069	3.06
0.104	4.81	0.202	4.34	0.118	5.19	0.096	5.85	0.131	6.07	0.111	4.98	0.241	8.84	0.100	4.78
0.120	5.80	0.112	5.51	0.127	5.97	0.083	4.61	0.080	4.19	0.107	6.09	0.104	4.04	0.194	4.69
0.065	3.57	0.093	4.03	0.106	401	0.132	5.47	0.038	2.63	0.026	1.20	0.059	1.05	0.142	8.37
0.129	6.08	0.151	7.85	0.095	4.75	0.095	3.24	0.096	5.20	0.067	4.00	0.073	2.14	0.095	3.54
0.111*	**5.65***	**0.105***	**4.982***	**0.103***	**4.65***	**0.103***	**4.77***	**0.106***	**4.66***	**0.091***	**4.25***	**0.093***	**4.45***	**0.092***	**4.32***
0.032**	**1.374****	**0.037****	**1.82****	**0.036****	**1.66****	**0.031****	**1.49****	**0.035****	**1.43****	**0.036****	**1.72****	**0.038****	**1.58****	**0.036****	**1.58****

*** Average Value of the Results**
**** Standard Deviation of the Results**

Blank		Blue 1		Blue 2		Blue 3		Blue 4		Blue 5		Blue 6	
B. L.	**B. E.**	**B. L.**	**B. E.**	**B. L.**	**B. E.**	**B. L.**	**B. E.**	**B. L.**	**B. E.**	**B. L.**	**B. E.**	**B. L.**	**B. E.**
0.078	4.65	0.112	5.12	0.095	5.72	0.060	2.51	0.049	5.47	0.091	6.51	0.083	5.13
0.077	4.93	0.138	4.13	0.100	4.55	0.131	4.27	0.083	3.82	0.067	2.89	0.042	1.79
0.083	3.79	0.075	4.59	0.063	2.82	0.097	4.51	0.071	1.95	0.103	4.23	0.064	4.44
0.185	5.55	0.054	6.39	0.064	4.71	0.106	4.73	0.096	4.69	0.081	5.97	0.040	1.07
0.129	5.00	0.097	4.88	0.178	6.11	0.104	4.69	0.104	3.59	0.138	7.41	0.064	1.32
0.059	2.72	0.092	4.91	0.085	4.59	0.121	8.66	0.163	8.86	0.134	5.43	0.063	2.49
0.091	4.65	0.100	4.81	0.042	6.39	0.077	5.29	0.040	2.57	0.108	5.54	0.085	5.48
0.115	7.22	0.099	8.39	0.131	4.48	0.096	3.72	0.092	4.20	0.056	3.48	0.143	5.44
0.137	6.25	0.083	3.90	0.111	5.24	0.089	3.88	0.111	3.54	0.107	5.28	0.103	5.76
0.081	3.91	0.093	5.56	0.118	6.14	0.075	3.74	0.075	4.55	0.068	2.93	0.079	2.71
0.079	1.77	0.145	8.64	0.076	2.57	0.085	4.74	0.104	4.17	0.089	2.32	0.084	3.53
0.099	5.65	0.121	8.66	0.102	4.96	0.033	1.03	0.088	4.87	0.075	3.03	0.108	5.54
0.076	5.23	0.079	4.74	0.079	4.86	0.163	8.86	0.046	1.44	0.089	5.93	0.056	3.48
0.080	4.35	0.025	2.12	0.084	4.51	0.097	6.31	0.138	8.46	0.093	3.99	0.107	5.28
0.117	6.17	0.096	5.06	0.100	4.27	0.123	7.51	0.075	4.25	0.090	6.13	0.068	2.93
0.100	4.64	0.051	1.56	0.081	5.59	0.131	4.27	0.067	4.13	0.085	3.92	0.089	2.32
0.056	2.64	0.108	4.81	0.091	6.50	0.097	4.51	0.030	2.51	0.073	3.98	0.075	3.03
0.129	7.03	0.172	8.35	0.067	2.89	0.106	4.73	0.150	8.66	0.085	4.17	0.089	5.93
0.083	4.95	0.091	4.21	0.103	4.23	0.104	4.69	0.080	4.99	0.060	3.80	0.093	3.99
0.114	5.03	0.100	6.08	0.081	5.97	0.121	8.66	0.072	2.62	0.092	5.46	0.059	3.13
0.088	4.19	0.044	1.99	0.048	3.41	0.077	5.29	0.085	2.62	0.097	5.29	0.085	3.92
0.093	4.14	0.134	4.46	0.134	5.43	0.096	3.72	0.085	4.27	0.096	3.72	0.073	3.98
0.103	4.75	0.064	3.20	0.119	2.85	0.089	3.88	0.115	6.91	0.089	3.88	0.085	4.17
0.089	5.94	0.087	2.67	0.128	3.26	0.075	3.74	0.068	4.63	0.075	3.74	0.060	3.80
0.089	4.93	0.092	3.44	0.083	4.36	0.163	8.86	0.060	7.98	0.115	4.74	0.100	4.51
0.120	6.98	0.106	5.73	0.085	4.59	0.033	1.03	0.129	5.33	0.033	1.03	0.088	2.98
0.089	4.33	0.083	4.04	0.087	5.46	0.064	2.81	0.071	1.53	0.064	2.81	0.099	3.97
0.110	4.59	0.112	5.12	0.055	3.16	0.097	6.31	0.069	3.21	0.097	6.31	0.069	2.31
0.077	3.51	0.138	4.13	0.059	3.22	0.060	2.51	0.065	3.69	0.093	5.03	0.106	3.95
0.110	4.61	0.075	3.85	0.081	4.48	0.131	4.27	0.060	2.51	0.049	5.47	0.060	4.04
0.147	7.26	0.064	2.52	0.084	4.98	0.115	6.90	0.131	4.27	0.083	3.82	0.096	4.52
0.093	5.06	0.097	4.88	0.067	3.28	0.068	4.63	0.097	4.51	0.071	1.95	0.064	2.31

0.132	5.90	0.042	7.71	0.164	8.48	0.060	7.98	0.106	4.73	0.096	4.69	0.056	3.76
0.103	5.31	0.100	4.81	0.104	6.08	0.129	5.33	0.104	4.69	0.104	3.59	0.061	4.42
0.116	6.78	0.069	4.59	0.033	5.72	0.077	5.29	0.148	7.46	0.083	3.86	0.104	4.78
0.103	4.14	0.083	6.39	0.064	4.55	0.096	3.72	0.077	5.29	0.040	2.57	0.108	4.74
0.092	4.10	0.093	5.56	0.116	5.82	0.089	3.88	0.096	3.72	0.092	4.20	0.095	4.97
0.118	4.72	0.063	2.64	0.073	4.71	0.075	3.74	0.089	3.88	0.111	3.54	0.096	5.32
0.115	6.90	0.111	5.66	0.178	6.10	0.085	4.74	0.075	3.74	0.075	4.55	0.089	4.41
0.068	4.63	0.079	4.74	0.085	4.59	0.073	1.98	0.115	6.91	0.154	8.17	0.051	2.28
0.160	7.98	0.145	6.12	0.082	6.39	0.164	8.81	0.068	4.63	0.088	4.87	0.107	4.83
0.129	5.13	0.096	5.06	0.131	4.48	0.097	6.31	0.060	7.98	0.099	4.44	0.079	1.92
0.110	4.59	0.051	7.56	0.141	5.24	0.068	4.63	0.129	5.33	0.148	7.46	0.075	4.49
0.097	4.01	0.168	8.81	0.118	6.14	0.068	4.63	0.079	4.74	0.085	4.59	0.076	3.73
0.109	6.11	0.091	4.35	0.176	8.57	0.060	3.98	0.125	7.12	0.042	6.39	0.091	3.83
0.087	4.26	0.091	4.21	0.102	4.96	0.115	6.91	0.096	5.06	0.131	4.48	0.103	3.50
0.093	5.06	0.100	6.08	0.079	4.86	0.163	7.86	0.163	7.86	0.111	5.24	0.077	3.76
0.083	5.90	0.174	8.99	0.084	4.51	0.060	7.98	0.108	4.81	0.118	6.14	0.071	4.21
0.129	5.31	0.134	4.46	0.100	4.27	0.129	5.33	0.091	4.35	0.096	5.57	0.068	2.28
0.116	5.78	0.064	3.20	0.081	5.59	0.087	4.26	0.091	4.20	0.102	4.96	0.046	2.47
0.109*	**5.03***	**0.108***	**5.31***	**0.106***	**5.18***	**0.106***	**5.01***	**0.099***	**4.86***	**0.103***	**4.75***	**0.098***	**4.68***
0.024**	**1.21****	**0.032****	**1.82****	**0.033****	**1.26****	**0.031****	**1.95****	**0.030****	**1.82****	**0.025****	**1.42****	**0.020****	**1.18****

*** Average Value of the Results**
**** Standard Deviation of the Results**

E.2.2 Results of breaking load and breaking extension for the third set (fibres from different lots)

Undyed		Lt-blue green		Ginger		Dkl-taupe		Olive		De-petrol		Tobacco		Khaki	
B. L.	**B. E.**	**B. L.**	**B. E.**	**B. L.**	**B. E.**	**B. L.**	**B. E.**	**B. L.**	**B. E.**	**B. L.**	**B. E.**	**B. L.**	**B. E.**	**B. L.**	**B. E.**
0.087	4.80	0.077	1.70	0.107	4.77	0.081	4.09	0.069	3.90	0.076	4.38	0.103	4.44	0.112	3.98
0.120	5.22	0.046	2.77	0.120	5.85	0.072	3.17	0.079	3.82	0.118	5.60	0.158	5.44	0.034	1.44
0.095	4.18	0.076	4.37	0.068	2.97	0.069	4.33	0.022	1.90	0.072	6.53	0.181	5.41	0.094	4.52
0.067	2.93	0.099	2.34	0.073	3.42	0.065	5.59	0.068	2.37	0.030	4.40	0.140	5.66	0.068	2.28
0.084	3.75	0.096	3.55	0.073	4.46	0.044	1.91	0.071	3.40	0.065	2.90	0.112	5.02	0.129	6.18
0.123	6.34	0.045	1.66	0.093	3.89	0.095	3.69	0.111	3.98	0.080	6.34	0.139	4.94	0.067	2.64
0.065	1.16	0.108	4.83	0.149	6.47	0.038	1.80	0.083	3.59	0.100	4.08	0.088	4.06	0.072	5.53
0.154	7.67	0.073	3.90	0.063	3.07	0.079	4.28	0.085	3.45	0.099	3.41	0.056	2.04	0.073	3.92
0.115	6.43	0.116	5.62	0.080	4.17	0.099	4.83	0.080	3.39	0.048	4.47	0.059	3.06	0.127	5.03
0.128	7.64	0.106	4.70	0.079	3.35	0.067	1.18	0.134	5.10	0.093	3.18	0.079	2.35	0.059	2.62
0.197	9.55	0.108	4.20	0.056	1.80	0.115	5.53	0.089	4.25	0.041	1.01	0.084	4.09	0.084	4.29
0.174	6.01	0.120	5.53	0.041	1.68	0.088	3.85	0.132	5.68	0.091	5.24	0.063	1.70	0.089	3.87
0.173	9.45	0.095	5.69	0.052	2.34	0.064	1.79	0.065	4.97	0.085	3.45	0.092	3.63	0.085	3.67
0.122	5.70	0.138	6.50	0.064	3.41	0.028	1.41	0.107	5.85	0.088	3.93	0.081	2.85	0.079	3.69
0.126	8.18	0.093	4.09	0.080	3.61	0.072	3.17	0.064	3.01	0.076	3.20	0.102	3.90	0.085	3.92
0.048	1.69	0.088	4.19	0.044	1.99	0.134	5.43	0.077	5.29	0.085	2.62	0.077	5.29	0.073	3.98
0.089	6.17	0.093	4.14	0.134	4.46	0.119	2.85	0.096	3.72	0.085	4.27	0.096	6.72	0.085	4.17
0.124	6.30	0.103	4.75	0.064	3.20	0.128	3.26	0.089	3.88	0.044	2.54	0.089	3.88	0.060	3.80
0.162	8.04	0.088	4.94	0.087	2.67	0.083	4.36	0.075	3.74	0.071	4.17	0.075	3.74	0.100	4.50
0.145	8.67	0.068	4.63	0.092	3.44	0.085	4.59	0.085	4.74	0.075	1.65	0.085	4.74	0.088	2.98
0.142	7.53	0.060	3.98	0.106	5.73	0.087	5.46	0.033	1.03	0.085	4.55	0.033	1.03	0.099	3.97
0.112	5.22	0.110	4.59	0.083	4.04	0.055	3.16	0.064	2.81	0.071	1.53	0.064	2.81	0.069	2.30
0.131	7.12	0.077	3.51	0.112	5.12	0.059	3.22	0.097	6.31	0.069	3.21	0.097	6.31	0.106	3.95
0.126	6.69	0.100	4.11	0.138	4.13	0.081	4.48	0.060	2.51	0.065	3.69	0.049	5.47	0.060	4.04
0.147	7.49	0.087	4.26	0.075	3.85	0.084	4.98	0.131	4.27	0.060	2.51	0.083	3.82	0.096	4.52
0.155	7.21	0.093	5.06	0.044	2.52	0.067	3.28	0.097	4.51	0.131	4.27	0.071	1.95	0.064	2.31
0.103	4.95	0.083	5.90	0.097	4.88	0.064	2.48	0.106	4.73	0.097	4.51	0.096	4.69	0.056	3.76
0.068	3.31	0.103	5.31	0.042	1.71	0.104	6.08	0.104	4.69	0.106	4.73	0.104	3.59	0.061	1.42

0.174	7.73	0.106	4.78	0.100	4.80	0.095	5.72	0.022	1.46	0.104	4.69	0.083	3.86	0.104	4.78
0.120	4.48	0.103	4.14	0.069	3.39	0.100	4.55	0.077	5.29	0.042	4.46	0.130	8.57	0.108	4.74
0.093	3.12	0.112	9.07	0.083	3.90	0.185	8.78	0.096	3.72	0.077	5.29	0.157	6.71	0.108	9.14
0.069	1.42	0.185	9.17	0.185	9.17	0.126	5.44	0.109	3.75	0.047	3.72	0.143	6.19	0.115	4.61
0.153	7.82	0.084	2.77	0.084	2.77	0.175	8.03	0.085	2.65	0.124	5.13	0.147	8.39	0.100	6.11
0.142	7.72	0.173	8.44	0.073	3.44	0.150	6.34	0.162	6.42	0.110	3.55	0.065	3.40	0.124	7.56
0.169	6.32	0.124	5.65	0.124	5.65	0.185	6.08	0.150	8.57	0.104	5.17	0.107	6.12	0.209	6.16
0.110	7.81	0.060	1.25	0.060	1.25	0.182	7.56	0.107	5.14	0.120	6.29	0.093	4.69	0.131	7.43
0.146	6.78	0.102	2.44	0.102	2.44	0.103	2.29	0.128	5.30	0.115	5.34	0.079	2.06	0.021	1.57
0.119	5.81	0.075	2.91	0.075	2.91	0.118	5.25	0.181	9.32	0.182	8.12	0.065	1.43	0.084	1.62
0.099	3.88	0.170	6.54	0.170	6.54	0.171	5.01	0.190	7.91	0.091	3.51	0.186	8.74	0.122	4.48
0.038	1.11	0.150	7.01	0.150	7.01	0.169	6.75	0.065	1.62	0.059	1.19	0.130	4.23	0.123	5.42
0.068	3.30	0.111	5.39	0.111	5.39	0.085	2.65	0.107	4.27	0.170	8.06	0.221	7.22	0.132	3.04
0.174	7.73	0.149	7.78	0.149	7.78	0.162	6.42	0.027	1.72	0.130	6.44	0.128	5.67	0.151	8.03
0.120	4.48	0.052	1.19	0.185	8.78	0.130	2.57	0.124	5.13	0.160	8.55	0.115	7.20	0.124	5.10
0.093	3.12	0.158	6.27	0.126	5.44	0.107	5.14	0.110	3.55	0.118	4.87	0.100	3.94	0.125	6.59
0.069	1.42	0.101	5.49	0.175	8.03	0.128	5.30	0.104	5.17	0.182	8.12	0.196	7.03	0.158	7.51
0.153	7.82	0.079	3.85	0.150	6.34	0.181	9.32	0.120	6.29	0.091	3.51	0.159	6.99	0.145	6.64
0.142	7.71	0.063	1.76	0.052	2.08	0.190	7.91	0.115	5.34	0.059	1.19	0.165	8.47	0.169	6.75
0.169	6.42	0.087	3.53	0.142	7.56	0.065	1.62	0.182	8.12	0.170	8.06	0.185	8.78	0.085	2.65
0.123	5.68	0.201	1.51	0.103	2.29	0.107	4.27	0.091	3.51	0.130	6.44	0.126	5.44	0.162	6.42
0.122	5.98	0.096	4.48	0.118	5.25	0.081	4.27	0.059	1.19	0.160	8.55	0.175	8.03	0.150	8.57
0.102	5.08	0.093	4.44	0.139	5.66	0.128	5.52	0.118	4.87	0.118	4.87	0.150	6.34	0.107	5.14
0.12*	**5.67***	**0.110***	**4.50***	**0.096***	**4.20***	**0.107***	**4.32***	**0.092***	**4.20***	**0.098***	**4.38***	**0.112***	**5.00***	**0.105***	**4.35***
0.032**	**1.37****	**0.033****	**1.84****	**0.038****	**1.90****	**0.042****	**1.92****	**0.037****	**1.79****	**0.036****	**1.89****	**0.042****	**2.02****	**0.035****	**1.85****

*** Average Value of the Results**
**** Standard Deviation of the Results**

Brown I		Brown II		Grey		Blue-grey		Dr-grey		Olive-green		Brown III	
B. L.	**B. E.**	**B. L.**	**B. E.**	**B. L.**	**B. E.**	**B. L.**	**B. E.**	**B. L.**	**B. E.**	**B. L.**	**B. E.**	**B. L.**	**B. E.**
0.076	5.31	0.106	5.56	0.079	3.85	0.061	1.44	0.136	4.58	0.112	6.18	0.079	3.32
0.112	6.48	0.128	6.26	0.108	5.45	0.093	3.83	0.056	3.37	0.104	3.87	0.128	4.05
0.076	2.32	0.061	2.90	0.053	3.05	0.124	5.81	0.102	5.59	0.114	4.07	0.043	1.38
0.068	2.32	0.084	4.33	0.040	1.90	0.092	6.67	0.081	3.74	0.079	1.82	0.064	1.92
0.072	2.89	0.175	8.65	0.056	3.21	0.100	4.82	0.069	3.55	0.089	3.79	0.081	3.16
0.067	2.92	0.125	6.62	0.065	3.75	0.088	5.51	0.076	3.42	0.059	2.41	0.049	1.71
0.053	2.17	0.085	4.27	0.061	3.03	0.087	4.93	0.065	2.71	0.087	2.97	0.055	1.85
0.063	3.30	0.094	8.54	0.069	4.52	0.097	5.15	0.092	3.42	0.052	1.29	0.079	1.28
0.033	2.96	0.071	4.38	0.037	2.00	0.162	5.02	0.119	4.04	0.106	4.24	0.100	2.90
0.042	1.16	0.064	3.59	0.056	2.65	0.140	2.51	0.122	4.85	0.056	1.59	0.135	4.81
0.083	4.81	0.049	3.45	0.079	2.69	0.083	4.22	0.089	3.47	0.087	3.22	0.076	1.57
0.076	4.87	0.049	2.45	0.075	2.81	0.046	2.72	0.128	4.08	0.084	2.87	0.076	3.74
0.089	3.24	0.060	5.94	0.085	3.53	0.115	5.78	0.077	3.41	0.106	4.56	0.081	3.21
0.100	4.44	0.044	2.18	0.084	3.21	0.095	5.02	0.091	4.56	0.065	2.99	0.106	5.75
0.074	3.46	0.064	2.84	0.068	3.26	0.092	3.54	0.097	4.34	0.080	3.205	0.078	2.81
0.171	6.65	0.218	8.99	0.139	5.93	0.136	4.51	0.123	5.12	0.159	8.12	0.158	8.04
0.143	5.29	0.171	7.53	0.127	5.69	0.141	5.39	0.073	3.11	0.161	6.56	0.146	7.69
0.044	3.20	0.150	6.41	0.151	6.48	0.112	3.92	0.171	6.35	0.167	5.77	0.099	4.81
0.140	4.91	0.163	7.75	0.039	1.41	0.071	1.82	0.120	5.62	0.187	6.01	0.181	9.06
0.110	3.58	0.112	4.28	0.069	3.06	0.151	8.63	0.109	6.89	0.186	7.37	0.185	7.43
0.241	8.84	0.308	2.65	0.100	4.78	0.147	7.78	0.107	8.85	0.130	5.55	0.116	4.49
0.104	4.04	0.130	5.86	0.194	4.69	0.155	5.79	0.128	3.79	0.100	6.22	0.139	5.69
0.059	1.05	0.153	6.42	0.142	8.37	0.089	3.24	0.203	8.97	0.186	6.68	0.178	8.11
0.073	2.14	0.128	4.99	0.095	3.54	0.129	8.98	0.151	5.87	0.053	1.32	0.174	7.46
0.150	6.39	0.057	2.05	0.107	5.47	0.104	3.53	0.213	9.28	0.146	6.18	0.107	4.91
0.154	7.18	0.060	1.94	0.051	1.28	0.061	2.77	0.204	9.92	0.092	4.17	0.149	6.90
0.068	2.23	0.218	6.42	0.061	6.74	0.177	8.06	0.087	3.29	0.081	2.05	0.096	3.54
0.166	6.21	0.103	3.79	0.112	5.62	0.125	4.89	0.142	5.92	0.136	5.58	0.063	3.11
0.065	4.55	0.201	7.75	0.154	6.06	0.075	3.74	0.136	6.55	0.085	4.74	0.117	4.24
0.031	2.23	0.145	5.30	0.130	5.83	0.085	4.74	0.148	5.87	0.033	1.03	0.108	4.20

0.088	4.19	0.175	8.65	0.064	2.48	0.033	1.03	0.175	8.65	0.064	2.81	0.078	2.50
0.093	4.14	0.125	6.62	0.038	3.41	0.077	5.29	0.125	6.62	0.087	5.29	0.085	3.92
0.103	4.75	0.085	4.27	0.134	5.43	0.096	3.72	0.085	4.27	0.096	3.72	0.073	3.98
0.088	4.94	0.094	8.54	0.119	2.85	0.089	3.88	0.094	8.54	0.089	3.88	0.085	4.17
0.068	4.63	0.087	2.67	0.128	3.26	0.075	3.74	0.071	4.17	0.085	3.74	0.060	3.80
0.060	3.98	0.092	3.44	0.083	4.36	0.085	4.74	0.075	1.65	0.095	4.74	0.110	4.50
0.110	4.59	0.106	5.73	0.085	4.59	0.083	1.03	0.085	4.55	0.043	1.03	0.088	2.98
0.077	3.51	0.083	4.04	0.087	5.46	0.064	3.81	0.071	3.53	0.064	2.81	0.099	3.97
0.100	4.11	0.112	5.12	0.055	3.16	0.097	6.31	0.069	3.21	0.097	5.31	0.069	2.30
0.087	4.26	0.138	4.13	0.059	3.22	0.060	2.51	0.065	3.69	0.033	1.03	0.106	3.95
0.093	5.06	0.075	3.85	0.081	4.48	0.131	4.27	0.060	2.51	0.119	5.47	0.060	2.04
0.083	5.90	0.094	8.52	0.084	4.98	0.097	4.51	0.131	4.27	0.093	3.82	0.096	4.52
0.103	5.31	0.097	4.88	0.067	3.28	0.106	4.73	0.097	4.51	0.071	1.95	0.064	2.31
0.106	4.78	0.125	6.68	0.064	2.48	0.104	4.69	0.104	5.73	0.116	4.69	0.056	3.76
0.103	4.14	0.120	4.72	0.104	6.08	0.052	5.46	0.104	4.69	0.104	3.59	0.051	3.42
0.092	6.38	0.085	4.27	0.095	5.72	0.077	5.29	0.092	4.46	0.088	3.86	0.104	4.18
0.059	1.84	0.094	8.58	0.100	4.55	0.096	3.72	0.077	5.29	0.049	2.57	0.108	4.24
0.124	5.13	0.063	1.76	0.182	7.56	0.145	6.64	0.092	4.38	0.150	6.06	0.099	1.99
0.060	3.55	0.087	3.85	0.103	2.29	0.090	5.91	0.160	8.84	0.140	6.44	0.086	4.27
0.104	5.17	0.201	1.51	0.118	5.25	0.149	6.75	0.102	7.72	0.140	7.45	0.076	1.85
0.120	6.29	0.096	4.48	0.139	5.61	0.080	2.65	0.124	5.13	0.114	4.128	0.185	8.78
0.093*	**4.31***	**0.11***	**5.1***	**0.092***	**4.2***	**0.1***	**4.7***	**0.103***	**5.11***	**0.107***	**4.13***	**0.101***	**4.1***
0.038**	**1.58****	**0.052****	**2.09****	**0.036****	**1.58****	**0.031****	**1.74****	**0.037****	**1.95****	**0.038****	**1.82****	**0.037****	**1.96****

*** Average Value of the Results**
**** Standard Deviation of the Results**